

The Time-Dependent Gutzwiller Approximation
for Multi-Band Hubbard Models

Von der Fakultät für Mathematik, Naturwissenschaften und Informatik
der Brandenburgischen Technischen Universität Cottbus

zur Erlangung des akademischen Grades

Doktor der Naturwissenschaften
(Dr. rer. nat)

genehmigte Dissertation

vorgelegt von

Diplom-Physiker

Ernst Baron von Oelsen

geboren am 27. Mai 1983 in Kirchheim u. T.

Gutachter: Prof. Dr. Götz Seibold
Gutachter: Prof. Dr. Florian Gebhard
Gutachter: Prof. Dr. Vladimir Hizhnyakov

Tag der mündlichen Prüfung: 9. März 2012

The Time-Dependent Gutzwiller Approximation
for Multi-Band Hubbard Models

Von der Fakultät für Mathematik, Naturwissenschaften und Informatik
der Brandenburgischen Technischen Universität Cottbus

zur Erlangung des akademischen Grades

Doktor der Naturwissenschaften
(Dr. rer. nat.)

genehmigte Dissertation

vorgelegt von

Diplom-Physiker

Ernst Baron von Oelsen

geboren am 27. Mai 1983 in Kirchheim u. T.

Gutachter: Prof. Dr. Götz Seibold
Gutachter: Prof. Dr. Florian Gebhard
Gutachter: Prof. Dr. Vladimir Hizhnyakov

Tag der mündlichen Prüfung: 9. März 2012

Contents

Abstract	7
1 Introduction	9
2 Multi-Band Hubbard Models	13
2.1 Many-Body Description of Solids	13
2.2 Lattice Electrons	15
2.3 Second Quantization	16
2.4 Hubbard Models	17
2.5 Examples	19
2.5.1 The One-Band Hubbard Model	19
2.5.2 The Two-Band Hubbard Model	19
2.6 Simplifications	21
2.6.1 Hartree–Fock Approximation I	22
2.6.2 Limit of Large U and the $t - J$ -Model	23
3 Gutzwiller Wave Functions	25
3.1 Definitions and Notations	25
3.2 Multi-Band Gutzwiller Wave Functions	27
3.3 Limit of Infinite Spatial Dimensions	28
3.3.1 Local Constraints	29
3.3.2 Local Energy	30
3.3.3 Kinetic Energy	31
3.4 Energy Functional in Infinite Dimensions	32
3.5 Examples	35
3.5.1 The One-Band Hubbard Model and the Brinkman– Rice Transition	35
3.5.2 Two Decoupled Orbitals	40

4	Time-Dependent Hartree–Fock Approximation	43
4.1	Definitions and Notations	43
4.2	Hartree–Fock Approximation II	44
4.3	Equation of Motion for the Density Matrix	46
4.3.1	Expansion for Weak Perturbations	47
4.3.2	RPA Equations	48
5	Time-Dependent Gutzwiller Approximation	51
5.1	Definitions and Notations	51
5.2	Effective Energy Functional	51
5.3	Gutzwiller RPA Equations	53
5.4	Expansion of the Energy Functional	55
5.5	Lagrange-Functional Expansion	57
5.6	Response Functions for Lattice Models	58
5.6.1	Two-Particle Response Functions	58
5.6.2	Response Functions in the TDGA	60
6	Spin Susceptibility in the Time-Dependent Gutzwiller Approximation	63
6.1	Interaction Kernel	63
6.1.1	Specification of Fluctuations	64
6.1.2	Second-Order Expansion in the Spin-Channel	66
6.1.3	Anti-Adiabaticity and Effective Interaction Kernel	72
6.2	Transversal Spin Susceptibility	73
6.2.1	Response Functions	73
6.2.2	Phase Diagram	76
6.2.3	Magnon Dispersion and Excitation Spectrum	77
6.3	Spin Susceptibility in Infinite Dimensions	78
6.3.1	Model System	78
6.3.2	Results	78
6.4	Spin Susceptibility in Three Dimensions	82
6.4.1	Model System	82
6.4.2	Results	85
7	Conclusions	89
7.1	Summary	89
7.2	Outlook	90

A Two-Site Hubbard Models	93
A.1 The One-Orbital Model	93
A.2 The Two-Orbital Model	94
A.2.1 Exact Solution	94
A.2.2 Exact Evaluation of the GW Wave Function	97
A.2.3 Comparison of the Exact Solution to the GA	98
B Determination of Lagrange parameters	101
B.1 Pseudo-Inverse Matrix	101
C Invariance of the Second-Order Expansions	103
C.1 Equivalence of the Lagrange-Functional Expansion	103
C.2 Linear Transformations of the Density Matrix	106
D Explicit Form of the Second-Order Expansion	109
D.1 Local Fluctuations	109
D.2 Transitive Fluctuations	112
E Explicit Form of the Gutzwiller RPA Equations	115
E.1 Gutzwiller-RPA Equations	115
E.2 Decoupled Fluctuations	116
E.3 Coupled Fluctuations	117
F Kinetic Energy in Infinite Dimensions	121
F.1 Simplification of momentum-space sums	121
Bibliography	123

Abstract

We formulate a generalization of the time-dependent Gutzwiller theory for the application to multi-band Hubbard models. Our approach allows for the computation of general momentum- and frequency-dependent two-particle response functions. The in-depth knowledge of them is crucial for the understanding and interpretation of experiments in solid-state physics. In the calculation of ground-state properties of Hubbard models, the Gutzwiller approach is known to overcome the main shortcomings of the Hartree–Fock approximation, whose time-dependent generalization is the standard textbook method for the calculation of response functions. We therefore expect that the time-dependent Gutzwiller theory, that has been formulated only for the single-band Hubbard model so far, will offer a technique yielding new insight into the dynamics of strongly-correlated multi-orbital systems.

In this thesis, we motivate the employment of multi-orbital Hubbard models and give an introduction to multi-band Hubbard models in Chapters 1 and 2. Their treatment within the Gutzwiller variational approach is subject of Chapter 3, where it is supplemented by investigations that connect our new approach to previous results. We derive the random-phase approximation as the time-dependent Hartree–Fock theory in Chapter 4, followed by the derivation of the corresponding time-dependent Gutzwiller theory in Chapter 5. We demonstrate the applicability of our new approach in Chapter 6, where we calculate the transversal spin susceptibility of a Hubbard model with two degenerate bands and present numerical results for systems in infinite and three spatial dimensions. A summary and conclusion is given in the final Chapter. Mathematical details of our derivations are presented in several appendices.

Chapter 1

Introduction

The investigation of materials with medium to strong Coulomb interaction effects has been a long-standing subject in solid-state physics. Besides numerically exact techniques (like exact diagonalization or quantum Monte-Carlo methods) that are limited to systems of only a few lattice sites, the Density-Functional Theory (DFT) in combination with the Local-Density Approximation (LDA) has established as the standard tool for the investigation of metallic systems. For transition metals and their compounds, however, the LDA becomes insufficient. The reasons for the shortcomings of the LDA are believed to be due to an inadequate treatment of the Coulomb interaction effects.

For the investigation of transition-metal compounds, e.g., manganites, pnictides and cobaltates, more reliable many-particle techniques are desirable. A realistic model for the description of the aforementioned compounds requires the treatment of multi-orbital systems since their constituents possess partially-filled d -shells.

The single-band Hubbard model has become the standard model for the investigation of systems with short-range interactions. Within the Hartree–Fock (HF) approximation it allows for a relatively simple calculation of ground-state properties and of one-particle excitations within the Fermi-liquid theory. The HF approximation covers the weak-coupling limit only, therefore its application to strongly correlated electron systems is questionable.

A big progress in the treatment of many-particle systems was achieved by the limit of infinite spatial dimensions or infinite coordinate numbers, respectively. In this limit, the Hubbard model can be evaluated exactly leading to the Dynamical Mean-Field Theory (DMFT), in which the original lattice model is mapped onto an effective single-impurity system that

has to be solved numerically [1, 2, 3, 4, 5]. In recent years, sophisticated numerical techniques have been developed for the solution of the DMFT equations. However, it is quite challenging from a numerical point of view, and difficulties arise in the investigation of multi-band systems when the full local Coulomb and exchange interaction is taken into account.

Another approach that becomes exact in the limit of infinite spatial dimensions is the Gutzwiller approximation (GA) applied to Gutzwiller variational wave functions. Exact statements on the evaluation of Gutzwiller wave functions in the limit of infinite spatial dimensions have been reported in [1] for the single-band Hubbard model and in [6, 7] for multi-band Hubbard models. Systematic improvements have been achieved by calculating first-order corrections for finite dimensions [8]. The Gutzwiller variational method allows for an investigation of ground-state properties with much less computational effort compared to the DMFT. Originally developed for the investigation of ferromagnetism in the one-band Hubbard model [9, 10, 11], Gutzwiller wave functions provided a starting point for the investigation of (orbital selective) metal-to-insulator transitions [7, 12, 13, 14, 15, 16], quasi-particle properties within a Landau-Gutzwiller approach for Fermi liquids [17, 8, 18], magnetic properties of nickel and pnictides [19, 20, 21, 22] and ground-state properties of plutonium [23]. Specially the quasi-particle dispersion relation of nickel obtained within the Gutzwiller variational approach exhibits good accordance with results from ARPES experiments [17] and overcomes the shortcomings from other theoretical approaches. Furthermore, significant improvements in DFT calculations were achieved when Gutzwiller-correlated interacting electron systems were taken as reference systems [24, 25, 26, 27].

The Gutzwiller variational method yields an energy functional depending on the single-particle density matrix of the non-interacting system and a set of variational parameters. Another approach leading to an equivalent energy functional is the mean-field approximation of the slave-boson formalism originally introduced by Kotliar and Ruckenstein for the single-band Hubbard model [28]. It has been applied successfully to the single-band Hubbard model in two dimensions as approach to cuprate superconductors [29, 30]. The slave-boson formalism was generalized to multi-band Hubbard models [31, 32] and has been applied to several systems [33, 34, 35]. The equivalence of the Gutzwiller variational method and the slave-boson mean-field formalism has been proven in [36].

For the interpretation of experimental results, a profound knowledge of two-particle excitations is required. For example, magnetic neutron scatter-

ing experiments allow for the measurement of the frequency- and momentum-dependent magnetic susceptibility. The standard textbook method for the theoretical investigation of two-particle excitations is the Random-Phase Approximation (RPA), which can be interpreted as a time-dependent generalization of the HF approximation in the small-amplitude limit, i.e., as long as the external perturbations are sufficiently small. As the ground-state description within the HF approximation is known to be inaccurate for moderately to strongly correlated electron systems, its time-dependent generalization is also questionable.

A time-dependent generalization of the Gutzwiller approximation (in the following labelled as ‘TDGA’) within the slave-boson formalism has been developed by Seibold *et al* for the investigation of two-particle response functions in the single-band Hubbard model [37, 38]. Their approach has been applied to a number of systems where inhomogeneous solutions in high- T_c superconductors were investigated [39, 40, 41, 42, 43, 44, 45, 46]. The TDGA turned out to be in astonishing good agreement with exact results [47] and DMFT results [48] for the calculation of magnetic phase boundaries [49]. Another topic investigated by means of the TDGA is the influence of the electron-phonon coupling on two-particle response functions in the single-band Hubbard model [50].

As pointed out, the investigation of transition-metal compounds requires a description by multi-orbital Hubbard models. The success of the TDGA for the single-band model and its quite low computational effort compared to the DMFT encouraged us to investigate to what extent the TDGA can be generalized to such multi-band systems. That is the subject of this thesis. We achieved to derive RPA-like equations for two-particle response functions for Hubbard models with an arbitrary number of orbitals. The method was implemented for numerical calculations of spin-excitations on the Hubbard model with two degenerate electron bands as the simplest multi-band model. The calculations were carried out in finite and infinite spatial dimensions. By means of the two-band model, we were able to study multi-orbital effects like phase transitions towards spin-symmetry broken states as well as orbitally ordered phases. The results differ both qualitatively and quantitatively from the corresponding quantities obtained within the HF approximation.

Chapter 2

Multi-Band Hubbard Models

We summarize the derivation of a Hamiltonian that describes correlated electrons in a crystal. The interaction between the electrons and the lattice atoms is neglected, and so are any spin-orbit coupling effects. The electrons' interactions are reduced to the purely local Coulomb interactions. We present the single- and two-band Hubbard models and briefly sketch two common approximations.

2.1 Many-Body Description of Solids

Solid state physics aims for deducing electronic, magnetic and optical properties of matter from the microscopic properties of its constituents and their interaction. Based on the picture of N_s atomic nuclei occupying the sites of a regular lattice with N_e electrons in between them, one can define the basic solid state Hamilton operator as [51]

$$\begin{aligned}\hat{H}^{\text{ss}} = & \sum_i \frac{\hat{\mathbf{P}}_i^2}{2M_i} + \frac{e^2}{2} \sum_{i \neq j} \frac{Z_i Z_j}{|\hat{\mathbf{R}}_i - \hat{\mathbf{R}}_j|} + \\ & + \sum_k \frac{\hat{\mathbf{p}}_k^2}{2m_e} + \frac{e^2}{2} \sum_{k \neq l} \frac{1}{|\hat{\mathbf{r}}_k - \hat{\mathbf{r}}_l|} + \\ & - \frac{e^2}{2} \sum_{i,k} \frac{Z_i}{|\hat{\mathbf{R}}_i - \hat{\mathbf{r}}_k|}.\end{aligned}\tag{2.1.1}$$

The first line of Eq. (2.1.1) describes the dynamics and Coulomb interaction of the atomic nuclei, characterized by the set of momentum operators $\hat{\mathbf{P}}_i$, position operators $\hat{\mathbf{R}}_i$, masses M_i and charge number Z_i , while the second line does the same for the electrons which are characterized by the set of momentum operators $\hat{\mathbf{p}}_k$ and position operators $\hat{\mathbf{r}}_k$. Their charge and mass

are standard e and m_e , respectively. The last line counts for the (attractive) interaction between the nuclei and the electrons.

Equation (2.1.1) is given in first quantization. Atomic radii are of the order of a few Å. The natural length scale in solid state physics is therefore the Bohr radius $a_0 = \hbar^2/m_e e^2 \approx 0.5\text{Å}$. Energies are measured in units of $E_0 = a_0/e^2$. In real space representation, we find $\hat{\mathbf{P}}_i \equiv -i\nabla_{\mathbf{R}_i}$, $\hat{\mathbf{R}}_i \equiv \mathbf{R}_i$, $\hat{\mathbf{p}}_k \equiv -i\nabla_{\mathbf{r}_k}$ and $\hat{\mathbf{r}}_k \equiv \mathbf{r}_k$. Introducing the scaled position vectors $\tilde{\mathbf{R}} = a_0\hat{\mathbf{R}}$ and replacing $\nabla_{\mathbf{R}} = \frac{1}{a_0}\nabla_{\tilde{\mathbf{R}}}$, one finds the dimensionless Hamiltonian

$$\begin{aligned} \hat{H}^{\text{ss}}/E_0 = & -\frac{1}{2}\sum_i \frac{m_e}{M_i} \frac{\partial^2}{\partial \tilde{\mathbf{R}}_i^2} + \frac{1}{2}\sum_{i \neq j} \frac{Z_i Z_j}{|\tilde{\mathbf{R}}_i - \tilde{\mathbf{R}}_j|} + \\ & -\frac{1}{2}\sum_k \frac{\partial^2}{\partial \tilde{\mathbf{r}}_k^2} + \frac{1}{2}\sum_{k \neq l} \frac{1}{|\tilde{\mathbf{r}}_k - \tilde{\mathbf{r}}_l|} + \\ & + \frac{1}{2}\sum_{i,k} \frac{Z_i}{|\tilde{\mathbf{R}}_i - \tilde{\mathbf{r}}_k|} \end{aligned} \quad (2.1.2)$$

which depends on the charge numbers and the ratio of electron and nucleus mass only. For alkaline or transition metals, the ratio is of the order of $m_e/M_i = \mathcal{O}(10^{-4})$. Born and Oppenheimer proved in [52] that the kinetic energy of the nuclei is smaller than the electrons' kinetic energy by a factor of $\sqrt[4]{m_e/M}$ where M is some mean value of all core masses. Within the 'Born-Oppenheimer' or 'adiabatic' approximation, one therefore neglects the motion of the cores. One is then left with the description of an (interacting) electron gas in front of the background of the nuclei. At sufficiently low temperatures, the nuclei will usually occupy the sites of a regular lattice leading to a periodic effective one-particle potential for the electrons. In this limit, the interaction between the nuclei is a constant and can be neglected.

Small deviations of the nuclei from their equilibrium positions can be treated as coupled harmonic oscillators. Perturbation theory then leads to effective electron-phonon coupling models, which may expose qualitatively new physics, e.g., an attractive electron-electron interaction as in the Fröhlich model. As we are interested in electronic properties only, we will not go into detail here.

With the aforementioned assumptions, the class of Hamiltonians that will be subject of this thesis finally reads

$$\begin{aligned} \hat{H}^{\text{el}} = & \sum_k \left[\frac{\hat{\mathbf{p}}_k^2}{2m_e} + V(\mathbf{r}_k) \right] + \frac{e^2}{2} \sum_{k \neq l} \frac{1}{|\mathbf{r}_k - \mathbf{r}_l|} \\ \equiv & \hat{H}_0 + \hat{H}_{\text{int}}, \end{aligned} \quad (2.1.3)$$

where \hat{H}_0 describes the motion of single electrons in the effective periodic potential caused by the static distribution of the nuclei $V(\mathbf{r})$, while the Coulomb interaction is expressed in \hat{H}_{int} .

2.2 Lattice Electrons

For the description of crystal electrons, one would like to consider infinite, perfect crystals in order to ensure translational invariance. As real crystals are never infinite in space, one rather assumes finite crystals that are sufficiently large, supplemented with periodic boundary conditions. This assumption is not applicable for the investigation of surface properties, but it is justified for the investigation of bulk properties. Non-interacting electrons on a lattice are described by the one-particle Hamiltonian \hat{H}_0 :

$$\hat{H}_0 = \sum_l \left[\frac{\hat{\mathbf{p}}_l^2}{2m_e} + \hat{V}(\mathbf{r}_l) \right]. \quad (2.2.1)$$

The effective one-particle potential of the cores \hat{V} is determined by the core positions. It therefore exhibits the same periodicity as the lattice itself,

$$\hat{V}(\mathbf{r} + \mathbf{R}) = \hat{V}(\mathbf{r}), \quad (2.2.2)$$

where \mathbf{R} is a vector of the underlying Bravais lattice.

A wave function describing the motion of non-interacting electrons in a periodic potential is a Bloch function $\Psi_{n,\mathbf{k}}(\mathbf{r})$. Bloch functions are solutions to the eigenvalue equation

$$\hat{H}_0 \Psi_{n,\mathbf{k}}(\mathbf{r}) = \varepsilon_{n,\mathbf{k}} \Psi_{n,\mathbf{k}}(\mathbf{r}), \quad (2.2.3)$$

with n as an abbreviation for a complete set of quantum numbers. As derived in [53], these solutions must obey the relation

$$\Psi_{n,\mathbf{k}}(\mathbf{r} + \mathbf{R}) = e^{i\mathbf{k}\mathbf{R}} \Psi_{n,\mathbf{k}}(\mathbf{r}), \quad (2.2.4)$$

with a wave vector \mathbf{k} in the first Brillouin zone. Bloch functions can therefore be written as a product of a plane wave with a periodic amplitude function $u_{n,\mathbf{k}}(\mathbf{r})$, the so-called Bloch factor:

$$\Psi_{n,\mathbf{k}}(\mathbf{r}) = e^{i\mathbf{k}\mathbf{r}} u_{n,\mathbf{k}}(\mathbf{r}) \quad \text{with} \quad u_{n,\mathbf{k}}(\mathbf{r} + \mathbf{R}) = u_{n,\mathbf{k}}(\mathbf{r}). \quad (2.2.5)$$

The Bloch factor is the solution of the Schrödinger equation

$$\frac{1}{2m_e} [(\mathbf{k} - i\nabla)^2 + \hat{V}(\mathbf{r})] u_{n,\mathbf{k}}(\mathbf{r}) = \varepsilon_{n,\mathbf{k}} u_{n,\mathbf{k}}(\mathbf{r}) \quad (2.2.6)$$

and thus fully determined by the core potential $\hat{V}(\mathbf{r})$.

Bloch functions describe delocalized electrons. Their Fourier transforms yield the ‘Wannier functions’ $w_n(\mathbf{r})$ as

$$w_n(\mathbf{r} - \mathbf{R}) = \frac{1}{\sqrt{N_s}} \sum_{\mathbf{k}} e^{-i\mathbf{k}\mathbf{R}} \Psi_{n,\mathbf{k}}(\mathbf{r}), \quad (2.2.7)$$

which—under certain circumstances—describe an electron state localized in the vicinity of lattice site \mathbf{R} .

2.3 Second Quantization

Due to the Pauli principle, the wave function for the electrons must obey the antisymmetry condition for indistinguishable fermions. The easiest way to take the Pauli principle into consideration is the framework of second quantization where the antisymmetry of the wave function is introduced automatically via the anticommutator relations for fermionic annihilation and creation operators. In order to derive the representation of the Hamiltonian (2.1.3) in second quantization, one usually starts from the field operators in real space:

$$\hat{\Psi}_s(\mathbf{r}) = \sum_{i=1}^{N_s} \sum_a w_{a,s}(\mathbf{r} - \mathbf{R}_i) \hat{c}_{i,a,s} \quad (2.3.1)$$

$$\hat{\Psi}_s^\dagger(\mathbf{r}) = \sum_{i=1}^{N_s} \sum_a w_{a,s}^*(\mathbf{r} - \mathbf{R}_i) \hat{c}_{i,a,s}^\dagger. \quad (2.3.2)$$

The Wannier states $w_{a,s}(\mathbf{r} - \mathbf{R}_i)$ are localized in the vicinity of the lattice site \mathbf{R}_i . The $\hat{c}_{i,a,s}^{(\dagger)}$ are the usual annihilation (creation) operators for an electron on lattice site \mathbf{R}_i in the state (a, s) . The field operators $\hat{\Psi}_s^{(\dagger)}$ annihilate (create) an electron with spin s at the position \mathbf{r} . The sum runs over all N_s lattice sites and the discrete index a counts the Wannier states at each lattice site. As the Hamiltonian (2.1.3) does not depend on the electrons’ spin, one can split the state $w_{a,s}(\mathbf{r})$ into a spatial state $w_a(\mathbf{r})$ and a two-dimensional spinor χ_s for the two spin projections $s = \uparrow, \downarrow$.

The effective electronic Hamiltonian (2.1.3) is then expressed via the field operators (2.3.1) and (2.3.2) as

$$\hat{H}_0 = \sum_{s_1 s_2} \int d\mathbf{r} \hat{\Psi}_{s_1}^\dagger(\mathbf{r}) \left[\frac{\hat{\mathbf{p}}^2}{2m_e} + V(\mathbf{r}) \right] \hat{\Psi}_{s_2}(\mathbf{r}) \quad (2.3.3)$$

$$\hat{H}_{\text{int}} = \frac{1}{2} \sum_{\substack{s_1 s_2 \\ s_3 s_4}} \iint d\mathbf{r} d\mathbf{r}' \hat{\Psi}_{s_1}^\dagger(\mathbf{r}) \hat{\Psi}_{s_2}^\dagger(\mathbf{r}') \frac{e^2}{|\mathbf{r} - \mathbf{r}'|} \hat{\Psi}_{s_3}(\mathbf{r}') \hat{\Psi}_{s_4}(\mathbf{r}), \quad (2.3.4)$$

leading to the result

$$\hat{H}_0 = \sum_{ij} \sum_{\sigma_1 \sigma_2} t_{ij}^{\sigma_1 \sigma_2} \hat{c}_{i, \sigma_1}^\dagger \hat{c}_{j, \sigma_2} \quad (2.3.5)$$

$$\hat{H}_{\text{int}} = \frac{1}{2} \sum_{\substack{ij \\ kl}} \sum_{\substack{\sigma_1 \sigma_2 \\ \sigma_3 \sigma_4}} U_{ijkl}^{\sigma_1 \sigma_2 \sigma_3 \sigma_4} \hat{c}_{i, \sigma_1}^\dagger \hat{c}_{j, \sigma_2}^\dagger \hat{c}_{k, \sigma_3} \hat{c}_{l, \sigma_4}, \quad (2.3.6)$$

where the abbreviations

$$t_{ij}^{\sigma_1 \sigma_2} = \delta_{\chi_{\sigma_1} \chi_{\sigma_2}} \int d\mathbf{r} w_{\sigma_1}^*(\mathbf{r} - \mathbf{R}_i) \left[-\frac{\Delta}{2m_e} + V(\mathbf{r}) \right] w_{\sigma_2}(\mathbf{r} - \mathbf{R}_j) \quad (2.3.7)$$

and

$$U_{ijkl}^{\sigma_1 \sigma_2 \sigma_3 \sigma_4} = \delta_{\chi_{\sigma_1} \chi_{\sigma_4}} \delta_{\chi_{\sigma_2} \chi_{\sigma_3}} \times \\ \times e^2 \iint d\mathbf{r} d\mathbf{r}' \frac{w_{\sigma_1}^*(\mathbf{r} - \mathbf{R}_i) w_{\sigma_2}^*(\mathbf{r}' - \mathbf{R}_j) w_{\sigma_3}(\mathbf{r}' - \mathbf{R}_k) w_{\sigma_4}(\mathbf{r} - \mathbf{R}_l)}{|\mathbf{r} - \mathbf{r}'|} \quad (2.3.8)$$

were introduced using the combined spin-orbit index $\sigma \equiv (a, s)$.

The representation Eqs. (2.3.5) and (2.3.6) of the Hamiltonian (2.1.3) is still exact. One can see from Eqs. (2.3.7) and (2.3.8) that these matrix elements depend on the spatial overlap of the Wannier states. This fact will be the starting point for crucial approximations in the next section.

2.4 Hubbard Models

The Hubbard model was proposed for the description of electrons in narrow bands where the model of a gas of free electrons fails both qualitatively and quantitatively. The low mobility of the electrons is a consequence of the small overlap of two Wannier states localized around different lattice sites. The effective potential $V(\mathbf{r})$ in the domain where the Wannier state $w_\sigma(\mathbf{r} - \mathbf{R}_i)$ has not yet tended to zero will be dominated by the spherical atomic potential of the nuclei at lattice site \mathbf{R}_i . Hubbard thus suggested to replace the exact Wannier states by the solution of the Schrödinger equation of the isolated atoms. The field operators then read

$$\hat{\Psi}_s(\mathbf{r}) \approx \sum_{i, a} \chi_s \phi_a(\mathbf{r} - \mathbf{R}_i) \hat{c}_{i, a, s} \quad (2.4.1)$$

$$\hat{\Psi}_s^\dagger(\mathbf{r}) \approx \sum_{i, a} \chi_s \phi_a^*(\mathbf{r} - \mathbf{R}_i) \hat{c}_{i, a, s}^\dagger, \quad (2.4.2)$$

where the index a is now identified with the orbital index.

Due to the small overlap of the atomic orbitals, the hopping amplitudes will decrease fast with increasing distance $|\mathbf{R}_i - \mathbf{R}_j|$. Thus, one will limit the

finite hopping amplitudes (2.3.7) only to a certain number of neighboring sites. This is the basic idea of the ‘tight-binding’ or Bloch approximation [53]. In order to derive suitable hopping amplitudes, one has to take the special geometry of the underlying lattice and the anisotropy of atomic orbitals’ spatial distribution into account. Slater and Koster developed a systematic scheme that allows for the determination of hopping amplitudes that expose the correct symmetries for the most common crystal structures [54].

The interaction matrix element (2.3.8) is simplified analogously by neglecting all contributions that arise from electron states that are localized around at least two different lattice sites. Taking Coulomb interactions between electrons on *different* lattice sites into account would lead to the class of ‘extended Hubbard models’ that are not subject of this thesis.

One is then left with the multi-orbital tight-binding Hamiltonian and the purely local interaction Hamiltonian

$$\begin{aligned} \hat{H}^{\text{el}} = & \sum_{\substack{i \neq j \\ \sigma_1 \sigma_2}} t_{ij}^{\sigma_1 \sigma_2} \hat{c}_{i, \sigma_1}^\dagger \hat{c}_{j, \sigma_2} + \sum_{\substack{i \\ \sigma_1 \sigma_2}} \epsilon_i^{\sigma_1 \sigma_2} \hat{c}_{i, \sigma_1}^\dagger \hat{c}_{i, \sigma_2} \\ & + \frac{1}{2} \sum_i \sum_{\substack{\sigma_1 \sigma_2 \\ \sigma_3 \sigma_4}} U_i^{\sigma_1 \sigma_2 \sigma_3 \sigma_4} \hat{c}_{i, \sigma_1}^\dagger \hat{c}_{i, \sigma_2}^\dagger \hat{c}_{i, \sigma_3} \hat{c}_{i, \sigma_4}, \end{aligned} \quad (2.4.3)$$

with the matrix element (2.3.8) evaluated for $i = j = k = l$. Here, we split the one-particle Hamiltonian into the inter-site hopping part and the site-diagonal part with the orbital energies $\epsilon_i^{\sigma_1 \sigma_2} \equiv t_{ii}^{\sigma_1 \sigma_2}$.

The orbital index has no upper boundary. We transform the Hamiltonian (2.4.3) into momentum space via

$$\hat{c}_{\mathbf{k}, \sigma}^{(\dagger)} = \frac{1}{\sqrt{N_s}} \sum_i e^{\mp i \mathbf{k} \mathbf{R}_i} \hat{c}_{i, \sigma}^{(\dagger)} \quad (2.4.4)$$

$$\epsilon_{\mathbf{k}}^{\sigma_1 \sigma_2} = \frac{1}{N_s} \sum_{i, j} e^{i \mathbf{k} (\mathbf{R}_i - \mathbf{R}_j)} t_{ij}^{\sigma_1 \sigma_2}, \quad (2.4.5)$$

leading to band states $|\mathbf{k}\sigma\rangle$. We diagonalize the resulting Hamiltonian via some unitary transformation

$$\hat{h}_{\mathbf{k}, \alpha}^\dagger = \sum_{\sigma} [u_{\sigma, \alpha}(\mathbf{k})]^* \hat{c}_{\mathbf{k}, \sigma}^\dagger. \quad (2.4.6)$$

At $T = 0$, the lowest energy band states are occupied up to the Fermi energy E_F which must be determined from

$$N_e = \sum_{\mathbf{k}, \alpha} \Theta[E_F - E_{\mathbf{k}, \alpha}]. \quad (2.4.7)$$

Orbital states that are energetically far below or above the Fermi energy will be either fully occupied or unoccupied, respectively. If one is interested in low-energy excitations only, one can restrict oneself to a small (finite) number of orbitals that are energetically close to E_F .

2.5 Examples

We briefly present the one-band Hubbard model as *the* standard model in the theory of correlated electrons. Furthermore, we sketch the two-band Hubbard model to enter the universe of multi-band Hubbard models.

2.5.1 The One-Band Hubbard Model

The one-band Hubbard model was introduced independently by Gutzwiller [9], Hubbard [55] and Kanamori [56] in 1963. The simplest Hubbard model contains only one orbital per lattice site and arises if one considers the conduction band of a solid as totally separated from the valence band and any higher energy bands. This assumption may be justified to a certain degree if the electronic structure ensures that the Fermi energy crosses exactly one electron band. On the one hand, this picture holds for Na, Mg, K and Ca, for example. On the other hand, the three-orbital Emery model—describing the dynamics in the copper-oxide planes in high- T_c superconductors—at half-filling can be mapped onto an effective single-band Hubbard model for holes in Cu- d -orbitals [57].

The electronic Hamiltonian reads

$$\hat{H}_{1B}^{\text{el}} = \hat{H}_{1B}^0 + \hat{H}_{1B}^{\text{int}} = \sum_{i \neq j, s} t_{ij} \hat{c}_{i,s}^\dagger \hat{c}_{j,s} + \sum_{i,s} \epsilon_i \hat{n}_{i,s} + \sum_i U_i \hat{n}_{i,\uparrow} \hat{n}_{i,\downarrow}. \quad (2.5.1)$$

Note that we do not have to indicate the specific orbital. Thus, the electrons' spin projection s is the only degree of freedom. The only contributions to the interaction energy arise from doubly occupied lattice sites. For many systems, one can assume that the lattice sites are occupied with equivalent atoms. If the number of electrons is fixed, the site-diagonal one-particle term leads to a constant energy contribution which can be dropped.

2.5.2 The Two-Band Hubbard Model

The two-band Hubbard model is the simplest non-trivial multi-band Hubbard model. As sketched in the introduction, the participation of transition metals in pnictides, manganites and cobaltates requires an adequate description of d -orbitals. In a cubic environment, the fivefold degeneracy of

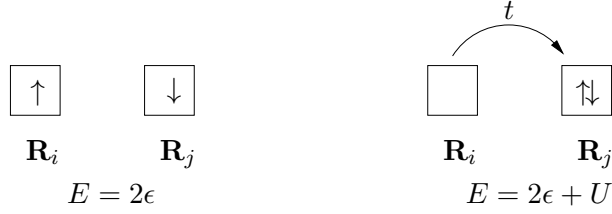


Figure 2.5.1: Sketch of the single-band Hubbard model. **Left:** neutral configuration with singly occupied sites; **Right:** charge fluctuations (hopping amplitude t) between lattice sites \mathbf{R}_i and \mathbf{R}_j induce doubly occupied sites leading to an increase of the system's energy by the local interaction U .

the atomic d -orbitals is partially lifted. The orbitals are split into three t_{2g} -orbitals (usually labelled as d_{xy} -, d_{xz} - and d_{yz} -orbitals) and two e_g -orbitals (usually labelled as $d_{x^2-y^2}$ - and $d_{3z^2-z^2}$ -orbitals). If the central atom, i.e., the one contributing the d -orbitals, is surrounded by six negatively charged ions (each one sitting on a corner of a regular octahedron), the e_g -orbitals are shifted towards higher energies due to their spatial orientation along the crystal axes. For an illustrative description of crystal field effects, see [58].

The multi-orbital character leads to inter-orbital hopping processes and thus increases the number of finite hopping amplitudes $t_{ij}^{\sigma_1\sigma_2}$. As the structure of the hopping amplitudes strongly depends on the lattice geometry (e.g., its dimension and symmetry), we skip the detailed specification of the one-particle Hamiltonian here.

In the numerical application of the TDGA in Chapter 6, we consider two degenerate e_g -orbitals on a simple cubic and a hyper-cubic lattice. The local interaction Hamiltonian (2.3.8) for two e_g -orbitals on a three-dimensional cubic lattice reads [7]

$$\begin{aligned} \hat{H}_{\text{int}} = & U \sum_{b=1,2} \hat{n}_{b,\uparrow} \hat{n}_{b,\downarrow} + U' \sum_{s,s'=\uparrow,\downarrow} \hat{n}_{1,s} \hat{n}_{2,s'} - J \sum_{s=\uparrow,\downarrow} \hat{n}_{1,s} \hat{n}_{2,s} \\ & + J \sum_{s=\uparrow,\downarrow} \hat{c}_{1,s}^\dagger \hat{c}_{2,\bar{s}}^\dagger \hat{c}_{1,\bar{s}} \hat{c}_{2,s} + J_C [\hat{c}_{1,\uparrow}^\dagger \hat{c}_{1,\downarrow}^\dagger \hat{c}_{2,\downarrow} \hat{c}_{2,\uparrow} + \hat{c}_{2,\uparrow}^\dagger \hat{c}_{2,\downarrow}^\dagger \hat{c}_{1,\downarrow} \hat{c}_{1,\uparrow}], \end{aligned} \quad (2.5.2)$$

where we used the convention $\bar{\uparrow} = \downarrow$ and $\bar{\downarrow} = \uparrow$. For simplicity, we skipped the site index on both the interaction parameters (U , U' , J and J_C) and the operators. The eigenstates and eigenenergies of \hat{H}_{int} are listed in Table 2.5.1, supplemented by their spin quantum numbers. All interaction parameters have positive values. Only two of them can be chosen independently as the cubic symmetry in three dimensions requires $U - U' = 2J$ and $J = J_C$. The ratio of J and U is thus limited to $\frac{J}{U} < \frac{1}{3}$. Otherwise an unphysical *attractive*

interaction $U' < 0$ for electrons occupying different orbitals on the same lattice site would arise, which may lead to a superconducting ground state. We use the same interaction Hamiltonian and the same symmetry conditions also in the case of the hyper-cubic lattice, although, strictly speaking, it does not make sense to define a cubic environment in infinite spatial dimensions.

No.	$ \Gamma\rangle$	$E_{ \Gamma\rangle}$	S_{at}	S_{at}^z
1	$ \circ, \circ\rangle$	0	0	0
2	$ \uparrow, \circ\rangle$	0	$\frac{1}{2}$	$\frac{1}{2}$
3	$ \circ, \uparrow\rangle$	0	$\frac{1}{2}$	$\frac{1}{2}$
4	$ \downarrow, \circ\rangle$	0	$\frac{1}{2}$	$-\frac{1}{2}$
5	$ \circ, \downarrow\rangle$	0	$\frac{1}{2}$	$-\frac{1}{2}$
6	$ \uparrow, \uparrow\rangle$	$U' - J$	1	1
7	$\frac{1}{\sqrt{2}} [\uparrow, \downarrow\rangle + \downarrow, \uparrow\rangle]$	$U' - J$	1	0
8	$ \downarrow, \downarrow\rangle$	$U' - J$	1	-1
9	$\frac{1}{\sqrt{2}} [\uparrow, \downarrow\rangle - \downarrow, \uparrow\rangle]$	$U' + J$	0	0
10	$\frac{1}{\sqrt{2}} [\uparrow\downarrow, \circ\rangle - \circ, \uparrow\downarrow\rangle]$	$U - J_C$	0	0
11	$\frac{1}{\sqrt{2}} [\uparrow\downarrow, \circ\rangle + \circ, \uparrow\downarrow\rangle]$	$U + J_C$	0	0
12	$ \uparrow, \uparrow\downarrow\rangle$	$U + 2U' - J$	$\frac{1}{2}$	$\frac{1}{2}$
13	$ \uparrow\downarrow, \uparrow\rangle$	$U + 2U' - J$	$\frac{1}{2}$	$\frac{1}{2}$
14	$ \downarrow, \uparrow\downarrow\rangle$	$U + 2U' - J$	$\frac{1}{2}$	$-\frac{1}{2}$
15	$ \uparrow\downarrow, \downarrow\rangle$	$U + 2U' - J$	$\frac{1}{2}$	$-\frac{1}{2}$
16	$ \uparrow\downarrow, \uparrow\downarrow\rangle$	$2U + 4U' - 2J$	0	0

Table 2.5.1: The 16 atomic eigenstates $|\Gamma\rangle$ of the two-band Hubbard interaction Hamiltonian (2.5.2). The eigenenergies $E_{|\Gamma\rangle}$, the total spin S_{at} and its z -component for each eigenstate are listed. The three triplet states with $S_{\text{at}} = 1$ possess the lowest energy among the two-electron states, in accordance with Hund's first rule. A representation of the eigenstates and their symmetry properties can be found in [7].

2.6 Simplifications

In spite of the crucial simplifications, Hubbard models cannot be solved analytically without further assumptions. Exact solutions exist for the one-band Hubbard model in one dimension and for systems with a small number

of lattice sites, where the diagonalization of Eq. (2.1.3) can be carried out explicitly. For any other system, further approximation techniques are required that are shortly discussed in the following.

2.6.1 Hartree–Fock Approximation I

The HF approximation is the standard textbook method to deal with correlated-electron systems. It can be derived in various ways, all leading to equivalent results. In Chapter 4.2, we derive the HF equations variationally by minimizing the ground-state energy of the Hamiltonian (2.1.3) with respect to the one-particle density matrix of a trial wave function.

An equivalent result is obtained if the Hamiltonian itself is approximated by an effective one-particle Hamiltonian

$$\hat{H}^{\text{HF}} = \sum_{\gamma} E_{\gamma} \hat{h}_{\gamma}^{\dagger} \hat{h}_{\gamma}. \quad (2.6.1)$$

The one-particle energies E_{γ} and operators $\hat{h}_{\gamma}^{\dagger}$ will be specified later. Its ground-state wave function is a Slater determinant

$$|\Phi_0^{\text{HF}}\rangle = \prod_{E_{\gamma} \leq E_{\text{F}}} \hat{h}_{\gamma}^{\dagger} |0\rangle, \quad (2.6.2)$$

where certain one-particle states γ are occupied. The Fermi energy E_{F} was introduced as a variational parameter in order to conserve the total number of electrons,

$$N_e = \sum_{\substack{\gamma \\ \text{occ.}}} 1 = \sum_{\gamma} \Theta[E_{\text{F}} - E_{\gamma}]. \quad (2.6.3)$$

The creation operators $\hat{h}_{\gamma}^{\dagger}$ and $\hat{c}_{\sigma}^{\dagger}$ are connected via the unitary transformation

$$\hat{h}_{\gamma}^{\dagger} = \sum_{\sigma} u_{\sigma, \gamma} \hat{c}_{\sigma}^{\dagger} \quad (2.6.4)$$

$$\hat{c}_{\sigma}^{\dagger} = \sum_{\gamma} [u_{\sigma, \gamma}]^* \hat{h}_{\gamma}^{\dagger} \quad (2.6.5)$$

that must be determined self-consistently.

Based on the operator identity

$$\hat{A}\hat{B} = [\hat{A} - \langle\hat{A}\rangle][\hat{B} - \langle\hat{B}\rangle] + \hat{A}\langle\hat{B}\rangle + \hat{B}\langle\hat{A}\rangle - \langle\hat{A}\rangle\langle\hat{B}\rangle, \quad (2.6.6)$$

the HF approximation neglects the fluctuation around the expectation value, i.e., the first two brackets in Eq. (2.6.6),

$$\hat{A}\hat{B} \xrightarrow{\text{HFA}} \hat{A}\langle\hat{B}\rangle + \hat{B}\langle\hat{A}\rangle - \langle\hat{A}\rangle\langle\hat{B}\rangle, \quad (2.6.7)$$

and only one-operator expressions and c -numbers remain. If each of the operators \hat{A} or \hat{B} is an operator product itself, the decoupling procedure has to be repeated until one is left with one-particle operators only. In the latter case, each possible pairing of operators has to be taken into account. For fermionic systems, each interchange of two operators leads to a factor of -1 .

For the product of four fermionic operators as they appear in two-particle interaction Hamiltonians, the aforementioned decoupling scheme leads to

$$\begin{aligned} \hat{c}_{\sigma_1}^\dagger \hat{c}_{\sigma_2}^\dagger \hat{c}_{\sigma_3} \hat{c}_{\sigma_4} &= \hat{c}_{\sigma_1}^\dagger \hat{c}_{\sigma_4} \langle \hat{c}_{\sigma_2}^\dagger \hat{c}_{\sigma_3} \rangle + \hat{c}_{\sigma_2}^\dagger \hat{c}_{\sigma_3} \langle \hat{c}_{\sigma_1}^\dagger \hat{c}_{\sigma_4} \rangle - \langle \hat{c}_{\sigma_1}^\dagger \hat{c}_{\sigma_4} \rangle \langle \hat{c}_{\sigma_2}^\dagger \hat{c}_{\sigma_3} \rangle \\ &\quad - \hat{c}_{\sigma_1}^\dagger \hat{c}_{\sigma_3} \langle \hat{c}_{\sigma_2}^\dagger \hat{c}_{\sigma_4} \rangle - \hat{c}_{\sigma_2}^\dagger \hat{c}_{\sigma_4} \langle \hat{c}_{\sigma_1}^\dagger \hat{c}_{\sigma_3} \rangle + \langle \hat{c}_{\sigma_2}^\dagger \hat{c}_{\sigma_4} \rangle \langle \hat{c}_{\sigma_1}^\dagger \hat{c}_{\sigma_3} \rangle \\ &\quad + \hat{c}_{\sigma_1}^\dagger \hat{c}_{\sigma_2}^\dagger \langle \hat{c}_{\sigma_3} \hat{c}_{\sigma_4} \rangle + \hat{c}_{\sigma_3} \hat{c}_{\sigma_4} \langle \hat{c}_{\sigma_1}^\dagger \hat{c}_{\sigma_2}^\dagger \rangle - \langle \hat{c}_{\sigma_3} \hat{c}_{\sigma_4} \rangle \langle \hat{c}_{\sigma_1}^\dagger \hat{c}_{\sigma_2}^\dagger \rangle. \end{aligned} \quad (2.6.8)$$

Note that the last line contributes for superconducting systems only and is mentioned here only for the sake of completeness. The expectation values that appear in Eq. (2.6.8) are to be taken with respect to the HF ground-state wave function (2.6.2).

Applied to the multi-band Hubbard Hamiltonian (2.5.2), the effective one-particle Hamiltonian in its general form reads

$$\hat{H}^{\text{HF}} = \sum_{ij} \sum_{\sigma_1 \sigma_2} [t_{ij}^{\sigma_1 \sigma_2} + \delta_{ij} \sum_{\sigma_3 \sigma_4} \tilde{U}_i^{\sigma_1 \sigma_2, \sigma_3 \sigma_4} \langle \hat{c}_{i\sigma_3}^\dagger \hat{c}_{i\sigma_4} \rangle_{\Phi_0^{\text{HF}}}] \hat{c}_{i\sigma_1}^\dagger \hat{c}_{j\sigma_2} \quad (2.6.9)$$

and must be diagonalized via the unitary transformations (2.6.4) and (2.6.5). The one-particle energies depend implicitly on the Slater determinant (2.6.2) through the expectation values $\langle \hat{c}_{i\sigma_3}^\dagger \hat{c}_{i\sigma_4} \rangle_{\Phi_0^{\text{HF}}}$. With a certain starting wave function $|\Phi_0^{\text{HF}}\rangle$, one calculates the particle densities $\langle \hat{c}_{i\sigma}^\dagger \hat{c}_{i\sigma'} \rangle_{\Phi_0^{\text{HF}}}$ defining new one-particle energies in \hat{H}^{HF} . This procedure is continued until self-consistency is reached.

2.6.2 Limit of Large U and the $t - J$ -Model

The $t - J$ -model evolves from the one-band Hubbard model perturbatively in the limit of infinite local interactions ($U \rightarrow \infty$). For band-fillings below or equal to $\frac{1}{2}$, the system will avoid any double occupancies. Via a canonical transformation, the Hamiltonian (2.5.1) can be transformed into an effective Hamiltonian

$$\hat{H}_{tJ}^{\text{aux}} = \sum_{i \neq j} \sum_{s=\uparrow, \downarrow} t_{ij} [1 - \hat{n}_{i, \bar{s}}] \hat{c}_{i, s}^\dagger [1 - \hat{n}_{j, \bar{s}}] \hat{c}_{j, s} + \frac{1}{2} \sum_{i \neq j} \frac{4t_{ij}^2}{U} [\hat{\mathbf{S}}_i \hat{\mathbf{S}}_j - \frac{1}{4} \hat{n}_i \hat{n}_j], \quad (2.6.10)$$

in which high-energy excitations (induced by doubly occupied sites) are eliminated to order $\mathcal{O}(\frac{t_{ij}^2}{U})$. The unconstrained hopping processes of the Hamiltonian (2.4.3) are replaced by *projected* hopping events in the sense that an electron can reach lattice site \mathbf{R}_j only if that is not covered by an electron of opposite spin yet. The formerly *local* density-like interaction is now represented by a spin-spin interaction between electrons on *neighboring* lattice sites. For exactly half-filled systems, the Hamiltonian (2.6.10) turns into the Heisenberg Hamiltonian for the description of localized spins

$$\hat{H}_{\text{HB}} = \sum_{i \neq j} J_{ij} \hat{\mathbf{S}}_i \hat{\mathbf{S}}_j, \quad (2.6.11)$$

with the anti-ferromagnetic coupling constant $J_{ij} = \frac{4t_{ij}^2}{U}$. For an overview of the development of the $t - J$ -model, cf., [59].

Chapter 3

Gutzwiller Wave Functions

We briefly summarize some basic definitions and expressions that are very useful to develop the multi-band Gutzwiller theory. An overview of the basic ideas leading to the class of Gutzwiller wave functions as they were developed in order to examine the single-band Hubbard model is given.

We present a symmetric formulation that allows for a straight-forward generalization to multi-band systems. We recapitulate the results that arise from the limit of infinite spatial dimensions, known as the ‘Gutzwiller approximation’ (GA).

3.1 Definitions and Notations

In order to formulate the general multi-band Gutzwiller formalism, we set up some definitions that will remain valid for the rest of this thesis. We follow the ideas of Bünemann, Weber and Gebhard in [7]. Each lattice site with N orbitals allows for an occupation with up to $2N$ electrons. Thus, the dimension of the atomic Hilbert space is 2^{2N} . For a given set of combined spin-orbit indices $\sigma = (a, s)$, we introduce some arbitrary, but fixed, order $\sigma_1 < \sigma_2 < \dots < \sigma_{2N}$.

Each atomic configuration I is characterized by its occupied spin-orbit states. If the configuration I contains the occupied spin-orbit states $\sigma_{\alpha_1}, \sigma_{\alpha_2}, \dots, \sigma_{\alpha_{|I|}}$, the corresponding state $|I\rangle$ is defined as

$$|I\rangle = \hat{c}_{\sigma_{\alpha_1}}^\dagger \hat{c}_{\sigma_{\alpha_2}}^\dagger \dots \hat{c}_{\sigma_{\alpha_{|I|}}}^\dagger |0\rangle, \quad (3.1.1)$$

where the creation operators are in ascending order. Sequences of annihilation operators, as in

$$[|I\rangle]^\dagger \equiv \langle I| = \langle 0| \hat{c}_{\sigma_{\alpha_{|I|}}} \dots \hat{c}_{\sigma_2} \hat{c}_{\sigma_1}, \quad (3.1.2)$$

always appear in descending order. Here, we also introduced $|I|$ as the total number of electrons within the configuration I .

Configurations I are treated as sets in the common mathematical sense. This allows for the usual set operations. For example, the configuration $J = I \setminus I'$ will contain all occupied states as I except the occupied ones from I' . Analogously, the state $J = I \cup I'$ is made of those spin-orbit states that are occupied within I or I' , respectively, while the state $J = I \cap I'$ only contains states that are occupied in both states I and I' simultaneously. The complement to a given state I is defined as $\bar{I} = (\sigma_1, \sigma_2, \dots, \sigma_{2N}) \setminus I$.

If an additional electron is added to a given configuration I by $\hat{c}_\sigma^\dagger |I\rangle$, the result will be finite only if $\sigma \notin I$. We define the sign function

$$\text{sign}(\sigma, I) \equiv \langle I \cup \sigma | \hat{c}_\sigma^\dagger | I \rangle, \quad (3.1.3)$$

which is 1 (−1) if an even (odd) number of anti-commutations are required in order to move \hat{c}_σ^\dagger to its proper position in the state $|I \cup \sigma\rangle$ and zero if $\sigma \in I$.

The transfer operators $\hat{m}_{I,I'} = |I\rangle\langle I'|$ are expressed as

$$\hat{m}_{I,I'} = \prod_{\sigma \in I} \hat{c}_\sigma^\dagger \prod_{\sigma' \in I'} \hat{c}_{\sigma'} \prod_{\sigma'' \in J} [1 - \hat{n}_{\sigma''}], \quad (3.1.4)$$

with the overall complement $J = \overline{I \cup I'}$. A special case of transfer operators is the projector $\hat{m}_{I,I} = |I\rangle\langle I|$, which is written as

$$\hat{m}_{I,I} = \prod_{\sigma \in I} \hat{n}_\sigma \prod_{\sigma' \notin I} [1 - \hat{n}_{\sigma'}]. \quad (3.1.5)$$

The Fock states $|I\rangle$ provide a basis of the local Hilbert space. The eigenstates $|\Gamma\rangle$ of the local interaction Hamiltonian can be written as

$$|\Gamma\rangle = \sum_I T_{I,\Gamma} |I\rangle, \quad (3.1.6)$$

where the coefficients $T_{I,\Gamma}$ are obtained from a diagonalization of

$$H_{\text{int}}^{I,I'} = \langle I | \hat{H}_{\text{int}} | I' \rangle. \quad (3.1.7)$$

As long as the particle number on each lattice site is conserved by \hat{H}_{int} , we have $T_{I,\Gamma} \sim \delta_{|I|,|\Gamma|}$. The set of local eigenstates $|\Gamma\rangle$ and eigenenergies E_Γ will be used to set up the generalized Gutzwiller correlator in the following sections.

3.2 Multi-Band Gutzwiller Wave Functions

Uncorrelated many-electron systems are described by a product of one-particle states, i.e., a Slater determinant. For example, the ground state of an infinite system is usually described by the non-interacting ‘Fermi sea’ $|\text{FS}\rangle$ defined as

$$|\Phi_0\rangle = |\text{FS}\rangle \equiv \prod_{E_\sigma \leq E_F} \hat{c}_\sigma^\dagger |0\rangle. \quad (3.2.1)$$

For interacting electrons, such a description is insufficient since the local occupancies in $|\Phi_0\rangle$ are independent of the local interaction energies. Nevertheless, product states as defined in Eq. (3.2.1) provide a starting point for a variational approach to interacting electron systems. In the one-orbital model, the interaction energy can be reduced by optimizing variationally the number of doubly occupied lattice sites. A more general approach applicable for multi-orbital Hubbard models has been developed by Bünemann *et al* [6, 7]. The product-state $|\Phi_0\rangle$ is multiplied with the ‘Gutzwiller correlation operator’ \hat{P}_G in order to obtain the Gutzwiller wave function $|\Psi_G\rangle$:

$$|\Psi_G\rangle = \hat{P}_G |\Phi_0\rangle. \quad (3.2.2)$$

The Gutzwiller correlator for multi-band Hubbard models with purely local interactions has the special form

$$\hat{P}_G = \prod_i \hat{P}_{i,G} = \prod_i \sum_{\Gamma \Gamma'} \lambda_{i,\Gamma\Gamma'} |\Gamma\rangle_{ii} \langle \Gamma'|. \quad (3.2.3)$$

It is a product of local correlation operators which, on each lattice site \mathbf{R}_i , are set up by the 2^{2N} eigenstates $|\Gamma\rangle_i$ of the local interaction Hamiltonian. The local parameters $\lambda_{i,\Gamma\Gamma'}$ allow for the variation of the weight of the local eigenstates, i.e., of the local electron configurations. The energy expectation value $\langle \Psi_G | \hat{H} | \Psi_G \rangle / \langle \Psi_G | \Psi_G \rangle$ must be minimized with respect to all $\{\lambda_{\Gamma\Gamma'}\}$ in order to obtain the variational ground state.

Throughout this thesis, we work with Hermitian Gutzwiller correlators only, which implies that

$$\lambda_{i,\Gamma\Gamma} = \lambda_{i,\Gamma\Gamma'}^* \quad (3.2.4)$$

must hold for all non-diagonal variational parameters. Due to Eq. (3.2.4), we have to choose the diagonal parameters $\lambda_{i,\Gamma\Gamma}$ to be real. The necessity of non-diagonal and non-Hermitian projectors in the context of symmetry-broken phases has been discussed in [12].

Usually, the interaction Hamiltonian does not change the total number of electrons. Thus, the Gutzwiller wave function should be an eigenstate of

the total electron number operator $\hat{N}_e = \sum_{i,\sigma} \hat{n}_{i,\sigma}$. The disappearance of the commutator $[\hat{P}_G, \hat{N}_e]$ leads to

$$\sum_{\Gamma'} \lambda_{i,\Gamma'} (|\Gamma\rangle - |\Gamma'\rangle) |\Gamma\rangle_{ii} \langle \Gamma'| = 0. \quad (3.2.5)$$

From Eq. (3.2.5) one can conclude that only those variational parameters for states $|\Gamma\rangle$, $|\Gamma'\rangle$ with the same particle number can be finite.

The situation is different if one deals with superconducting systems. One then usually chooses $|\Phi_0\rangle$ as an BCS ground state instead of a non-interacting Fermi sea. As we are not interested in superconductivity in this thesis, we refer the reader to the literature [60].

Finally we state that, in the following, expectation values with respect to $|\Psi_G\rangle$ will be denoted as ‘correlated’ expectation values while those with respect to $|\Phi_0\rangle$ will be denoted as ‘uncorrelated’ expectation values.

3.3 Limit of Infinite Spatial Dimensions

In general, Gutzwiller wave functions cannot be evaluated without approximations. Analytically exact results were derived for the single-band Hubbard model in one dimension [1], that are in good agreement with the exact solution. Another strategy to evaluate Gutzwiller wave functions is based on combinatorial counting arguments [11, 61, 62] known as the ‘Gutzwiller approximation’.

Gutzwiller wave functions can be evaluated exactly in the limit of infinite spatial dimensions. The exact solvability in this limit originates from the fact that all expectation values turn out to be purely local. Metzner and Vollhard proved that the evaluation of Gutzwiller wave functions in the limit of infinite spatial dimensions yields the same results as the GA [63] for paramagnetic systems. Corrections for finite-dimensional systems can be obtained by an expansion of expectation values with respect to the inverse of the dimensionality D . The resulting corrections are small [8, 63, 64, 65] and the limit of infinite spatial dimensions turns out to be a good starting point for the investigation of finite-dimensional systems.

As pointed out in the introduction, the single-band Hubbard model can also be evaluated within the mean-field approximation of the slave-boson formalism. Both the variational approach and the slave-boson formalism have been generalized to multi-band systems [31, 7] and the equivalence of both approaches has been proved [36].

In this section, we summarize the results of the diagrammatic approach for multi-band Hubbard models as reported in [7]. The limit $D \rightarrow \infty$ affects

both the kinetic and interaction energy, i.e., both \hat{H}_0 and \hat{H}_{int} , and both will be investigated separately. Furthermore, it leads to a set of constraints that the local variational parameters have to obey and that will be discussed.

3.3.1 Local Constraints

The $D \rightarrow \infty$ -limit leads to a set of physical constraints that the local variational parameters $\lambda_{i,\Gamma'}$ have to obey on each lattice site [7]. These are

$$1 = \langle \hat{P}_i^\dagger \hat{P}_i \rangle_{\Phi_0} \quad (3.3.1)$$

$$C_{i,\sigma\sigma'}^0 = \langle \hat{c}_{i,\sigma}^\dagger \hat{P}_i^\dagger \hat{P}_i \hat{c}_{i,\sigma'} \rangle_{\Phi_0}. \quad (3.3.2)$$

Within this subsection, we re-introduced the lattice site index i in order to emphasize the local character of Eqs. (3.3.1) and (3.3.2). Using the expansion of \hat{P}_i from Eq. (3.5.1), the constraints can be explicitly written as

$$1 = \sum_{\Gamma_1\Gamma_2} \lambda_{i,\Gamma_1}^* \lambda_{i,\Gamma_2} m_{\Gamma_1,\Gamma_2}^0 \quad (3.3.3)$$

$$C_{i,\sigma\sigma'}^0 = \sum_{\substack{\Gamma_1\Gamma_2\Gamma_3 \\ \Gamma_1\Gamma_2\Gamma_3}} \lambda_{i,\Gamma_2\Gamma_1}^* \lambda_{i,\Gamma_2\Gamma_3} \langle \Gamma | \hat{c}_\sigma^\dagger | \Gamma_1 \rangle \times \langle \Gamma_3 | \hat{c}_{\sigma'} | \Gamma' \rangle m_{\Gamma,\Gamma'}^0. \quad (3.3.4)$$

One must not conclude from Eq. (3.3.2) that the correlated and the uncorrelated local density matrix have to coincide. In particular, the occupancy of orbitals in the correlated local density matrix

$$C_{i,\sigma\sigma'}^c = \langle \hat{c}_{i,\sigma}^\dagger \hat{c}_{i,\sigma'} \rangle_{\Psi_G} = \frac{\langle \hat{P}_G^\dagger \hat{c}_{i,\sigma}^\dagger \hat{c}_{i,\sigma'} \hat{P}_G \rangle_{\Phi_0}}{\langle \hat{P}_G^\dagger \hat{P}_G \rangle_{\Phi_0}} \quad (3.3.5)$$

may be different from the uncorrelated local density matrix. Nevertheless, as long as the Gutzwiller correlator \hat{P}_G commutes with the total number operator $\hat{N}_e = \sum_{i,\sigma} \hat{n}_{i,\sigma}$, the total numbers of electrons in $|\Phi_0\rangle$ and $|\Psi_G\rangle$ are the same

$$N_e = \sum_{i,\sigma} \langle \hat{n}_{i,\sigma} \rangle_{\Psi_G} = \sum_{i,\sigma} \langle \hat{n}_{i,\sigma} \rangle_{\Phi_0}. \quad (3.3.6)$$

A detailed study of the diagrammatic evaluation of expectation values in infinite spatial dimensions has been published in [6]. The main result is that expectation values of local and non-local operators \hat{O}_i and $\hat{O}_{ij} = \hat{c}_{i\sigma}^\dagger \hat{c}_{j\sigma'}$, respectively, are simplified to

$$\begin{aligned} \langle \hat{O}_i \rangle_{\Psi_G} &= \frac{\langle \Phi_0 | \hat{P}_G^\dagger \hat{O}_i \hat{P}_G | \Phi_0 \rangle}{\langle \Phi_0 | \hat{P}_G^\dagger \hat{P}_G | \Phi_0 \rangle} = \frac{\langle \Phi_0 | \prod_{m \neq i} \hat{P}_m^\dagger \hat{P}_m [\hat{P}_i^\dagger \hat{O}_i \hat{P}_i] | \Phi_0 \rangle}{\langle \Phi_0 | \prod_m \hat{P}_m^\dagger \hat{P}_m | \Phi_0 \rangle} \\ &\stackrel{D \rightarrow \infty}{=} \langle \Phi_0 | \hat{P}_i^\dagger \hat{O}_i \hat{P}_i | \Phi_0 \rangle \end{aligned} \quad (3.3.7)$$

and

$$\begin{aligned} \langle \hat{O}_{ij} \rangle_{\Psi_G} &= \frac{\langle \Phi_0 | \hat{P}_G^\dagger \hat{O}_{ij} \hat{P}_G | \Phi_0 \rangle}{\langle \Phi_0 | \hat{P}_G^\dagger \hat{P}_G | \Phi_0 \rangle} = \frac{\langle \Phi_0 | \prod_{m \neq i,j} \hat{P}_m^\dagger \hat{P}_m [\hat{P}_i^\dagger \hat{P}_j^\dagger \hat{O}_{ij} \hat{P}_j \hat{P}_i] | \Phi_0 \rangle}{\langle \Phi_0 | \prod_m \hat{P}_m^\dagger \hat{P}_m | \Phi_0 \rangle} \\ &\stackrel{D \rightarrow \infty}{\equiv} \langle \Phi_0 | \hat{P}_i^\dagger \hat{P}_j^\dagger \hat{O}_{ij} \hat{P}_j \hat{P}_i | \Phi_0 \rangle, \end{aligned} \quad (3.3.8)$$

respectively, if the constraints (3.3.1) and (3.3.2) are taken into account. Note that the local Gutzwiller correlators \hat{P}_i and \hat{P}_j always commute for $i \neq j$ (cf., Eq. (3.1.4) in combination with Eq. (3.2.5)), which leads to the simplification in the numerator of Eqs. (3.3.7) and (3.3.8). Equation (3.3.7) holds for both one- and two-particle local operators while Eq. (3.3.8) is valid for non-local one-particle operators only.

3.3.2 Local Energy

Due to the local character of the interaction energy, one can diagonalize \hat{H}_{int} in Eq. (2.4.3) on each lattice site,

$$\hat{H}_{i,\text{int}} |\Gamma\rangle_i = E_{\Gamma_i}^{\text{loc}} |\Gamma\rangle_i, \quad (3.3.9)$$

which yields the eigenstates $|\Gamma\rangle_i$ and eigenenergies $E_{\Gamma_i}^{\text{loc}}$. We drop the lattice site index i in the following. For the expectation value E_{loc} of the interaction energy with respect to the Gutzwiller trial wave function $|\Psi_G\rangle$ we find

$$\begin{aligned} \langle \hat{H}_{\text{int}} \rangle_{\Psi_G} &\equiv E^{\text{loc}} = \frac{\langle \Psi_G | \hat{H}_{\text{int}} | \Psi_G \rangle}{\langle \Psi_G | \Psi_G \rangle} = \frac{\langle \Phi_0 | \hat{P}_G^\dagger \hat{H}_{\text{int}} \hat{P}_G | \Phi_0 \rangle}{\langle \Phi_0 | \hat{P}_G^\dagger \hat{P}_G | \Phi_0 \rangle} \\ &\stackrel{D \rightarrow \infty}{\equiv} \sum_{\Gamma} E_{\Gamma}^{\text{loc}} \langle \hat{m}_{\Gamma,\Gamma} \rangle_{\Psi_G}, \end{aligned} \quad (3.3.10)$$

where the expectation value of the transfer operators

$$\langle \hat{m}_{\Gamma,\Gamma'} \rangle_{\Psi_G} = \sum_{\tilde{\Gamma}\tilde{\Gamma}'} \lambda_{\tilde{\Gamma}\tilde{\Gamma}'}^* \lambda_{\Gamma\tilde{\Gamma}'} m_{\tilde{\Gamma}\tilde{\Gamma}'}^0, \quad (3.3.11)$$

is a weighted sum of the uncorrelated expectation values $m_{\tilde{\Gamma}\tilde{\Gamma}'}^0 = \langle \hat{m}_{\tilde{\Gamma}\tilde{\Gamma}'} \rangle_{\Phi_0}$. The states $|\Gamma\rangle$ are set up by the Fock states $|I\rangle$ via a unitary transformation

$$|\Gamma\rangle = \sum_I T_{I,\Gamma} |I\rangle, \quad (3.3.12)$$

which allows us to express $m_{\tilde{\Gamma}\tilde{\Gamma}'}^0$ as

$$m_{\tilde{\Gamma}\tilde{\Gamma}'}^0 = \sum_{II'} T_{I,\tilde{\Gamma}} T_{I',\tilde{\Gamma}'}^* m_{II'}^0, \quad (3.3.13)$$

my means of the uncorrelated expectation values of the transfer operators $m_{I,I'}^0 = \langle |I\rangle\langle I'| \rangle_{\Phi_0}$. Using the uncorrelated local density-matrix elements

$$C_{i,\sigma\sigma'}^0 = \langle \hat{c}_{i,\sigma}^\dagger \hat{c}_{i,\sigma'} \rangle_{\Phi_0}, \quad (3.3.14)$$

the expectation value $m_{I,I'}^0$ can be written as

$$m_{I,I'}^0 = \begin{vmatrix} \tilde{\Omega}^{I,I'} & -\tilde{\Omega}^{I,J} \\ \tilde{\Omega}^{J,I'} & \tilde{\Omega}^{J,J} \end{vmatrix}, \quad (3.3.15)$$

with the matrices $\tilde{\Omega}^{I,I'}$ defined as

$$\tilde{\Omega}^{I,I'} = \begin{pmatrix} C_{\sigma_1\sigma'_1}^0 & C_{\sigma_1\sigma'_2}^0 & \cdots & C_{\sigma_1\sigma'_{|I'|}}^0 \\ C_{\sigma_2\sigma'_1}^0 & C_{\sigma_2\sigma'_2}^0 & \cdots & C_{\sigma_2\sigma'_{|I'|}}^0 \\ \vdots & \vdots & \ddots & \vdots \\ C_{\sigma_{|I|}\sigma'_1}^0 & C_{\sigma_{|I|}\sigma'_2}^0 & \cdots & C_{\sigma_{|I|}\sigma'_{|I'|}}^0 \end{pmatrix} \quad (3.3.16)$$

for the electronic configurations $I = (\sigma_1, \dots, \sigma_{|I|})$ and $I' = (\sigma'_1, \dots, \sigma'_{|I'|})$, respectively, and

$$\tilde{\Omega}^{J,J} = \begin{pmatrix} 1 - C_{\sigma_1\sigma_1}^0 & -C_{\sigma_1\sigma_2}^0 & \cdots & -C_{\sigma_1\sigma_{|J|}}^0 \\ -C_{\sigma_2\sigma_1}^0 & 1 - C_{\sigma_2\sigma_2}^0 & \cdots & -C_{\sigma_2\sigma_{|J|}}^0 \\ \vdots & \vdots & \ddots & \vdots \\ -C_{\sigma_{|J|}\sigma_1}^0 & -C_{\sigma_{|J|}\sigma_2}^0 & \cdots & 1 - C_{\sigma_{|J|}\sigma_{|J|}}^0 \end{pmatrix} \quad (3.3.17)$$

for states $\sigma_\alpha \in J \equiv \overline{I \cup I'}$.

3.3.3 Kinetic Energy

As sketched in Eq. (3.3.8), hopping expectation values factorize according to

$$\langle \hat{c}_{i,\sigma_1}^\dagger \hat{c}_{j,\sigma_2} \rangle_{\Psi_G} \stackrel{D \rightarrow \infty}{\equiv} \langle [\hat{P}_i^\dagger \hat{c}_{i,\sigma_2}^\dagger \hat{P}_i] [\hat{P}_j^\dagger \hat{c}_{j,\sigma_2} \hat{P}_j] \rangle_{\Phi_0} \quad (3.3.18)$$

in infinite spatial dimensions. This leads to the expression

$$\langle \hat{c}_{i,\sigma_1}^\dagger \hat{c}_{j,\sigma_2} \rangle_{\Psi_G} = \sum_{\sigma'_1\sigma'_2} q_{i,\sigma_1}^{\sigma'_1} [q_{j,\sigma_2}^{\sigma'_2}]^* \langle \hat{c}_{i,\sigma'_1}^\dagger \hat{c}_{j,\sigma'_2} \rangle_{\Phi_0}, \quad (3.3.19)$$

where the ‘renormalization matrix’ $q_\sigma^{\sigma'}$ with

$$q_\sigma^{\sigma'} = \sum_{\substack{\Gamma_1\Gamma_2 \\ \Gamma_3\Gamma_4}} \lambda_{\Gamma_2\Gamma_1}^* \lambda_{\Gamma_3\Gamma_4} \langle \Gamma_2 | \hat{c}_\sigma^\dagger | \Gamma_3 \rangle \sum_{I_1 I_4} T_{I_1, \Gamma_1} T_{I_4, \Gamma_4}^* H_{I_1, I_4}^{\sigma'} \quad (3.3.20)$$

was introduced. The matrix $\tilde{H}^{\sigma'}$ contains three different contributions depending on whether the index σ' is an element of $I_1 \cap I_4$, $I_4 \setminus (I_1 \cap I_4)$ or $\overline{I_1 \cup I_4}$. $\tilde{H}^{\sigma'}$ can be written as

$$H_{I_1, I_4}^{\sigma'} = (1 - f_{\sigma', I_1}) \langle I_4 | \hat{c}_{\sigma'} | I_4 \cup \sigma' \rangle m_{I_1, I_4 \cup \sigma'}^0 + \langle I_1 \setminus \sigma' | \hat{c}_{\sigma'} | I_1 \rangle \left[f_{\sigma', I_4} m_{I_1 \setminus \sigma', I_4}^0 + (1 - f_{\sigma', I_4}) m_{I_1 \setminus \sigma', I_4}^{0; \sigma'} \right], \quad (3.3.21)$$

with the abbreviation $f_{\sigma, I} \equiv \langle I | \hat{c}_{\sigma}^{\dagger} \hat{c}_{\sigma} | I \rangle$. The expectation value $m_{I_1 \setminus \sigma', I_4}^{0; \sigma'}$ is determined from Eq. (3.3.15), except that the subset J has to be replaced by $J \setminus \sigma'$.

For homogeneous systems, the expectation value of the kinetic energy can explicitly written as

$$\langle \hat{H}_0 \rangle_{\Psi_G} = N_s \sum_{\substack{\sigma_1 \sigma_2 \\ \sigma_1' \sigma_2'}} q_{\sigma_1}^{\sigma_1'} [q_{\sigma_2}^{\sigma_2'}]^* E_{\sigma_1 \sigma_2, \sigma_1' \sigma_2'}, \quad (3.3.22)$$

where we used Eq. (3.3.19) and introduced the tensor

$$E_{\sigma_1 \sigma_2, \sigma_1' \sigma_2'} = \frac{1}{N_s} \sum_{i \neq j} t_{ij}^{\sigma_1 \sigma_2} \langle \hat{c}_{i, \sigma_1}^{\dagger} \hat{c}_{j, \sigma_2} \rangle_{\Phi_0}, \quad (3.3.23)$$

whose elements are the expectation value of the kinetic energy for the uncorrelated system.

3.4 Energy Functional in Infinite Dimensions

We summarize the results of the previous section that lead to the expression for the Gutzwiller energy functional. We sketch how its minimization (adopted from [66]) yields both the ground-state energy and an effective one-particle Gutzwiller Hamiltonian whose eigenenergies will be interpreted as quasi-particle energies in the TDGA in Chapters 5 and 6.

The correlated expectation value $\langle \hat{H} \rangle_{\Psi_G}$ can be split into the kinetic energy and the local interaction energy:

$$E^{\text{GA}} \equiv \langle \hat{H} \rangle_{\Psi_G} = \langle \hat{H}_0 \rangle_{\Psi_G} + \langle \hat{H}_{\text{int}} \rangle_{\Psi_G} = E_0(\{\tilde{\lambda}_i\}, \{\tilde{C}_i^0\}, |\Phi_0\rangle) + \sum_i E_i^{\text{loc}}(\tilde{\lambda}_i, \tilde{C}_i^0). \quad (3.4.1)$$

Both the kinetic and the interaction energy are functionals of the variational parameter matrices $\tilde{\lambda}$ and the uncorrelated local density matrix \tilde{C}^0 , where

the kinetic energy

$$\begin{aligned} E_0(\{\tilde{\lambda}_i\}, \{\tilde{C}_i^0\}, |\Phi_0\rangle) &= \sum_{i \neq j} \sum_{\substack{\sigma_1 \sigma_2 \\ \sigma'_1 \sigma'_2}} t_{ij}^{\sigma_1 \sigma_2} q_{i, \sigma_1}^{\sigma'_1} [q_{j, \sigma_2}^{\sigma'_2}]^* \langle \hat{c}_{i, \sigma'_1}^\dagger \hat{c}_{j, \sigma'_2} \rangle_{\Phi_0} \\ &= \sum_{i \neq j} \sum_{\sigma \sigma'} \tilde{t}_{ij}^{\sigma \sigma'} \langle \hat{c}_{i, \sigma}^\dagger \hat{c}_{j, \sigma'} \rangle_{\Phi_0} \end{aligned} \quad (3.4.2)$$

is additionally a functional of the uncorrelated one-particle wave function $|\Phi_0\rangle$. In the second line of Eq. (3.4.2) the abbreviation

$$\tilde{t}_{ij}^{\sigma \sigma'} = \sum_{\sigma_1 \sigma_2} t_{ij}^{\sigma_1 \sigma_2} q_{i, \sigma_1}^{\sigma} [q_{j, \sigma_2}^{\sigma'}]^* \quad (3.4.3)$$

for the effective hopping-parameter matrix elements has been introduced.

The variational ground-state energy is found by minimizing E^{GA} with respect to all variational parameters $\{\tilde{\lambda}\}$ and the one-particle states $|\Phi_0\rangle$, where the n_c constraints (3.3.1) and (3.3.2) must be fulfilled. As this section is meant to treat the Gutzwiller scheme on a formal level, we assume from now on—without loss of generality—that the constraints are fulfilled explicitly, i.e., we assume that we can resolve the constraints and eliminate n_c *dependent* variational parameters and are left with $n_{\text{par}} - n_c$ *independent* variational parameters $\lambda_{i, \Gamma \Gamma'}^i$.

When one minimizes the energy with respect to the one-particle states $|\Phi_0\rangle$, the additional constraints

$$1 = \langle \Phi_0 | \Phi_0 \rangle \quad (3.4.4)$$

$$C_{\sigma \sigma'}^0 = \langle \hat{c}_{\sigma}^\dagger \hat{c}_{\sigma'} \rangle_{\Phi_0} \quad (3.4.5)$$

$$N_e = \sum_{i, \sigma} \langle \hat{n}_{i, \sigma} \rangle_{\Phi_0} \quad (3.4.6)$$

have to be fulfilled. For the last two constraints, see Eqs. (3.3.6) and (3.3.14). The constraints are taken into account by Lagrange multipliers E^{SP} , $\eta_{i, \sigma \sigma'}$ and E_{F} , respectively. The resulting constricted energy functional E_c then reads

$$\begin{aligned} E_c(\{\tilde{\lambda}_i^i\}, \{\tilde{C}_i^0\}, |\Phi_0\rangle, E^{\text{SP}}, \{\tilde{\eta}_i\}, E_{\text{F}}) \\ = E^{\text{GA}}(\{\tilde{\lambda}_i^i\}, \{\tilde{C}_i^0\}, |\Phi_0\rangle) - E^{\text{SP}}[\langle \Phi_0 | \Phi_0 \rangle - 1] + \\ + \sum_{i, \sigma \sigma'} \eta_{i, \sigma \sigma'} [C_{i, \sigma \sigma'}^0 - \langle \Phi_0 | \hat{c}_{i, \sigma}^\dagger \hat{c}_{i, \sigma'} | \Phi_0 \rangle] + E_{\text{F}} [N_e - \sum_{i, \sigma} \langle \Phi_0 | \hat{c}_{i, \sigma}^\dagger \hat{c}_{i, \sigma} | \Phi_0 \rangle]. \end{aligned} \quad (3.4.7)$$

The variational ground-state energy is then found as the overall minimum

$$E_0^{\text{GA}} = \underset{\substack{\{\tilde{\lambda}_i^i\}, \{\tilde{C}_i^0\}, |\Phi_0\rangle \\ E^{\text{SP}}, \{\tilde{\eta}_i\}, E_{\text{F}}}}{\text{Minimum}} E_c(\{\tilde{\lambda}_i^i\}, \{\tilde{C}_i^0\}, |\Phi_0\rangle, E^{\text{SP}}, \{\tilde{\eta}_i\}, E_{\text{F}}). \quad (3.4.8)$$

As shown in [67], the minimization with respect to $|\Phi_0\rangle$ can be carried out analytically leading to an effective one-particle Schrödinger equation

$$\hat{H}_0^{\text{eff}}|\Phi_0\rangle = E^{\text{SP}}(\{\tilde{\lambda}_i^1\}, \{\tilde{C}_i^0\}, \{\tilde{\eta}_i\})|\Phi_0\rangle, \quad (3.4.9)$$

with the effective one-particle Hamiltonian

$$\hat{H}_0^{\text{eff}} = \sum_{i \neq j} \sum_{\sigma\sigma'} \tilde{t}_{ij}^{\sigma\sigma'} \hat{c}_{i,\sigma'}^\dagger \hat{c}_{j,\sigma'} - \sum_i \sum_{\sigma\sigma'} [\eta_{i,\sigma\sigma'} + \delta_{\sigma\sigma'} E_F] \hat{c}_{i,\sigma}^\dagger \hat{c}_{i,\sigma'}. \quad (3.4.10)$$

For translationally invariant systems, the effective Hamiltonian (3.4.10) has the rather simple form

$$\hat{H}_0^{\text{eff}} = \sum_{\mathbf{k}, \sigma\sigma'} \left[\sum_{\tilde{\sigma}\tilde{\sigma}'} q_{\tilde{\sigma}}^\sigma [q_{\tilde{\sigma}'}^{\sigma'}]^* \varepsilon_{\mathbf{k}}^{\tilde{\sigma}\tilde{\sigma}'} - \eta_{\sigma\sigma'} - \delta_{\sigma\sigma'} E_F \right] \hat{c}_{\mathbf{k},\sigma}^\dagger \hat{c}_{\mathbf{k},\sigma'}, \quad (3.4.11)$$

where the operators $\hat{c}_{\mathbf{k},\sigma}^{(\dagger)}$ and the dispersion relation $\varepsilon_{\mathbf{k}}^{\tilde{\sigma}\tilde{\sigma}'}$ have been defined in Eqs. (2.4.4) and (2.4.5), respectively. The Hamiltonian (3.4.11) can be diagonalized easily by a proper unitary transformation

$$\hat{h}_{\mathbf{k},\gamma}^\dagger = \sum_{\sigma} u_{\gamma,\sigma}(\mathbf{k}) \hat{c}_{\mathbf{k},\sigma}^\dagger, \quad (3.4.12)$$

leading to

$$\hat{H}_0^{\text{eff}} = \sum_{\mathbf{k},\gamma} [E_{\mathbf{k},\gamma} - E_F] \hat{h}_{\mathbf{k},\gamma}^\dagger \hat{h}_{\mathbf{k},\gamma}, \quad (3.4.13)$$

where the eigenenergies $E_{\mathbf{k},\gamma}$ of \hat{H}_0^{eff} and the dispersion relation $\varepsilon_{\mathbf{k}}^{\tilde{\sigma}\tilde{\sigma}'}$ are related through the elements of the transformation matrix \tilde{u} :

$$E_{\mathbf{k},\gamma} = \sum_{\sigma\sigma'} \left[\sum_{\tilde{\sigma}\tilde{\sigma}'} q_{\tilde{\sigma}}^\sigma [q_{\tilde{\sigma}'}^{\sigma'}]^* \varepsilon_{\mathbf{k}}^{\tilde{\sigma}\tilde{\sigma}'} - \eta_{\sigma\sigma'} \right] u_{\gamma,\sigma}(\mathbf{k}) u_{\gamma,\sigma'}^*(\mathbf{k}). \quad (3.4.14)$$

Motivated by the corresponding HF results [68], we assume that $|\Phi_0\rangle$ can be written as

$$|\Phi_0\rangle = \prod_{\substack{\mathbf{k},\gamma \\ E_{\mathbf{k},\gamma} \leq E_F}} \hat{h}_{\mathbf{k},\gamma}^\dagger |0\rangle, \quad (3.4.15)$$

which still is a functional of $\{\tilde{\lambda}_i^1\}$, $\{\tilde{C}_i^0\}$ and $\{\tilde{\eta}_i\}$. The variational ground-state energy is then found as

$$E_0^{\text{GA}} = \text{Minimum}_{\substack{\{\tilde{\lambda}_i^1\}, \{\tilde{C}_i^0\} \\ \{\tilde{\eta}_i\}, E_F}} E_c^{\text{eff}}(\{\tilde{\lambda}_i^1\}, \{\tilde{C}_i^0\}, \{\tilde{\eta}_i\}, E_F) \quad (3.4.16)$$

of the function

$$E_c^{\text{eff}}(\{\tilde{\lambda}_i^i\}, \{\tilde{C}_i^0\}, \{\tilde{\eta}_i\}, E_F) = E^{\text{SP}}(\{\tilde{\lambda}_i^i\}, \{\tilde{C}_i^0\}, \{\tilde{\eta}_i\}) + E^{\text{loc}}(\{\tilde{\lambda}_i^i\}, \{\tilde{C}_i^0\}) + \sum_{i,\sigma\sigma'} \eta_{i,\sigma\sigma'} C_{i,\sigma\sigma'}^0 + E_F N_e. \quad (3.4.17)$$

Up to now, \hat{H}_0^{eff} has been introduced as an auxiliary object without physical counterpart. The effective one-particle Hamiltonian (3.4.10) yields the eigenenergies $E_{\mathbf{k},\gamma}$ that will be interpreted as quasi-particle energies within a Fermi-liquid scheme. \hat{H}_0^{eff} is thus of great importance for both obtaining the variational ground-state energy and deriving the time-dependent theory as well.

Note that the aforementioned scheme has to be seen as a formal treatment only. A more sophisticated algorithm for the minimization with respect to the variational parameters has been developed by Bünemann *et al* and will be published elsewhere [69].

3.5 Examples

In this section, we apply the Gutzwiller theory to the single- and the two-band Hubbard model. With the help of the one-band model, we illustrate the essential steps derived in the previous sections leading to the ground-state energy functional. In case of the two-band model, we decouple the orbitals and prove that in the limit of vanishing inter-orbital correlations the results of the single-band model are reproduced.

3.5.1 The One-Band Hubbard Model and the Brinkman–Rice Transition

We illustrate the Gutzwiller formalism for the one-band Hubbard model. We assume translational invariance and therefore drop the lattice site index i in most expressions. M. C. Gutzwiller proposed a variational approach in order to deal with correlated electron systems [9]. The aim of [9] and the consecutive works [10, 11] was the investigation of ferromagnetism in the single-band Hubbard model. The ansatz is based on the picture that hopping processes between two lattice sites become more and more improbable with increasing on-site interaction if the site is already occupied by an electron of opposite spin.

Starting from a single-particle product state $|\Phi_0\rangle$, the number of doubly occupied sites is $N_d = \langle \Phi_0 | \sum_i \hat{n}_{i,\uparrow} \hat{n}_{i,\downarrow} | \Phi_0 \rangle$, each one contributing the energy

U . Gutzwiller introduced a local variational parameter g_i to reduce the weight of doubly occupied sites in a Slater determinant by means of the Gutzwiller correlator

$$\hat{P}_G^{1b} = \prod_i [1 - (1 - g_i) \hat{n}_{i,\uparrow} \hat{n}_{i,\downarrow}] \quad (3.5.1)$$

acting on the uncorrelated ground state:

$$|\Psi_G\rangle = \hat{P}_G^{1b} |\Phi_0\rangle. \quad (3.5.2)$$

The local variational parameters $g_i \in [0, 1]$ adjust the weight of the local double occupancies. For $g_i \equiv 0$, the Gutzwiller correlator \hat{P}_G^{1b} is the projector onto the subspace without any double occupancies that already appeared in the $t - J$ -model. The Gutzwiller wave function $|\Psi_G\rangle$ allows for the interpolation between the two limiting cases of uncorrelated electrons ($U \rightarrow 0$ and $g = 1$) and the atomic limit ($t \rightarrow 0$ and $g = 0$) describing isolated atoms. The energy expectation value must be varied with respect to all g_i to obtain the variational ground-state energy, i.e., an upper bound for the exact ground-state energy.

The correlator \hat{P}_G^{1b} (3.5.1) focusses on the doubly occupied state and its energy contribution U . One can set up a more symmetric correlator based on the whole set of local eigenstates as

$$\hat{P}_G = \prod_i \hat{P}_{i,G} = \prod_i \sum_{\Gamma'} \lambda_{i,\Gamma'} |\Gamma\rangle_{ii} \langle \Gamma'|, \quad (3.5.3)$$

allowing to vary the weight of *all* local eigenstates $|\Gamma_i\rangle$ by means of the elements of a local variational parameter matrix $\tilde{\lambda}_{i,\Gamma'}$. For the one-band model, the local correlator reads

$$\begin{aligned} \hat{P}_{i,G}^{1b} = & \lambda_{i,o} |\circ\rangle_{ii} \langle \circ| + \lambda_{i,\uparrow} |\uparrow\rangle_{ii} \langle \uparrow| + \lambda_{i,\uparrow\downarrow} |\uparrow\downarrow\rangle_{ii} \langle \uparrow\downarrow| + \\ & + \lambda_{i,\downarrow\uparrow} |\downarrow\uparrow\rangle_{ii} \langle \downarrow\uparrow| + \lambda_{i,\downarrow} |\downarrow\rangle_{ii} \langle \downarrow| + \lambda_{i,d} |\uparrow\downarrow\rangle_{ii} \langle \uparrow\downarrow|, \end{aligned} \quad (3.5.4)$$

which is the most general ansatz for the one-band correlator for systems without superconductivity. Superconductivity would lead to contributions $\sim |\circ\rangle_{ii} \langle \uparrow\downarrow|$ and $|\uparrow\downarrow\rangle_{ii} \langle \circ|$ in Eq. (3.5.4). It has been proven that both correlators (3.5.1) and (3.5.3) define the same variational space [70].

The interaction Hamiltonian reads

$$\hat{H}_{\text{int}}^{1b} = U \sum_i \hat{n}_{i,\uparrow} \hat{n}_{i,\downarrow} = U \sum_i |\uparrow\downarrow\rangle_{ii} \langle \uparrow\downarrow| \quad (3.5.5)$$

and leads to the four local eigenstates $|\circ\rangle_i$, $|\uparrow\rangle_i$, $|\downarrow\rangle_i$ and $|\uparrow\downarrow\rangle_i$. The most general local density matrix

$$\tilde{C}^0 = \begin{pmatrix} \langle \hat{c}_\uparrow^\dagger \hat{c}_\uparrow \rangle_{\Phi_0} & \langle \hat{c}_\uparrow^\dagger \hat{c}_\downarrow \rangle_{\Phi_0} \\ \langle \hat{c}_\downarrow^\dagger \hat{c}_\uparrow \rangle_{\Phi_0} & \langle \hat{c}_\downarrow^\dagger \hat{c}_\downarrow \rangle_{\Phi_0} \end{pmatrix} = \begin{pmatrix} n_\uparrow^0 & \Delta_{\uparrow\downarrow}^0 \\ \Delta_{\downarrow\uparrow}^0 & n_\downarrow^0 \end{pmatrix} \quad (3.5.6)$$

with $\Delta_{\downarrow\uparrow}^0 = [\Delta_{\uparrow\downarrow}^0]^* \equiv \Delta^0$ and the one-band Gutzwiller correlator (3.5.4) lead to the uncorrelated expectation values

$$m_o^0 = [1 - n_{\uparrow}^0][1 - n_{\downarrow}^0] - |\Delta^0|^2 \quad (3.5.7)$$

$$m_s^0 = n_s^0[1 - n_{\bar{s}}^0] + |\Delta^0|^2 \quad (3.5.8)$$

$$m_{s\bar{s}}^0 = \Delta_{s\bar{s}}^0 \quad (3.5.9)$$

$$m_d^0 = n_{\uparrow}^0 n_{\downarrow}^0 - |\Delta^0|^2 \quad (3.5.10)$$

of transfer operators. The interaction energy E^{loc} thus reads

$$E^{\text{loc}} = \sum_i U \langle |\uparrow\downarrow\rangle_{ii} \langle \uparrow\downarrow| \rangle_{\Phi_G} = N_s U |\lambda_d|^2 m_d^0. \quad (3.5.11)$$

The evaluation of Eq. (3.3.20) yields the explicit expressions

$$q_s^s = \lambda_s^* \lambda_o [1 - n_{\bar{s}}^0] + \lambda_d^* \lambda_{\bar{s}} n_{\bar{s}}^0 + [\lambda_d^* \lambda_{\bar{s}s} + \lambda_{s\bar{s}}^* \lambda_o] \Delta_{s\bar{s}}^0 \quad (3.5.12)$$

$$q_{\bar{s}}^{\bar{s}} = [\lambda_s^* \lambda_o - \lambda_d^* \lambda_{\bar{s}}] \Delta_{s\bar{s}}^0 \quad (3.5.13)$$

for the elements of the renormalization matrix. The constraints concerning the variational parameters are given by the expressions

$$1 = |\lambda_o|^2 m_o^0 + |\lambda_d|^2 + [|\lambda_{\uparrow}|^2 + |\lambda_{\uparrow\downarrow}|^2] m_{\uparrow}^0 + [|\lambda_{\downarrow}|^2 + |\lambda_{\uparrow\downarrow}|^2] m_{\downarrow}^0 \quad (3.5.14)$$

$$n_s^0 = [|\lambda_{\bar{s}}|^2 + |\lambda_{s\bar{s}}|^2] m_d^0 + |\lambda_o|^2 m_s^0 \quad (3.5.15)$$

$$\Delta_{s\bar{s}}^0 = -[\lambda_{s\bar{s}}^* \lambda_s + \lambda_{\bar{s}}^* \lambda_{\bar{s}s}] m_d^0 + |\lambda_o|^2 \Delta_{s\bar{s}}^0. \quad (3.5.16)$$

As we are free in the choice of the local basis, we can diagonalize \tilde{C}^0 via the unitary transformation

$$\hat{h}_{\gamma}^{\dagger} = \sum_s u_{s,\gamma} \hat{c}_s^{\dagger}, \quad (3.5.17)$$

leading to

$$\tilde{C}_h^0 = \begin{pmatrix} \langle \hat{h}_1^{\dagger} \hat{h}_1 \rangle_{\Phi_0} & \langle \hat{h}_1^{\dagger} \hat{h}_2 \rangle_{\Phi_0} \\ \langle \hat{h}_2^{\dagger} \hat{h}_1 \rangle_{\Phi_0} & \langle \hat{h}_2^{\dagger} \hat{h}_2 \rangle_{\Phi_0} \end{pmatrix} \equiv \begin{pmatrix} \tilde{n}_1^0 & 0 \\ 0 & \tilde{n}_2^0 \end{pmatrix}. \quad (3.5.18)$$

With the diagonal local density matrix, the transfer operators are written as

$$\tilde{m}_o = \tilde{\lambda}_o^2 m_o^0 = 1 - \tilde{n}_1^0 - \tilde{n}_2^0 + \tilde{m}_d \quad (3.5.19)$$

$$\tilde{m}_{\gamma} = \tilde{\lambda}_{\gamma}^2 m_{\gamma}^0 = \tilde{n}_{\gamma}^0 - \tilde{m}_d \quad (3.5.20)$$

$$\tilde{m}_d = \tilde{\lambda}_d^2 m_d^0. \quad (3.5.21)$$

The renormalization matrix becomes diagonal and has the well-known form [9, 10, 11]

$$q_{\gamma}^{\gamma} = \tilde{\lambda}_o \tilde{\lambda}_{\gamma} [1 - \tilde{n}_{\gamma}^0] + \tilde{\lambda}_d \tilde{\lambda}_{\gamma} \tilde{n}_{\gamma}^0 = \frac{1}{\sqrt{\tilde{n}_{\gamma}^0 [1 - \tilde{n}_{\gamma}^0]}} \left[\sqrt{\tilde{m}_o \tilde{m}_{\gamma}} + \sqrt{\tilde{m}_d \tilde{m}_{\bar{\gamma}}} \right]. \quad (3.5.22)$$

Finally, the constraints concerning the completeness and the local occupation numbers are expressed as

$$1 = \tilde{\lambda}_0^2 m_0^0 + \tilde{\lambda}_1^2 m_1^0 + \tilde{\lambda}_2^2 m_2^0 + \tilde{\lambda}_d^2 m_d^0 \quad (3.5.23)$$

$$\tilde{n}_\gamma^0 = \tilde{\lambda}_\gamma^2 m_\gamma^0 + \tilde{\lambda}_d^2 m_d^0, \quad (3.5.24)$$

while the constraints for the previously off-diagonal elements $\Delta_{s\bar{s}}^0$ are automatically fulfilled if the Gutzwiller correlator in the new basis $\hat{h}_\gamma^{(\dagger)}$ contains only diagonal variational parameters, i.e., $\tilde{\lambda}_{\gamma\bar{\gamma}} = 0$. Consequently, all variational parameters $\tilde{\lambda}_{\Gamma\bar{\Gamma}}$, and renormalization factors q_γ^\dagger are real.

For a given diagonal local density matrix \tilde{C}_h^0 , the minimization of the energy functional

$$E_{1b}^{\text{GA}} = \sum_{i \neq j} \sum_{\gamma} [q_\gamma^\dagger]^2 t_{ij} \langle \hat{h}_{i,\gamma}^\dagger \hat{h}_{j,\gamma} \rangle_{\Phi_0} + N_s U \tilde{m}_d \quad (3.5.25)$$

with respect to \tilde{m}_d can be carried out analytically.

We define the uncorrelated ground-state energy ϵ_0 per lattice site as

$$\bar{\epsilon} = \frac{1}{N_s} \sum_{i \neq j} \sum_{\gamma} t_{ij} \langle \hat{h}_{i,\gamma}^\dagger \hat{h}_{j,\gamma} \rangle_{\Phi_0} = \frac{1}{N_s} \sum_{\mathbf{k}} \epsilon_{\mathbf{k}} \langle \hat{n}_{\mathbf{k}} \rangle_{\Phi_0} = \frac{2}{N_s} \sum_{\mathbf{k}} \epsilon_{\mathbf{k}} \Theta[E_F - \epsilon_{\mathbf{k}}]. \quad (3.5.26)$$

Especially for a half-filled paramagnet, i.e., $\tilde{n}_1^0 = \tilde{n}_2^0 \equiv \frac{1}{2}$, we express the ground-state energy per lattice site (3.5.25) as

$$\bar{\epsilon}_{1b}^{\text{GA}} = 8[1 - 2\tilde{m}_d] \tilde{m}_d \bar{\epsilon} + U \tilde{m}_d, \quad (3.5.27)$$

whose minimization with respect to \tilde{m}_d leads to

$$[q_\gamma^\dagger]^2 = 1 - \left[\frac{U}{U_{\text{BR}}} \right]^2 \quad (3.5.28)$$

and

$$\tilde{m}_d = \frac{1}{4} \left[1 - \frac{U}{U_{\text{BR}}} \right], \quad (3.5.29)$$

with the critical interaction strength $U_{\text{BR}} = 8|\bar{\epsilon}|$. From Eq.(3.5.21) we conclude that the variational parameter $\tilde{\lambda}_d$ vanishes if U approaches U_{BR} from below. The average number of doubly occupied sites in $|\Psi_G\rangle$ tends to zero. Consequently, the renormalization factors also decrease and the system becomes insulating when $U = U_{\text{BR}}$.

For one-dimensional systems, these findings are in contrast to both exact results of the single-band Hubbard model [71] and the exact evaluation of the Gutzwiller-correlated wave function [1, 65]. In Fig.3.5.1 we plot the

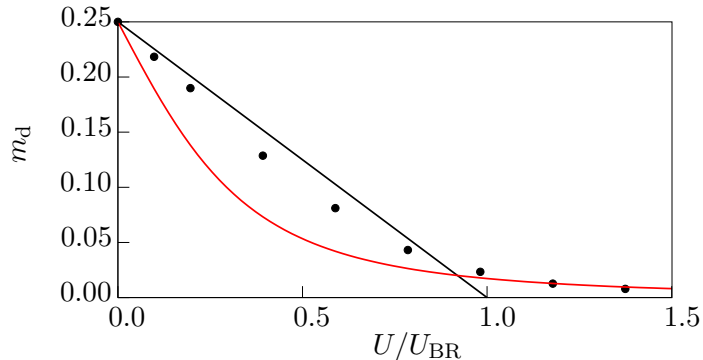


Figure 3.5.1: Mean double occupancy m_d for the one-dimensional single-band Hubbard model as a function of the on-site interaction U for a half-filled paramagnet ($n_\uparrow = n_\downarrow = \frac{1}{2}$). The circles mark the exact result in the thermodynamic limit ($N_s \rightarrow \infty$) while the solid lines are the results obtained within the GA (black) and of the two-site model (red). The exact results are excerpt from [65].

average number of doubly occupied sites of the one-dimensional single-band Hubbard model. We recognize that the linear decrease of \tilde{m}_d with increasing U reproduces the results from the exact evaluation of the Gutzwiller wave function for U up to $U \approx 0.8U_{BR}$ quantitatively well. For larger values of U , the exact evaluation of the Gutzwiller wave function yields a finite number of doubly occupied sites. For comparison, we also plot the mean double occupancy of the exact solution of the two-site model of the half-filled one-band Hubbard model, see Appendix A.1.

Brinkman and Rice predicted that, within the GA, this localization transition will occur for half-filled systems in arbitrary spatial dimensions [72]. In [73] it was shown that the Brinkman–Rice (BR) transition is an artefact of the limit of infinite spatial dimensions. Hence, corrections in leading order of $\frac{1}{D}$ may yield quantitatively better results [65], but the BR transition cannot be overcome by finite-order corrections in $\frac{1}{D}$.

The single-band Hubbard model was also applied to inhomogeneous states. It was shown that the single-band Hubbard model within the slave-boson mean-field formalism possesses solutions with various inhomogeneous solutions like spin polarons, domain walls [37] and vortex-antivortex and Skyrmion structures [29]. Later, the time-dependent generalization of the slave-boson formalism was applied in order to investigate the dynamic properties of inhomogeneous superconductors [30, 39, 42, 43, 44].

3.5.2 Two Decoupled Orbitals

The one-band Hubbard model has been extensively studied both within the Gutzwiller variational approach and the time-dependent Gutzwiller theory. It is therefore interesting to check to what extent the numerous one-band results are reproduced by the multi-band Gutzwiller scheme. In order to address this question, we consider the Hubbard model with two completely decoupled orbitals per lattice site. We talk about ‘decoupled’ orbitals if *both* the one-particle Hamiltonian \hat{H}_0 and the local interaction Hamiltonian \hat{H}_{int} are ‘orbital-diagonal’ in the sense that the Hamiltonian can be written as

$$\hat{H}_{\text{dec}}^{2b} = \sum_{b=1}^2 \hat{H}_{\text{dec}}^{2b,b} = \sum_{b=1}^2 \left[\sum_{i \neq j} \sum_{\sigma} t_{ij} \hat{c}_{i,b\sigma}^{\dagger} \hat{c}_{j,b\sigma} + U \sum_i \hat{n}_{i,b\uparrow} \hat{n}_{i,b\downarrow} \right], \quad (3.5.30)$$

where only the intra-orbital Coulomb interaction parameter U remains. We assume an orbital-independent hopping amplitude t_{ij} .

The local density matrix \tilde{C}^0 consists of two block matrices for the two orbitals:

$$\tilde{C}^0 = \begin{pmatrix} n_{1,\uparrow}^0 & \Delta_{1,\uparrow\downarrow}^0 & 0 & 0 \\ \Delta_{1,\uparrow\downarrow}^0 & n_{1,\downarrow}^0 & 0 & 0 \\ 0 & 0 & n_{2,\uparrow}^0 & \Delta_{2,\uparrow\downarrow}^0 \\ 0 & 0 & \Delta_{2,\uparrow\downarrow}^0 & n_{2,\downarrow}^0 \end{pmatrix}. \quad (3.5.31)$$

The atomic two-orbital eigenstates are simple product states

$$|\Gamma\rangle = |\gamma\rangle_1 \otimes |\gamma'\rangle_2 \equiv |\gamma\rangle_1 |\gamma'\rangle_2 \quad (3.5.32)$$

of the one-orbital eigenstates, i.e., $|\gamma^{(l)}\rangle_{1,2} \in \{|\circ\rangle, |\uparrow\rangle, |\downarrow\rangle, |\uparrow\downarrow\rangle\}$.

Due to the block structure of the local density matrix (3.5.31), the uncorrelated expectation values of transfer operators $\hat{m}_{\Gamma,\Gamma'}$ with respect to the two-orbital eigenstates

$$\langle \hat{m}_{\Gamma,\tilde{\Gamma}} \rangle \equiv \langle (|\gamma\rangle_1 |\gamma'\rangle_2) ({}_2\langle \tilde{\gamma}' | {}_1\langle \tilde{\gamma} |) \rangle = \langle |\gamma\rangle_{11} \langle \tilde{\gamma} | \rangle \times \langle |\gamma\rangle_{22} \langle \tilde{\gamma}' | \rangle \quad (3.5.33)$$

can be expressed as the product of two expectation values of one-orbital transfer operators $\hat{m}_{\gamma,\gamma'}$.

The factorization of the atomic eigenstates and the expectation values of transfer operators into the respective one-band quantities suggests the following decomposition for the elements of the Gutzwiller correlator (3.5.1):

$$\begin{aligned} \lambda_{\Gamma\tilde{\Gamma}} |\Gamma\rangle \langle \tilde{\Gamma}| &\equiv \lambda_{\Gamma\tilde{\Gamma}} |\gamma\rangle_1 |\gamma'\rangle_2 {}_2\langle \tilde{\gamma}' | {}_1\langle \tilde{\gamma} | \\ &= \lambda_{\gamma\tilde{\gamma}} |\gamma\rangle_{11} \langle \tilde{\gamma} | \times \lambda_{\gamma'\tilde{\gamma}'} |\gamma'\rangle_{22} \langle \tilde{\gamma}' |. \end{aligned} \quad (3.5.34)$$

In order to check the validity of this assumption, we first state that the relation

$$\sum_{\Gamma} \lambda_{\Gamma}^* \lambda_{\Gamma} = \sum_{\gamma \tilde{\gamma}} \lambda_{\gamma}^* \lambda_{\gamma} \times \lambda_{\tilde{\gamma}}^* \lambda_{\tilde{\gamma}} = 1 \quad (3.5.35)$$

holds after the minimization. Here, the λ_{Γ} are the diagonal variational parameters for the two-band model while the λ_{γ} are the variational parameters from the one-band model. Furthermore, a comparison of the single values λ_{Γ} to the products $\lambda_{\gamma} \lambda_{\tilde{\gamma}}$ yields a one-to-one correspondence of two-orbital states $|\Gamma\rangle$ and one-orbital product states $|\gamma\rangle|\tilde{\gamma}\rangle$. In this way, the validity of our assumption has been checked for both para- and ferromagnetic systems.

By replacing each sum over the multi-orbital states $|\Gamma\rangle$ by multiple sums over one-orbital states $|\gamma\rangle$, one derives the following results:

- The local completeness relation (3.3.1) factorizes into the completeness relations for the completeness within each orbital:

$$\begin{aligned} 1 &= \sum_{\Gamma_1 \Gamma_2} \lambda_{\Gamma_1}^* \lambda_{\Gamma_2} m_{\Gamma_1, \Gamma_2}^0 \\ &= \sum_{\gamma_1 \gamma_2} \lambda_{\gamma_1}^* \lambda_{\gamma_2} m_{\gamma_1, \gamma_2}^0 \times \sum_{\gamma'_1 \gamma'_2} \lambda_{\gamma'_1}^* \lambda_{\gamma'_2} m_{\gamma'_1, \gamma'_2}^0 \\ &= 1^{(1)} \times 1^{(2)}. \end{aligned} \quad (3.5.36)$$

The superscript denotes the orbitals.

- The constraint concerning the element $C_{as, as'}^0$ of the local density matrix can be cast into the corresponding constraint for $C_{s, s'}^0$ from the one-orbital model and the completeness relation within the other orbital:

$$\begin{aligned} C_{as, as'}^0 &= \sum_{\substack{\Gamma \Gamma' \\ \Gamma_1 \Gamma_2 \Gamma_3}} \lambda_{\Gamma_2 \Gamma_1}^* \lambda_{\Gamma_2 \Gamma_3} \langle \Gamma | \hat{c}_{as}^\dagger | \Gamma_1 \rangle \times \langle \Gamma_3 | \hat{c}_{as'} | \Gamma' \rangle m_{\Gamma, \Gamma'}^0 \\ &= \sum_{\substack{\gamma \gamma' \\ \gamma_1 \gamma_2 \gamma_3}} \lambda_{\gamma_2 \gamma_1}^* \lambda_{\gamma_2 \gamma_3} \langle \gamma | \hat{c}_{as}^\dagger | \gamma_1 \rangle \times \langle \gamma_3 | \hat{c}_{as'} | \gamma' \rangle m_{\gamma, \gamma'}^0 \times \\ &\quad \times \sum_{\gamma'_1 \gamma'_2} \lambda_{\gamma'_1}^* \lambda_{\gamma'_2} m_{\gamma'_1, \gamma'_2}^0 \\ &= C_{s, s'}^0 \times 1^{(\bar{a})}, \end{aligned} \quad (3.5.37)$$

where we used $\bar{1} = 2$ and $\bar{2} = 1$, respectively.

- The elements of the renormalization matrix $q_{as}^{as'}$ can also be cast into the corresponding one-band renormalization factor $q_s^{s'}$ and the completeness relation within the other orbital:

$$\begin{aligned}
q_{as}^{as'} &= \sum_{\substack{\Gamma_1\Gamma_2 \\ \Gamma_3\Gamma_4}} \lambda_{\Gamma_2\Gamma_1}^* \lambda_{\Gamma_3\Gamma_4} \langle \Gamma_2 | \hat{c}_{as}^\dagger | \Gamma_3 \rangle H_{\Gamma_1\Gamma_4}^{as'} \\
&= \sum_{\substack{\gamma_1'\gamma_2' \\ \gamma_3'\gamma_4'}} \lambda_{\gamma_3'\gamma_4'}^* \langle \gamma_2' | \hat{c}_s^\dagger | \gamma_3' \rangle H_{\gamma_1'\gamma_4'}^{s'} \times \sum_{\gamma_1\gamma_2} \lambda_{\gamma_1}^* \lambda_{\gamma_2} m_{\gamma_1,\gamma_2}^0 \quad (3.5.38) \\
&= q_s^{s'} \times 1^{(\bar{a})}
\end{aligned}$$

- The local interaction energy splits into the sum of the one-orbital interaction energies, multiplied by the completeness relation of the opposite orbital:

$$\begin{aligned}
E^{\text{loc}} &= \sum_{\Gamma} E_{\Gamma}^{\text{loc}} \sum_{\Gamma_1\Gamma_2} \lambda_{\Gamma\Gamma_1}^* \lambda_{\Gamma\Gamma_2} m_{\Gamma_1,\Gamma_2}^0 \\
&= \sum_{\gamma\gamma'} [E_{\gamma}^{\text{loc}} + E_{\gamma'}^{\text{loc}}] \sum_{\substack{\gamma_1\gamma_2 \\ \gamma_1'\gamma_2'}} \lambda_{\gamma\gamma_1}^* \lambda_{\gamma'\gamma_1'}^* \lambda_{\gamma\gamma_2} \lambda_{\gamma'\gamma_2'} m_{\gamma_1,\gamma_2}^0 m_{\gamma_1',\gamma_2'}^0 \quad (3.5.39) \\
&= E^{1,\text{loc}} \times 1^{(2)} + E^{2,\text{loc}} \times 1^{(1)}
\end{aligned}$$

These findings have also been checked and been confirmed numerically. They provided useful criteria for consistency checks in the development of the TDGA.

Chapter 4

Time-Dependent Hartree–Fock Approximation

The HF approximation as sketched Section 2.6.1 yields a decoupled Hamiltonian allowing for simple calculations of ground-state properties. The stability of the ground state can be checked by calculating the response functions for the charge, spin and pair channel by applying time-dependent external fields to the system. In the limit of small fluctuation amplitudes, the so-called RPA allows for the calculation of two-particle response functions. The RPA was developed by Pines [74] based on the equation of motion for the one-electron density matrix. Here, the RPA will be derived as a time-dependent generalization of the HF approximation in Section 4.2.

The HF ground-state wave function is included in the Gutzwiller variational space if we set $\lambda_{i,\Gamma\Gamma'} = \delta_{\Gamma\Gamma'}$. The derivation of the TDGA will thus go along the same lines in certain aspects. We start this chapter with a list of abbreviations that will be used both for the RPA and the TDGA.

4.1 Definitions and Notations

The HF theory aims for an effective one-particle description of the interacting electron system. The trial ground state is therefore written as a product state of non-interacting particles, i.e., the ground-state wave function $|\Phi_0^{\text{HF}}\rangle$ is approximated by a Slater determinant:

$$|\Phi_0^{\text{HF}}\rangle = \prod_{\gamma} \hat{h}_{\gamma}^{\dagger} |0\rangle. \quad (4.1.1)$$

The evaluation of expectation values with respect to one-particle product states is a simple task by means of Wick's theorem. It is time-independent

version, Wick's theorem states that expectation values of many-particle operators can be obtained by calculating all possible pairings of creation and annihilation operators. Expectation values with respect to Slater determinants thus become functionals of the one-particle density matrix $\tilde{\rho}$. We label the elements of $\tilde{\rho}$ as

$$\rho_{j\sigma',i\sigma} \equiv \langle \hat{c}_{i\sigma}^\dagger \hat{c}_{j\sigma'} \rangle_{\Phi_0}. \quad (4.1.2)$$

Note that the order of the indices as introduced in Eq. (4.1.2) is more useful than the one used in Chapter 3. For $i = j$, $\rho_{j\sigma',i\sigma}$ just recovers the elements of the local density matrix \tilde{C} .

We introduce the abbreviations

$$v \equiv (i\sigma) \quad (4.1.3)$$

for local one-particle states and

$$Y = (v, v') \quad (4.1.4)$$

for pairs of these indices. The elements of $\tilde{\rho}$ can then be written as

$$\rho_{j\sigma_1,i\sigma_2} = \rho_{(v_1,v_2)} = \rho_Y, \quad (4.1.5)$$

which allows us to interpret them as elements of a matrix $\tilde{\rho}$ (with respect to (v_1, v_2)) or as elements of a vector $\vec{\rho}$ (with respect to Y). To a given index pair $Y = (v_1, v_2)$ we define the 'inverse' index $\bar{Y} = (v_2, v_1)$.

4.2 Hartree–Fock Approximation II

The expectation value of a many-particle Hamiltonian with respect to a single-particle product state is a function of the single-particle density matrix. For example, for the Hamiltonian (2.4.3) it reads

$$\begin{aligned} E^{\text{HF}}(\tilde{\rho}) &\equiv \langle \hat{H} \rangle_{\Phi_0} \\ &= \sum_{\substack{i \neq j \\ \sigma \sigma'}} t_{ij}^{\sigma \sigma'} \rho_{j\sigma',i\sigma} + \sum_{\substack{i \\ \sigma \sigma'}} \epsilon_i^{\sigma \sigma'} \rho_{i\sigma',i\sigma} + \sum_i E_{\text{loc},i}^{\text{HF}}(\tilde{\rho}), \end{aligned} \quad (4.2.1)$$

where $\rho_{j\sigma',i\sigma}$ are the elements of the previously defined density matrix and

$$E_{\text{loc},i}^{\text{HF}}(\tilde{\rho}) = \frac{1}{2} \sum_{\substack{\sigma_1 \sigma_2 \\ \sigma_3 \sigma_4}} U_i^{\sigma_1 \sigma_2, \sigma_3 \sigma_4} \left[\rho_{i\sigma_4, i\sigma_1} \rho_{i\sigma_3, i\sigma_2} - \rho_{i\sigma_3, i\sigma_1} \rho_{i\sigma_4, i\sigma_2} \right] \quad (4.2.2)$$

is the expectation value of the two-particle interaction term in the Hamiltonian (2.4.3).

With the abbreviations (4.1.5), the HF energy (4.2.1) reads

$$\begin{aligned} E^{\text{HF}}(\tilde{\rho}) &= \sum_{v_1 v_2} \varepsilon_{v_1 v_2} \rho_{v_2, v_1} + \frac{1}{2} \sum_{\substack{v_1 v_2 \\ v_3 v_4}} \rho_{v_4, v_1} W_{v_1 v_4, v_3 v_2} \rho_{v_3, v_2} \\ &= \sum_Y \varepsilon_Y \rho_{\bar{Y}} + \frac{1}{2} \sum_{YY'} \rho_{\bar{Y}} W_{YY'} \rho_{Y'}, \end{aligned} \quad (4.2.3)$$

where

$$\varepsilon_{i\sigma_1, j\sigma_2} \equiv t_{ij}^{\sigma_1 \sigma_2} + \delta_{ij} \epsilon_i^{\sigma_1 \sigma_2} \quad (4.2.4)$$

denotes the one-particle energies and

$$W_{v_1 v_4, v_3 v_2} \equiv U_i^{\sigma_1 \sigma_2, \sigma_3 \sigma_4} - U_i^{\sigma_1 \sigma_2, \sigma_4 \sigma_3} \quad (4.2.5)$$

for indices $v_k = (i, \sigma_k)$ that belong to the same lattice site i . Note the symmetries

$$W_{v_1 v_4, v_3 v_2} = W_{v_2 v_3, v_4 v_1} = -W_{v_1 v_3, v_4 v_2}, \quad (4.2.6)$$

which will be employed in the following section.

The energy functional (4.2.3) has to be minimized with respect to all density matrices which belong to a single-particle product state. Such matrices are idempotent, i.e., they obey the matrix equation

$$\tilde{\rho}^2 = \tilde{\rho}, \quad (4.2.7)$$

which must be imposed as a constraint via a Lagrange parameter matrix $\tilde{\eta}$ with elements $\eta_{vv'}$. The resulting equation

$$\frac{\partial}{\partial \rho_{v, v'}} \left[E^{\text{HF}}(\tilde{\rho}) - \text{tr} \left(\tilde{\eta} (\tilde{\rho}^2 - \tilde{\rho}) \right) \right] = 0 \quad (4.2.8)$$

has to be solved, leading to

$$\tilde{h}(\tilde{\rho}) + \tilde{\eta} - \tilde{\eta} \tilde{\rho} - \tilde{\rho} \tilde{\eta} = 0, \quad (4.2.9)$$

where we introduced the matrix $\tilde{h}(\tilde{\rho})$ with the elements

$$h_Y(\tilde{\rho}) = \frac{\partial}{\partial \rho_{\bar{Y}}} E^{\text{HF}}(\tilde{\rho}) = \varepsilon_Y + \sum_{Y'} W_{YY'} \rho_{Y'}. \quad (4.2.10)$$

Equation (4.2.9) is solved if $\tilde{\rho}$ satisfies both Eq. (4.2.7) and

$$[\tilde{h}(\tilde{\rho}), \tilde{\rho}] = 0. \quad (4.2.11)$$

Starting with a certain density matrix $\tilde{\rho}$, we can introduce the single-particle basis

$$|\alpha\rangle = \sum_v u_{v, \alpha} |v\rangle \quad (4.2.12)$$

of states which diagonalize the Hamilton matrix $\tilde{h}(\tilde{\rho})$, i.e.,

$$\sum_{v'} h_{v,v'}(\tilde{\rho}) u_{v',\alpha} = E_{\alpha} u_{v,\alpha}. \quad (4.2.13)$$

Equation (4.2.11) is then solved by setting

$$\rho_{\alpha,\alpha'} = \delta_{\alpha\alpha'} \Theta[E_{\text{F}} - E_{\alpha}], \quad (4.2.14)$$

where the Fermi energy E_{F} is determined by the total number of electrons

$$N_{\text{e}} = \sum_{\alpha} \Theta[E_{\text{F}} - E_{\alpha}]. \quad (4.2.15)$$

The density matrix (4.2.14) has to be reinserted into Eqs. (4.2.3) and (4.2.10) until self-consistency is reached. We denote the self-consistent solution of these equations as $\tilde{\rho}^0$ and introduce the corresponding Hamilton matrix

$$\tilde{h}^0 \equiv \tilde{h}(\tilde{\rho}^0). \quad (4.2.16)$$

4.3 Equation of Motion for the Density Matrix

We consider two-particle Green's functions of the form

$$\begin{aligned} G_{v_2 v_1, v_3 v_4}(t - t') &\equiv \langle\langle \hat{c}_{v_1}^{\dagger}(t) \hat{c}_{v_2}(t); \hat{c}_{v_3}^{\dagger}(t') \hat{c}_{v_4}(t') \rangle\rangle \\ &\equiv -i \Theta(t - t') \langle \Phi | [\hat{c}_{v_1}^{\dagger}(t) \hat{c}_{v_2}(t), \hat{c}_{v_3}^{\dagger}(t') \hat{c}_{v_4}(t')] | \Phi \rangle, \end{aligned} \quad (4.3.1)$$

where $|\Phi\rangle$ is the exact ground state of the multi-band Hubbard Hamiltonian (2.4.3), and $\hat{c}_v^{(\dagger)}(t)$ is the Heisenberg representation of the operator $\hat{c}_v^{(\dagger)}$ with respect to \hat{H} . As shown in most textbooks on many-particle physics, the Green's functions (4.3.1) naturally arise in 'linear-response theory' because they describe the time-dependent changes

$$\begin{aligned} \delta \langle \hat{c}_{v_1}^{\dagger} \hat{c}_{v_2} \rangle_t &\equiv \langle \hat{c}_{v_1}^{\dagger} \hat{c}_{v_2} \rangle_t - \langle \hat{c}_{v_1}^{\dagger} \hat{c}_{v_2} \rangle_{-\infty} \equiv \delta \rho_{v_2, v_1}(t) \\ &= \sum_{v_3 v_4} \int_{-\infty}^{\infty} dt' G_{v_2 v_1, v_3 v_4}(t - t') f_{v_3 v_4}(t') \end{aligned} \quad (4.3.2)$$

of the density matrix $\tilde{\rho}$ in the presence of a small time-dependent perturbation

$$\hat{V}_f(t) = \sum_{vv'} f_{vv'}(t) \hat{c}_v^{\dagger} \hat{c}_{v'} \quad (4.3.3)$$

added to \hat{H} [75, 76, 77]. After a Fourier transformation and using again the abbreviation $Y = (v, v')$, Eq. (4.3.2) reads

$$\delta \rho_Y(\omega) = \sum_{Y'} G_{YY'}(\omega) f_{Y'}(\omega), \quad (4.3.4)$$

with

$$G_{Y Y'}(\omega) \equiv \int_{-\infty}^{\infty} d\tau G_{Y Y'}(\tau) e^{i\omega\tau}, \quad (4.3.5)$$

and $f_Y(\omega)$ and $\delta\rho_Y(\omega)$ defined accordingly.

Ideally, we would like to calculate the time dependence of the density matrix

$$\rho_{v',v}(t) \equiv \langle \Phi(t) | \hat{c}_v^\dagger \hat{c}_{v'} | \Phi(t) \rangle, \quad (4.3.6)$$

where $|\Phi(t)\rangle$ is the exact solution of the time-dependent Schrödinger equation for the full Hamiltonian

$$\hat{H}(t) = \hat{H} + \hat{V}_f(t). \quad (4.3.7)$$

The expectation value (4.3.6) obeys the Heisenberg equation

$$i\dot{\rho}_{v',v}(t) = \langle \Psi(t) | [\hat{H}, \hat{c}_v^\dagger \hat{c}_{v'}] | \Psi(t) \rangle, \quad (4.3.8)$$

which contains the commutator

$$\begin{aligned} [\hat{H}(t), \hat{c}_v^\dagger \hat{c}_{v'}] &= \sum_{v_1} [\varepsilon_{v_1 v} + f_{v_1 v}(t)] \hat{c}_{v_1}^\dagger \hat{c}_{v'} - \sum_{v_1} [\varepsilon_{v' v_1} + f_{v' v_1}(t)] \hat{c}_v^\dagger \hat{c}_{v_1} \\ &+ \frac{1}{2} \sum_{v_1 v_2 v_3} \left(W_{v_1 v_3, v v_2} \hat{c}_{v_1}^\dagger \hat{c}_{v_2}^\dagger \hat{c}_{v'} \hat{c}_{v_3} + W_{v_1 v_2, v_3 v'} \hat{c}_{v_1}^\dagger \hat{c}_v^\dagger \hat{c}_{v_2} \hat{c}_{v_3} \right). \end{aligned} \quad (4.3.9)$$

In the time-dependent HF approximation, it is assumed that the solution $|\Phi(t)\rangle$ of the Schrödinger equation at any time t is approximately given by a single-particle product wave function. In this case, the expectation value of the commutator (4.3.9) can be evaluated by means of Wick's theorem. This leads to the equation of motion

$$i\dot{\tilde{\rho}}(t) = [\tilde{h}(\tilde{\rho}(t)) + \tilde{f}(t), \tilde{\rho}(t)] \quad (4.3.10)$$

for $\tilde{\rho}(t)$, where the matrix $\tilde{h}(\tilde{\rho})$ has been introduced in Eq. (4.2.10). Equations (4.2.10) and (4.3.10) will be crucial also for our formulation of the TDGA in Chapter 5.

4.3.1 Expansion for Weak Perturbations

We are only interested in cases where

$$\hat{V}_f(t) \rightarrow \delta\hat{V}_f(t) = \sum_{vv'} \delta f_{vv'}(t) \hat{c}_v^\dagger \hat{c}_{v'} \quad (4.3.11)$$

is a weak perturbation to the time-independent Hamiltonian \hat{H} . In this case, the density matrix $\tilde{\rho}(t)$ and the Hamilton matrix $\tilde{h}(t)$ are given as

$$\tilde{\rho}(t) \approx \tilde{\rho}^0 + \delta\tilde{\rho}(t) \quad (4.3.12)$$

$$\tilde{h}(t) \approx \tilde{h}^0 + \delta\tilde{h}(t), \quad (4.3.13)$$

where $\delta\tilde{\rho}(t)$ describes a ‘small’ time-dependent perturbation around the ground-state density matrix $\tilde{\rho}^0$, and

$$h_Y^0 = \varepsilon_Y + \sum_{Y'} W_{YY'} \rho_{Y'}^0, \quad (4.3.14)$$

$$\delta h_Y(t) = \sum_{Y'} W_{YY'} \delta \rho_{Y'}(t). \quad (4.3.15)$$

With the expansion (4.3.12) and (4.3.13), the equation of motion for the time-dependent density matrix (4.3.10) becomes

$$0 = [\tilde{h}^0, \tilde{\rho}^0] \quad (4.3.16)$$

$$i\delta\dot{\tilde{\rho}}(t) = [\tilde{h}^0, \delta\tilde{\rho}(t)] + [\delta\tilde{h}(t) + \delta\tilde{f}(t), \tilde{\rho}^0]. \quad (4.3.17)$$

These equations have to be solved for density matrices $\tilde{\rho}(t)$ that fulfill Eq. (4.2.7). After applying the expansion Eq. (4.3.12), Eq. (4.2.7) reads (to leading order in $\delta\tilde{\rho}(t)$)

$$\tilde{\rho}^0 = [\tilde{\rho}^0]^2 \quad (4.3.18)$$

$$\delta\tilde{\rho}(t) = \tilde{\rho}^0 \delta\tilde{\rho}(t) + \delta\tilde{\rho}(t) \tilde{\rho}^0. \quad (4.3.19)$$

Note that Eqs. (4.3.16) and (4.3.18) just recover the time-independent HF equations (4.2.7) and (4.2.11) derived in Section 4.2.

4.3.2 RPA Equations

Mathematically, the density matrix is a projector onto ‘hole’-states, $\tilde{\rho}_h \equiv \tilde{\rho}^0$. In addition, we define the projector onto ‘particle’-states as

$$\tilde{\rho}_p \equiv 1 - \tilde{\rho}^0. \quad (4.3.20)$$

With these two operators, we can decompose all matrices into their four components

$$\delta\tilde{\rho}^{vw}(t) \equiv \tilde{\rho}_v \delta\tilde{\rho}(t) \tilde{\rho}_w \quad (4.3.21)$$

$$\delta\tilde{f}^{vw}(t) \equiv \tilde{\rho}_v \delta\tilde{f}(t) \tilde{\rho}_w \quad (4.3.22)$$

$$\tilde{h}^{0;vw} \equiv \tilde{\rho}_v \tilde{h}^0 \tilde{\rho}_w, \quad (4.3.23)$$

where $v, w \in \{p, h\}$ denotes the particle and hole channel, respectively. Note that $\tilde{h}^{0;vw}$ has the elements

$$h_{\alpha, \alpha'}^{0;vw} = \delta_{vw} \delta_{\alpha\alpha'} E_{\alpha}. \quad (4.3.24)$$

An evaluation of the condition (4.3.19) for the components $\delta\tilde{\rho}^{vw}(t)$ yields

$$\delta\tilde{\rho}^{vw}(t) = \delta\tilde{\rho}^{vw}(t) + \delta\tilde{\rho}^{vv}(t)\delta\tilde{\rho}^{vw}(t) + \delta\tilde{\rho}^{vw}(t)\delta\tilde{\rho}^{ww}(t) \quad (4.3.25)$$

and

$$\delta\tilde{\rho}^{ww}(t) = 0, \quad (4.3.26)$$

where $v \neq w$. Hence, the components $\delta\tilde{\rho}^{pp}(t)$ and $\delta\tilde{\rho}^{hh}(t)$ can be neglected in the following compared to the leading fluctuations $\delta\tilde{\rho}^{hp}(t)$ and $\delta\tilde{\rho}^{ph}(t)$.

We express the time-dependent quantities $\delta\tilde{\rho}^{vw}(t)$ and $\delta\tilde{f}^{vw}(t)$ by their respective Fourier transforms $\delta\tilde{\rho}^{vw}(\omega)$ and $\delta\tilde{f}^{vw}(\omega)$. The equation of motion (4.3.17) then leads to

$$+\omega\delta\rho_{\alpha_1, \alpha_2}^{vw}(\omega) = [E_{\alpha_1} - E_{\alpha_2}]\delta\rho_{\alpha_1, \alpha_2}^{vw}(\omega) \pm [\delta h_{\alpha_1, \alpha_2}^{vw}(\omega) + \delta f_{\alpha_1, \alpha_2}^{vw}(\omega)], \quad (4.3.27)$$

where the plus and minus signs correspond to $vw = ph$ and $vw = hp$, respectively. With the abbreviation $A = (\alpha_1, \alpha_2)$ for pairs of indices α we find

$$\delta h_A^{vw}(\omega) = - \sum_{A'} U_{AA'} [\delta\rho_{A'}^{vw}(\omega) + \delta\rho_{A'}^{wv}(\omega)]. \quad (4.3.28)$$

Here, the elements of the matrix \tilde{U} are given as

$$U_{AA'} = U_{\alpha_1\alpha_2, \alpha'_1\alpha'_2} \equiv - \sum_{\substack{v_1v_2 \\ v'_1v'_2}} u_{v_1, \alpha_1}^* u_{v_2, \alpha_2} W_{v_1v_2, v'_1v'_2} u_{v'_1, \alpha'_1} u_{v'_2, \alpha'_2}^*. \quad (4.3.29)$$

The coefficients $u_{v, \alpha}$ in Eq. (4.3.29) have been introduced in Eq. (4.2.12) and determine the solutions $|\alpha\rangle$ of the HF equations. Equations (4.3.27) and (4.3.28) then yield

$$\left[(\omega - \tilde{E}) \begin{pmatrix} 1 & 0 \\ 0 & -1 \end{pmatrix} + \tilde{U} \right] \begin{pmatrix} \delta\tilde{\rho}^{ph}(\omega) \\ \delta\tilde{\rho}^{hp}(\omega) \end{pmatrix} = \begin{pmatrix} \delta\tilde{f}^{ph}(\omega) \\ \delta\tilde{f}^{hp}(\omega) \end{pmatrix}, \quad (4.3.30)$$

with a matrix \tilde{E} defined as

$$E_{AA'} = E_{\alpha_1\alpha_2, \alpha'_1\alpha'_2} = \delta_{\alpha_1\alpha'_1} \delta_{\alpha_2\alpha'_2} [E_{\alpha_1} - E_{\alpha_2}]. \quad (4.3.31)$$

By comparing Eqs. (4.3.30) and (4.3.4) we find

$$\tilde{G}^{-1}(\omega) = \left[(\omega + i\delta - \tilde{E}) \begin{pmatrix} 1 & 0 \\ 0 & -1 \end{pmatrix} + \tilde{U} \right] \quad (4.3.32)$$

for the inverse of the two-particle Green's function

$$\begin{aligned} G_{AA'}(\omega) &= G_{\alpha_1\alpha_2,\alpha'_1\alpha'_2}(\omega) \\ &= \sum_{\substack{v_1v_2 \\ v'_1v'_2}} u_{v_1,\alpha_1} u_{v_2,\alpha_2}^* G_{v_1v_2,v'_1v'_2}(\omega) u_{v'_1,\alpha'_1}^* u_{v'_2,\alpha'_2}. \end{aligned} \quad (4.3.33)$$

In Eq. (4.3.32) we added an infinitesimal increment $i\delta$ with $\delta = 0^+$ in order to ensure the correct boundary conditions of a retarded Green's function. For $\tilde{U} = 0$, the inverse Green's function (4.3.32) reads

$$\tilde{\Gamma}^{-1}(\omega) \equiv \pm[\omega + i\delta - \tilde{E}], \quad (4.3.34)$$

which leads to

$$\Gamma_{AA'}(\omega) = \Gamma_{\alpha_1\alpha_2,\alpha'_1\alpha'_2}(\omega) = \delta_{\alpha_1\alpha'_1} \delta_{\alpha_2\alpha'_2} \frac{\rho_{\alpha_2,\alpha_2}^0 - \rho_{\alpha_1,\alpha_1}^0}{\omega - [E_{\alpha_1} - E_{\alpha_2}] + i\delta}. \quad (4.3.35)$$

Note that $\tilde{\Gamma}$ is not the exact Green's function for the single-particle Hamiltonian \hat{H}_0 since we just set $\tilde{U} = 0$ in Eq. (4.3.32), but kept finite the 'HF self-energy' contributions

$$\Sigma_A \equiv \sum_{A'} W_{AA'} \rho_{A'}^0, \quad (4.3.36)$$

which usually change the 'eigenvalues' E_α in Eq. (4.3.35); cf., Eqs. (4.2.10) and (4.2.13).

With the Green's function (4.3.35) we can write Eq. (4.3.32) as

$$\tilde{G}(\omega) = \tilde{\Gamma}(\omega)[1 + \tilde{U}\tilde{\Gamma}(\omega)]^{-1} \quad (4.3.37)$$

$$= \tilde{\Gamma}(\omega) + \tilde{\Gamma}(\omega)\tilde{U}\tilde{G}(\omega), \quad (4.3.38)$$

where, in the second line, we expanded $[1 + \tilde{U}\tilde{\Gamma}(\omega)]^{-1}$ into a power series with respect to $\tilde{U}\tilde{\Gamma}$. Both Eqs. (4.3.37) and (4.3.38) are familiar expressions for the two-particle Green's function in the RPA.

Chapter 5

Time-Dependent Gutzwiller Approximation

Based on the slave-boson mean-field formalism, Seibold *et al* developed the TDGA for the single-band Hubbard model [37, 38]. In later works, the TDGA yielded results that were in both qualitatively and quantitatively good agreement with DMFT and exact results [47, 48, 49].

In this chapter, we generalize this approach for the investigation of multi-band models. To this end, we set up an effective energy functional of the density matrix in Section 5.2, which is used in Sections 5.3 and 5.5 to derive the Gutzwiller RPA equations. We first present a list of abbreviations that will be used in the following sections.

5.1 Definitions and Notations

As in the previous chapter, we start with a list of definitions and abbreviations. The elements of the density matrix will be denoted as

$$\rho_{j\sigma',i\sigma} = \rho_{v'v} = \rho_Y = \langle \hat{c}_{i\sigma}^\dagger \hat{c}_{j\sigma'} \rangle_{\Phi_0}, \quad (5.1.1)$$

with the abbreviation $Y = (v', v)$ for a pair of local spin-orbit states ($i\sigma$) and ($j\sigma'$) already defined in Eqs. (4.1.3) and (4.1.4). We further introduce the abbreviation

$$X \equiv (i, \Gamma\Gamma') \quad \text{or} \quad Z \equiv (i, \Gamma\Gamma') \quad (5.1.2)$$

to label the elements of the variational parameter matrix, see below.

5.2 Effective Energy Functional

As summarized in Chapter 3, the expectation value of the multi-band Hamiltonian (2.4.3) in the Gutzwiller theory is a function of the variational param-

eters $\lambda_{\Gamma\Gamma'}$ and of the one-particle wave function $|\Phi_0\rangle$. As in the HF theory, the single-particle wave function $|\Phi_0\rangle$ enters the energy functional solely through the elements of the non-interacting density matrix $\tilde{\rho}$, Eq. (4.1.2). It is therefore possible to consider the energy

$$E^{\text{GA}} = E^{\text{GA}}(\vec{\lambda}, \tilde{\rho}) \equiv \frac{\langle \Psi_{\text{G}} | \hat{H} | \Psi_{\text{G}} \rangle}{\langle \Psi_{\text{G}} | \Psi_{\text{G}} \rangle} \quad (5.2.1)$$

as a function of the density matrix $\tilde{\rho}$ and of the ‘vector’

$$\vec{\lambda} = (\{\lambda_{\Gamma\Gamma'}^*\}, \{\lambda_{\Gamma\Gamma'}\}) = (\lambda_1, \dots, \lambda_{n_{\text{var}}}) \quad (5.2.2)$$

of n_{var} variational parameters $\lambda_{\Gamma\Gamma'}$ (and $\lambda_{\Gamma\Gamma'}^*$ for $\Gamma \neq \Gamma'$). The density matrix in the energy functional (5.2.1) must be derived from a single-particle wave function and, therefore, it has to obey the condition (4.2.7).

The constraints (3.3.1) and (3.3.2) are also functions of $\vec{\lambda}$ and $\tilde{\rho}$ and will be denoted as

$$g_n(\vec{\lambda}, \tilde{\rho}) = 0, \quad 1 \leq n \leq n_c. \quad (5.2.3)$$

The dependence on $\vec{\lambda}$ is given in Eqs. (3.3.3) and (3.3.4). Here, n_c is the (maximum) number of independent constraints, which, due to symmetries, is usually smaller than its maximum value $N_{\text{so}}^2 + 1$, where N_{so} is the number of spin-orbital states per lattice site. We assume that the functions (5.2.3) are real, i.e., in case of complex expressions in Eqs. (3.3.3) and (3.3.4) their real and imaginary parts are treated separately.

By solving Eqs. (5.2.3) we can, at least in principle, express n_c of the variational parameters ($\equiv \lambda_X^{\text{d}}$) through the density matrix $\tilde{\rho}$ and the remaining ‘independent’ parameters ($\equiv \lambda_Z^{\text{i}}$),

$$\lambda_X^{\text{d}} = \lambda_X^{\text{d}}(\vec{\lambda}^{\text{i}}, \tilde{\rho}). \quad (5.2.4)$$

In this way, we obtain an energy functional

$$E^{\text{GA}}(\vec{\lambda}^{\text{i}}, \tilde{\rho}) \equiv E^{\text{GA}}(\vec{\lambda}^{\text{d}}(\vec{\lambda}^{\text{i}}, \tilde{\rho}), \vec{\lambda}^{\text{i}}, \tilde{\rho}) \quad (5.2.5)$$

which has to be minimized without constraints apart from Eq. (4.2.7) and the condition that the total electron number

$$N_{\text{e}} = \sum_v \rho_{vv} \quad (5.2.6)$$

is conserved.

For a fixed density matrix $\tilde{\rho}$, the minimization of Eq. (5.2.5) with respect to the parameters λ_Z^{i} ,

$$\frac{\partial}{\partial \lambda_Z^{\text{i}}} E^{\text{GA}}(\vec{\lambda}^{\text{i}}, \tilde{\rho}) = 0, \quad (5.2.7)$$

determines these parameters

$$\vec{\lambda}^i = \vec{\lambda}^i(\vec{\rho}) \quad (5.2.8)$$

as a function of $\vec{\rho}$. This allows us to define the ‘effective’ energy functional

$$E^{\text{eff}}(\vec{\rho}) = E^{\text{GA}}(\vec{\lambda}^i(\vec{\rho}), \vec{\rho}), \quad (5.2.9)$$

which, for a fixed density matrix $\vec{\rho}$, is given as the minimum of E^{GA} with respect to $\vec{\lambda}^i$. With this effective functional we will formulate the time-dependent Gutzwiller theory in the following section.

Using a Lagrange-parameter matrix $\tilde{\eta}$ as in Chapter 4, we find

$$\left. \frac{\partial \left[E^{\text{eff}}(\tilde{\rho}) - \text{tr} \left(\tilde{\eta} (\tilde{\rho}^2 - \tilde{\rho}) \right) \right]}{\partial \rho_{\nu\nu'}} \right|_{\tilde{\rho}=\tilde{\rho}^0} = 0, \quad (5.2.10)$$

which leads to

$$[\tilde{h}(\tilde{\rho}), \tilde{\rho}] = 0. \quad (5.2.11)$$

Here we introduced the matrix $\tilde{h}(\tilde{\rho})$ with the elements

$$h_Y(\tilde{\rho}) = \frac{\partial E^{\text{eff}}(\tilde{\rho})}{\partial \rho_{\bar{Y}}} \quad (5.2.12)$$

and used again the notation $\bar{Y} \equiv (j\sigma', i\sigma)$ for $Y = (i\sigma, j\sigma')$. The self-consistent solution of Eqs. (5.2.11) and (5.2.12) then yields the ground-state density matrix $\tilde{\rho}^0$, the matrix $\tilde{h}^0 \equiv \tilde{h}(\tilde{\rho}^0)$, and the corresponding single-particle ‘Gutzwiller-Hamiltonian’

$$\hat{h}^0 \equiv \sum_{\substack{ij \\ \sigma\sigma'}} h_{i\sigma, j\sigma'}^0 \hat{c}_{i,\sigma}^\dagger \hat{c}_{j,\sigma'}. \quad (5.2.13)$$

5.3 Gutzwiller RPA Equations

The derivation of RPA-type equations within the time-dependent Gutzwiller theory goes along the same lines as discussed in Chapter 4 for the time-dependent HF theory. We add a small time-dependent field

$$\delta \hat{V}_f(t) = \sum_{\substack{ij \\ \sigma\sigma'}} \delta f_{i\sigma, j\sigma'}^0(t) \hat{c}_{i,\sigma}^\dagger \hat{c}_{j,\sigma'} + \text{h.c.} \quad (5.3.1)$$

to our multi-band Hamiltonian (2.4.3). With the particular time dependence

$$\delta f_{i\sigma, j\sigma'}^0(t) = \delta \tilde{f}_{i\sigma, j\sigma'}^0(\omega) e^{-i\omega t}, \quad (5.3.2)$$

the expectation value of $\delta\hat{V}(t)$ reads

$$E_f(\tilde{\rho}) = \sum_{\substack{ij \\ \sigma\sigma'}} \delta\tilde{f}_{i\sigma,j\sigma'}(\omega) e^{-i\omega t} \rho_{j\sigma',i\sigma} + \text{c.c.}, \quad (5.3.3)$$

where

$$\begin{aligned} \delta\tilde{f}_{i\sigma_1,j\sigma_2}(\omega) &= \delta_{ij} \delta\tilde{f}_{i\sigma_1,i\sigma_2}^0(\omega) \frac{C_{i\sigma_1,i\sigma_2}^c}{\rho_{i\sigma_2,i\sigma_1}} \\ &+ [1 - \delta_{ij}] \sum_{\sigma'_1\sigma'_2} \delta f_{i\sigma'_1,j\sigma'_2}^0(\omega) q_{\sigma'_1}^{\sigma_1} [q_{\sigma'_2}^{\sigma_2}]^*. \end{aligned} \quad (5.3.4)$$

The (correlated) local density matrix \tilde{C}^c and the renormalization matrix \tilde{q} are defined in Eqs. (3.3.5) and (3.3.20), respectively. With Eq. (5.2.8) they can both be considered as functions of $\tilde{\rho}$.

The time-dependent field induces small fluctuations of the density matrix elements,

$$\rho_Y = \rho_Y^0 + \delta\rho_Y(t). \quad (5.3.5)$$

Our main assumption is now that $\delta\rho_Y(t)$ obeys the same equation of motion,

$$i\delta\dot{\tilde{\rho}}(t) = [\tilde{h}^0, \delta\tilde{\rho}(t)] + [\delta\tilde{h}(t) + \delta\tilde{f}(t), \tilde{\rho}^0], \quad (5.3.6)$$

as the density matrix in the time-dependent HF theory; cf., Eq. (4.3.17). Here, however, the Hamilton matrix

$$\tilde{h}(t) \approx \tilde{h}^0(t) + \delta\tilde{h}(t) \quad (5.3.7)$$

is not derived from the HF energy functional (4.2.3), but from the effective energy functional (5.2.9),

$$h_Y(t) = \frac{\partial}{\partial\rho_{\tilde{Y}}} E^{\text{eff}}(\tilde{\rho}) \approx h_Y^0 + \sum_{Y'} K_{YY'} \delta\rho_{Y'}(t) \equiv h_Y^0 + \delta h_Y(t), \quad (5.3.8)$$

where the matrix \tilde{K} is given as

$$\tilde{K}_{YY'} \equiv \left. \frac{\partial^2 E^{\text{eff}}}{\partial\rho_{\tilde{Y}} \partial\rho_{Y'}} \right|_{\tilde{\rho}=\tilde{\rho}^0}. \quad (5.3.9)$$

The diagonalization of \tilde{h}^0 (or equivalently of the Gutzwiller Hamiltonian \hat{h}^0) yields a basis $|\alpha\rangle$ with

$$h_{\alpha\alpha'}^0 = h_A^0 = \delta_{\alpha\alpha'} E_\alpha \quad (5.3.10)$$

and a ground-state density matrix that is given as

$$\rho_{\alpha\alpha'}^0 = \rho_A^0 = \delta_{\alpha\alpha'} \Theta[E_F - E_\alpha]. \quad (5.3.11)$$

With the projectors $\tilde{\rho}_h \equiv \tilde{\rho}^0$ and $\tilde{\rho}_p \equiv 1 - \tilde{\rho}^0$, we define the particle and hole components of all matrices, as we did in Eqs.(4.3.21)–(4.3.23). The components $\delta\tilde{\rho}^{vw}(t)$ of the density-matrix fluctuations obey Eqs.(4.3.25) and (4.3.26), i.e., to leading order we can neglect $\delta\tilde{\rho}^{\text{hh}}(t)$ and $\delta\tilde{\rho}^{\text{pp}}(t)$. Hence, after a Fourier transformation we end up with the same form of RPA equations,

$$\left[(\omega - \tilde{E}) \begin{pmatrix} 1 & 0 \\ 0 & -1 \end{pmatrix} + \tilde{K} \right] \begin{pmatrix} \delta\tilde{\rho}^{\text{ph}}(\omega) \\ \delta\tilde{\rho}^{\text{hp}}(\omega) \end{pmatrix} = \begin{pmatrix} \delta\tilde{f}^{\text{ph}}(\omega) \\ \delta\tilde{f}^{\text{hp}}(\omega) \end{pmatrix}, \quad (5.3.12)$$

as in Eq.(4.3.30). Here, however, the bare matrix of Coulomb parameters \tilde{U} is replaced by the matrix \tilde{K} , defined in Eq.(5.3.9), and the energies E_α in the matrix \tilde{E} , Eq.(4.3.31), are the eigenvalues of the Gutzwiller Hamiltonian (5.2.13). The comparison with Eq.(4.3.4) leads to the final result

$$\tilde{G}(\omega) \equiv \left[(\omega + i\delta - \tilde{E}) \begin{pmatrix} 1 & 0 \\ 0 & -1 \end{pmatrix} + \tilde{K} \right]^{-1} \quad (5.3.13)$$

for the two-particle response functions matrix within the TDGA.

5.4 Saddle-Point Expansion of the Energy Functional

For an evaluation of the Gutzwiller RPA equations (5.3.12), we need to determine the matrix \tilde{K} which is given by the second derivatives (5.3.9) of the effective energy functional (5.2.9). To this end, we expand E^{GA} up to second order around the ground-state values $\tilde{\rho}^0$ and $\tilde{\lambda}^{i;0} \equiv \tilde{\lambda}^i(\tilde{\rho}^0)$,

$$\begin{aligned} E^{\text{GA}}(\tilde{\lambda}^i, \tilde{\rho}) &= E_0 + \text{tr}(\tilde{h}^0 \delta\tilde{\rho}) + \frac{1}{2} \left[\sum_{YY'} \delta\rho_Y M_{YY'}^{\rho\rho} \delta\rho_{Y'} + \sum_{ZZ'} \delta\lambda_Z^i M_{ZZ'}^{\lambda\lambda} \delta\lambda_{Z'}^i \right. \\ &\quad \left. + \sum_{ZY} \left(\delta\lambda_Z^i M_{ZY}^{\lambda\rho} \delta\rho_Y + \delta\rho_Y M_{YZ}^{\rho\lambda} \delta\lambda_Z^i \right) \right] \\ &\equiv E_0 + \text{tr}(\tilde{h}^0 \delta\tilde{\rho}) + \delta E^{(2)}. \end{aligned} \quad (5.4.1)$$

Here, we introduced the matrices $\widetilde{M}^{\rho\rho}$, $\widetilde{M}^{\lambda\rho}$, $\widetilde{M}^{\rho\lambda}$ and $\widetilde{M}^{\lambda\lambda}$ with the elements

$$M_{YY'}^{\rho\rho} = \frac{\partial^2 E^{\text{GA}}}{\partial \rho_Y \partial \rho_{Y'}} \quad (5.4.2)$$

$$M_{ZY}^{\lambda\rho} = \frac{\partial^2 E^{\text{GA}}}{\partial \lambda_Z^i \partial \rho_Y} = M_{YZ}^{\rho\lambda} \quad (5.4.3)$$

$$M_{ZZ'}^{\lambda\lambda} = \frac{\partial^2 E^{\text{GA}}}{\partial \lambda_Z^i \partial \lambda_{Z'}^i}, \quad (5.4.4)$$

where the second derivatives on the r.h.s. are evaluated for $\tilde{\rho} = \tilde{\rho}^0$ and $\tilde{\lambda}^i = \tilde{\lambda}^{i;0}$. Note that there is no linear term $\sim \lambda_Z^i$ in Eq. (5.4.1) because of the minimization condition (5.2.7). For our further evaluation, it is useful to write the second-order terms in Eq. (5.4.1) in a more compact form by means of matrix-vector products, i.e.,

$$\delta E^{(2)} = \frac{1}{2} \left[(\delta \tilde{\rho})^T \widetilde{M}^{\rho\rho} \delta \tilde{\rho} + 2 (\delta \tilde{\lambda}^i)^T \widetilde{M}^{\lambda\rho} \delta \tilde{\rho} + (\delta \tilde{\lambda}^i)^T \widetilde{M}^{\lambda\lambda} \delta \tilde{\lambda}^i \right]. \quad (5.4.5)$$

Here we used the symmetry

$$\widetilde{M}^{\lambda\rho} = [\widetilde{M}^{\rho\lambda}]^T. \quad (5.4.6)$$

In the effective energy functional (5.2.9) the parameters $\tilde{\lambda}^i$ are determined by the minimization condition (5.2.7). Applied to our second-order expansion (5.4.5), this condition yields

$$\frac{\partial}{\partial \delta \lambda_Z^i} \delta E^{(2)}(\delta \tilde{\lambda}^i, \delta \tilde{\rho}) = 0, \quad (5.4.7)$$

which provides us the multiplet-amplitudes

$$\delta \tilde{\lambda}^i = - [\widetilde{M}^{\lambda\lambda}]^{-1} \widetilde{M}^{\lambda\rho} \delta \tilde{\rho} \quad (5.4.8)$$

as a linear function of the densities $\delta \tilde{\rho}$. This result leads to the quadratic expansion

$$E^{\text{eff}}(\tilde{\rho}^0 + \delta \tilde{\rho}) = E_0 + \text{tr}(\tilde{h}^0 \delta \tilde{\rho}) + \frac{1}{2} (\delta \tilde{\rho})^T \tilde{K} \delta \tilde{\rho}, \quad (5.4.9)$$

with

$$\tilde{K} \equiv \widetilde{M}^{\rho\rho} - \widetilde{M}^{\rho\lambda} [\widetilde{M}^{\lambda\lambda}]^{-1} \widetilde{M}^{\lambda\rho}, \quad (5.4.10)$$

of the effective energy functional as a function of the density fluctuations $\delta \tilde{\rho}$. In earlier work on the TDGA, Eqs. (5.4.7) and (5.4.8) have been denoted as

the ‘anti-adiabaticity assumption’. In fact, these equations have the physical meaning that the local multiplet dynamics, described by fluctuations $\delta\lambda_Z^i(t)$, are fast compared to those of the density-matrix fluctuations $\delta\rho_Y(t)$.

With the functional (5.4.9), we could now proceed with our evaluation of the Gutzwiller RPA equations (5.3.12). For practical applications, however, it is more convenient to determine the ‘interaction kernel’ (5.4.10) in a way that avoids the explicit solution of the constraints (5.2.3). This alternative procedure is the subject of the following section.

5.5 Lagrange-Functional Expansion

In the second-order expansion, described in Section 5.4, we implemented the constraints (5.2.3) by explicitly eliminating a certain set of n_c variational parameters. Although such a procedure can, at least in principle, always be applied, for the numerical implementation it is more convenient to impose the constraints by means of Lagrange parameters. To this end, we define the ‘Lagrange functional’

$$L^{\text{GA}}(\vec{\lambda}, \vec{\rho}, \vec{\Lambda}) \equiv E^{\text{GA}}(\vec{\lambda}, \vec{\rho}) + \sum_n^{n_c} \Lambda_n g_n(\vec{\lambda}, \vec{\rho}), \quad (5.5.1)$$

which depends on *all* variational parameters $\vec{\lambda}$, the density matrix $\vec{\rho}(\doteq\vec{\rho})$ and the n_c Lagrange parameters Λ_n . The optimum variational parameters λ_Z^0 , density-matrix elements ρ_Y^0 , and Lagrange parameters Λ_n^0 are then determined by the equations

$$\left. \frac{\partial L^{\text{GA}}}{\partial \lambda_Z} \right|_{\vec{\lambda}=\vec{\lambda}^0, \vec{\Lambda}=\vec{\Lambda}^0, \vec{\rho}=\vec{\rho}^0} = \left. \frac{\partial L^{\text{GA}}}{\partial \Lambda_n} \right|_{\vec{\lambda}=\vec{\lambda}^0, \vec{\Lambda}=\vec{\Lambda}^0, \vec{\rho}=\vec{\rho}^0} = \left. \frac{\partial L^{\text{GA}}}{\partial \rho_Y} \right|_{\vec{\lambda}=\vec{\lambda}^0, \vec{\Lambda}=\vec{\Lambda}^0, \vec{\rho}=\vec{\rho}^0} = 0, \quad (5.5.2)$$

which have to be solved simultaneously.

We expand the Lagrange functional to leading order with respect to parameter $(\delta\lambda_Z, \delta\Lambda_n)$ and density fluctuations $(\delta\rho_Y)$. The second-order contribution has the form

$$\begin{aligned} \delta L^{(2)} = & \frac{1}{2} \sum_{YY'} \delta\rho_Y L_{YY'}^{\rho\rho} \delta\rho_{Y'} + \sum_{ZY} \delta\lambda_Z L_{ZY}^{\lambda\rho} \delta\rho_Y + \frac{1}{2} \sum_{ZZ'} \delta\lambda_Z L_{ZZ'}^{\lambda\lambda} \delta\lambda_{Z'} \\ & + \sum_n \delta\Lambda_n \left\{ \sum_Z \frac{\partial g_n}{\partial \lambda_Z} \delta\lambda_Z + \sum_Y \frac{\partial g_n}{\partial \rho_Y} \delta\rho_Y \right\}, \end{aligned} \quad (5.5.3)$$

with matrices $\tilde{L}^{\rho\rho}$, $\tilde{L}^{\lambda\rho}$ and $\tilde{L}^{\lambda\lambda}$ defined as in Eqs. (5.4.2)–(5.4.4) only with

E^{GA} replaced by L^{GA} . The anti-adiabaticity conditions

$$\frac{\partial}{\partial \delta \lambda_Z} \delta L^{(2)} = 0 \quad (5.5.4)$$

$$\frac{\partial}{\partial \delta \Lambda_n} \delta L^{(2)} = 0 \quad (5.5.5)$$

yield the n_c equations

$$\sum_Z \frac{\partial g_n}{\partial \lambda_Z} \delta \lambda_Z + \sum_Y \frac{\partial g_n}{\partial \rho_Y} \delta \rho_Y = 0 \quad (5.5.6)$$

and the n_{var} equations

$$\sum_{Z'} L_{ZZ'}^{\lambda\lambda} \delta \lambda_{Z'} + \sum_Y L_{ZY}^{\lambda\rho} \delta \rho_Y + \sum_n \frac{\partial g_n}{\partial \lambda_Z} \delta \Lambda_n = 0. \quad (5.5.7)$$

Together, these equations allow us to express the $n_{\text{var}} + n_c$ parameter fluctuations $\delta \Lambda_n$, $\delta \lambda_Z$ in terms of the density fluctuations $\delta \rho_Y$. These can be reinserted into Eq. (5.5.3) to obtain the desired quadratic functional solely of the density fluctuations,

$$\delta L^{(2)} = \frac{1}{2} \sum_{YY'} \delta \rho_Y \bar{K}_{YY'} \delta \rho_{Y'}. \quad (5.5.8)$$

In Appendix C, we prove that the interaction matrix $\bar{K}_{YY'}$ (5.5.8) is, in fact, identical to $K_{YY'}$ in Eqs. (5.4.9) and (5.4.10).

5.6 Response Functions for Lattice Models

In the previous section, we have developed the general formalism of the TDGA for the calculation of two-particle Green's functions. We will be more specific in this section and explain in detail how the response functions which are of interest in solid-state physics can be calculated within our approach.

5.6.1 Two-Particle Response Functions

In solid-state physics one is usually not interested in the full two-particle Green's function \tilde{G} as it has been defined in Eq. (4.3.1). The properties, relevant for experiments, are certain linear combinations of elements of \tilde{G} . For our translationally invariant model Hamiltonians (2.4.3), these are in particular the two-particle response functions

$$G_{\sigma_2\sigma_1,\sigma_3\sigma_4}(\mathbf{R}_i - \mathbf{R}_j, t - t') \equiv \langle\langle \hat{c}_{i,\sigma_1}^\dagger(t) \hat{c}_{i,\sigma_2}(t); \hat{c}_{j,\sigma_3}^\dagger(t') \hat{c}_{j,\sigma_4}(t') \rangle\rangle, \quad (5.6.1)$$

or, more importantly, their Fourier transforms

$$\begin{aligned} G_{\sigma_2\sigma_1,\sigma_3\sigma_4}(\mathbf{q}, \omega) &= \frac{1}{N_s} \int_{-\infty}^{\infty} d\tau e^{i\omega\tau} \sum_{ij} e^{i(\mathbf{R}_i - \mathbf{R}_j) \cdot \mathbf{q}} G_{\sigma_2\sigma_1,\sigma_3\sigma_4}(\mathbf{R}_i - \mathbf{R}_j, \tau) \\ &= \frac{1}{N_s} \sum_{\mathbf{k}\mathbf{k}'} \langle\langle \hat{c}_{\mathbf{k},\sigma_1}^\dagger \hat{c}_{\mathbf{k}+\mathbf{q},\sigma_2}; \hat{c}_{\mathbf{k}'+\mathbf{q},\sigma_3}^\dagger \hat{c}_{\mathbf{k}',\sigma_4} \rangle\rangle_{\omega}. \end{aligned} \quad (5.6.2)$$

Here, we introduced the fermionic operators

$$\hat{c}_{\mathbf{k},\sigma}^{(\dagger)} = \frac{1}{\sqrt{N_s}} \sum_i e^{\mp i\mathbf{R}_i \cdot \mathbf{k}} \hat{c}_{i,\sigma}^{(\dagger)} \quad (5.6.3)$$

and the usual notation

$$\langle\langle \hat{O}; \hat{O}' \rangle\rangle_{\omega} = \int_{-\infty}^{\infty} d\tau \langle\langle \hat{O}(\tau); \hat{O}'(0) \rangle\rangle e^{i\omega\tau} \quad (5.6.4)$$

for the Fourier transform of a Green's function with arbitrary operators \hat{O} , \hat{O}' . With the abbreviation $v = (\sigma, \sigma')$ for spin-orbit indices and the operators

$$\hat{A}_v^{\mathbf{q}} \equiv \hat{A}_{\sigma_2,\sigma_1}^{\mathbf{q}} \equiv \frac{1}{\sqrt{N_s}} \sum_{\mathbf{k}} \hat{c}_{\mathbf{k},\sigma_1}^\dagger \hat{c}_{\mathbf{k}+\mathbf{q},\sigma_2}, \quad (5.6.5)$$

we can write Eq. (5.6.2) as

$$G_{vv'}(\mathbf{q}, \omega) = \langle\langle \hat{A}_v^{\mathbf{q}}; (\hat{A}_{v'}^{\mathbf{q}})^\dagger \rangle\rangle_{\omega}. \quad (5.6.6)$$

The Green's functions (5.6.2) are still quite general since they include all possible channels of local coupling $\sigma_1 \leftrightarrow \sigma_2$, $\sigma_3 \leftrightarrow \sigma_4$. In experiments one usually measures response functions which are certain linear combinations

$$G_e(\mathbf{q}, \omega) = \sum_{vv'} \kappa_v G_{vv'}(\mathbf{q}, \omega) \kappa_{v'} \quad (5.6.7)$$

of some of the Green's functions (5.6.2), defined by the matrix $\kappa_v = \kappa_{\sigma,\sigma'}$. For example, the transversal spin susceptibility $\chi(\mathbf{q}, \omega)$ is given as

$$\chi(\mathbf{q}, \omega) = \frac{1}{N_s} \langle\langle \hat{S}_{\mathbf{q}}^+; \hat{S}_{-\mathbf{q}}^- \rangle\rangle_{\omega}, \quad (5.6.8)$$

where

$$\hat{S}_{\mathbf{q}}^+ = \sum_i e^{-i\mathbf{R}_i \cdot \mathbf{q}} \hat{S}_i^+ = \sum_{\mathbf{k}} \sum_b \hat{c}_{\mathbf{k},b\uparrow}^\dagger \hat{c}_{\mathbf{q}+\mathbf{k},b\downarrow} \quad (5.6.9)$$

$$\hat{S}_{-\mathbf{q}}^- = \sum_i e^{i\mathbf{R}_i \cdot \mathbf{q}} \hat{S}_i^- = \sum_{\mathbf{k}} \sum_b \hat{c}_{\mathbf{k}+\mathbf{q},b\downarrow}^\dagger \hat{c}_{\mathbf{k},b\uparrow} \equiv (\hat{S}_{\mathbf{q}}^+)^\dagger \quad (5.6.10)$$

$$\hat{S}_i^+ = \sum_b \hat{c}_{i,b\uparrow}^\dagger \hat{c}_{i,b\downarrow}, \quad \hat{S}_i^- = \sum_b \hat{c}_{i,b\downarrow}^\dagger \hat{c}_{i,b\uparrow} \quad (5.6.11)$$

are the usual spin-flip operators. The spin susceptibility of a two-band Hubbard model will be investigated in Chapter 6.

5.6.2 Response Functions in the TDGA

In order to apply the TDGA, as developed in Section 5.2, we have to expand the Lagrange functional (5.5.1) up to second order with respect to density-matrix $\delta\tilde{\rho}$ and variational-parameter fluctuations $\delta\lambda_{\Gamma\Gamma'}$. This means that we need an expansion of the constraints (3.3.1) and (3.3.2), of the local energies (3.3.10) and (3.3.11), and of the kinetic energy (3.3.22) and (3.3.23). The second-order expansion of the kinetic energy is more involved than that of the local energies and of the constraints. In the latter there are only contributions from fluctuations at *same* lattice sites while in the kinetic energy local and non-local fluctuations (such as $\delta\langle\hat{c}_{i,\sigma}^\dagger\hat{c}_{j,\sigma'}\rangle_{\Phi_0}$) couple. Nevertheless, the calculation of the second-order Lagrange functional is tedious but otherwise straightforward. We therefore refer to Appendix D where the details of this derivation are presented. As shown in that Appendix, it is useful to introduce the operators

$$\hat{B}_w^{\mathbf{q}} \equiv \hat{B}_{\sigma_1\sigma_2,\sigma'_1\sigma'_2}^{\mathbf{q}} \equiv \frac{1}{\sqrt{N_s}} \sum_{\mathbf{k}} \epsilon_{\mathbf{k}}^{\sigma_2\sigma_1} \hat{c}_{\mathbf{k},\sigma'_2}^\dagger \hat{c}_{\mathbf{k}+\mathbf{q},\sigma'_1} \quad (5.6.12)$$

$$\hat{\hat{B}}_w^{\mathbf{q}} \equiv \hat{\hat{B}}_{\sigma_1\sigma_2,\sigma'_1\sigma'_2}^{\mathbf{q}} \equiv \frac{1}{\sqrt{N_s}} \sum_{\mathbf{k}} \epsilon_{\mathbf{k}+\mathbf{q}}^{\sigma_2\sigma_1} \hat{c}_{\mathbf{k},\sigma'_2}^\dagger \hat{c}_{\mathbf{k}+\mathbf{q},\sigma'_1}, \quad (5.6.13)$$

and to define the auxiliary Green's function matrix $\tilde{\Pi}(\mathbf{q}, \omega)$ with the elements

$$\Pi_{\substack{v \ v' \\ (w) \ (w')}}(\mathbf{q}, \omega) = \begin{pmatrix} \langle\langle \hat{A}_v^{\mathbf{q}}; (\hat{A}_{v'}^{\mathbf{q}})^\dagger \rangle\rangle_\omega & \langle\langle \hat{A}_v^{\mathbf{q}}; (\hat{B}_{w'}^{\mathbf{q}})^\dagger \rangle\rangle_\omega & \langle\langle \hat{A}_v^{\mathbf{q}}; (\hat{\hat{B}}_{w'}^{\mathbf{q}})^\dagger \rangle\rangle_\omega \\ \langle\langle \hat{B}_w^{\mathbf{q}}; (\hat{A}_{v'}^{\mathbf{q}})^\dagger \rangle\rangle_\omega & \langle\langle \hat{B}_w^{\mathbf{q}}; (\hat{B}_{w'}^{\mathbf{q}})^\dagger \rangle\rangle_\omega & \langle\langle \hat{B}_w^{\mathbf{q}}; (\hat{\hat{B}}_{w'}^{\mathbf{q}})^\dagger \rangle\rangle_\omega \\ \langle\langle \hat{\hat{B}}_w^{\mathbf{q}}; (\hat{A}_{v'}^{\mathbf{q}})^\dagger \rangle\rangle_\omega & \langle\langle \hat{\hat{B}}_w^{\mathbf{q}}; (\hat{B}_{w'}^{\mathbf{q}})^\dagger \rangle\rangle_\omega & \langle\langle \hat{\hat{B}}_w^{\mathbf{q}}; (\hat{\hat{B}}_{w'}^{\mathbf{q}})^\dagger \rangle\rangle_\omega \end{pmatrix}. \quad (5.6.14)$$

We are actually interested only in the first 'element' of this matrix, i.e., the Green's functions (5.6.6), since they allow us to determine any response function of the form Eq. (5.6.7). As shown in Appendix E, however, the TDGA leads to the following equation for the entire matrix (5.6.14) from which Eq. (5.6.6) can be extracted,

$$\tilde{\Pi}(\mathbf{q}, \omega) = [1 + \tilde{\Pi}^0(\mathbf{q}, \omega)\tilde{V}^{\mathbf{q}}]^{-1}\tilde{\Pi}^0(\mathbf{q}, \omega). \quad (5.6.15)$$

Here, $\tilde{V}^{\mathbf{q}}$ is the effective second-order interaction matrix, introduced in Eq. (D.2.19), and $\tilde{\Pi}^0(\mathbf{q}, \omega)$ is the Green's function matrix (5.6.14) evaluated for the single-particle Gutzwiller Hamiltonian (5.2.13). As shown in

Refs. [8, 66], this Gutzwiller Hamiltonian $\hat{h}^0 \equiv \hat{H}_0^{\text{eff}}$ for our lattice Hamiltonian (2.4.3) has the form

$$\hat{H}_0^{\text{eff}} = \sum_{\mathbf{k}} \sum_{\sigma_1 \sigma_2} (\bar{\epsilon}_{\mathbf{k}}^{\sigma_1 \sigma_2} + \eta_{\sigma_1 \sigma_2}) \hat{c}_{\mathbf{k}, \sigma_1}^\dagger \hat{c}_{\mathbf{k}, \sigma_2} \equiv \sum_{\mathbf{k}} \sum_{\alpha} E_{\mathbf{k}, \alpha} \hat{h}_{\mathbf{k}, \alpha}^\dagger \hat{h}_{\mathbf{k}, \alpha}, \quad (5.6.16)$$

where the Lagrange parameters $\eta_{\sigma_1 \sigma_2}$ are determined by the minimization of the variational ground-state energy and $\bar{\epsilon}_{\mathbf{k}}^{\sigma_1 \sigma_2}$ is defined as

$$\bar{\epsilon}_{\mathbf{k}}^{\sigma_1 \sigma_2} \equiv \sum_{\sigma'_1 \sigma'_2} q_{\sigma'_1}^{\sigma_1} [q_{\sigma'_2}^{\sigma_2}]^* \epsilon_{\mathbf{k}}^{\sigma'_1 \sigma'_2}. \quad (5.6.17)$$

The creation and annihilation operators $\hat{h}_{\mathbf{k}, \alpha}^{(\dagger)}$ of the effective single-particle Hamiltonian (5.6.16) can be written as

$$\hat{h}_{\mathbf{k}, \alpha}^\dagger = \sum_{\sigma} u_{\sigma, \alpha}^{\mathbf{k}} \hat{c}_{\mathbf{k}, \sigma}^\dagger \quad (5.6.18)$$

$$\hat{h}_{\mathbf{k}, \alpha} = \sum_{\sigma} (u_{\sigma, \alpha}^{\mathbf{k}})^* \hat{c}_{\mathbf{k}, \sigma}, \quad (5.6.19)$$

where the coefficients of the transformation matrix \tilde{u} are determined from a diagonalization of Eq. (5.6.16). With these eigenstates, the calculation of $\tilde{\Pi}^0(\mathbf{q}, \omega)$ is now a simple task. For example, the first element $\langle\langle \hat{A}_{\sigma_1 \sigma_2}^{\mathbf{q}}; (\hat{A}_{\sigma'_1 \sigma'_2}^{\mathbf{q}})^\dagger \rangle\rangle_{\omega}^0$ is given as

$$\begin{aligned} & \langle\langle \hat{A}_{\sigma_1 \sigma_2}^{\mathbf{q}}; (\hat{A}_{\sigma'_1 \sigma'_2}^{\mathbf{q}})^\dagger \rangle\rangle_{\omega}^0 \\ &= \frac{1}{N_s} \sum_{\mathbf{k} \mathbf{k}'} \sum_{\substack{\alpha_1 \alpha_2 \\ \alpha'_1 \alpha'_2}} \langle\langle \hat{h}_{\mathbf{k}, \alpha_2}^\dagger \hat{h}_{\mathbf{k}+\mathbf{q}, \alpha_1}; \hat{h}_{\mathbf{k}'+\mathbf{q}, \alpha'_1}^\dagger \hat{h}_{\mathbf{k}', \alpha'_2} \rangle\rangle_{\omega}^0 [u_{\sigma_2, \alpha_2}^{\mathbf{k}}]^* u_{\sigma_1 \alpha_1}^{\mathbf{k}+\mathbf{q}} [u_{\sigma'_1, \alpha'_1}^{\mathbf{k}'}]^* u_{\sigma'_2, \alpha'_2}^{\mathbf{k}'} \\ &= \frac{1}{N_s} \sum_{\mathbf{k}} \sum_{\alpha_1 \alpha_2} \frac{[u_{\sigma_2, \alpha_2}^{\mathbf{k}}]^* u_{\sigma_1, \alpha_1}^{\mathbf{k}+\mathbf{q}} [u_{\sigma'_1, \alpha'_1}^{\mathbf{k}+\mathbf{q}}]^* u_{\sigma'_2, \alpha'_2}^{\mathbf{k}}}{\omega - (E_{\mathbf{k}+\mathbf{q}, \alpha_1} - E_{\mathbf{k}, \alpha_2}) + i\delta} [n_{\mathbf{k}, \alpha_2}^0 - n_{\mathbf{k}+\mathbf{q}, \alpha_1}^0], \end{aligned} \quad (5.6.20)$$

where

$$n_{\mathbf{k}, \alpha}^0 = \Theta[E_F - E_{\mathbf{k}, \alpha}] \quad (5.6.21)$$

is the ground-state distribution function (5.3.11). In the same way, we can calculate all other elements of $\tilde{\Pi}^0(\mathbf{q}, \omega)$. The result is always the same as in Eq. (5.6.20) only with additional factors $\sim \epsilon_{\mathbf{k}}^{\sigma \sigma'}$ or $\sim \epsilon_{\mathbf{k}+\mathbf{q}}^{\sigma \sigma'}$ due to the definition of the operators (5.6.12) and (5.6.13). For example, the second element in Eq. (5.6.14) leads to

$$\begin{aligned} & \langle\langle \hat{A}_{\sigma_1 \sigma_2}^{\mathbf{q}}; (\hat{B}_{\sigma_3 \sigma_4, \sigma'_3 \sigma'_4}^{\mathbf{q}})^\dagger \rangle\rangle_{\omega}^0 \\ &= \frac{1}{N_s} \sum_{\mathbf{k}} \sum_{\alpha_1 \alpha_2} \frac{[u_{\sigma_2, \alpha_2}^{\mathbf{k}}]^* u_{\sigma_1, \alpha_1}^{\mathbf{k}+\mathbf{q}} [u_{\sigma'_3, \alpha'_3}^{\mathbf{k}+\mathbf{q}}]^* u_{\sigma'_4, \alpha'_4}^{\mathbf{k}}}{\omega - (E_{\mathbf{k}+\mathbf{q}, \alpha_1} - E_{\mathbf{k}, \alpha_2}) + i\delta} [n_{\mathbf{k}, \alpha_2}^0 - n_{\mathbf{k}+\mathbf{q}, \alpha_1}^0] \times \epsilon_{\mathbf{k}}^{\sigma_3 \sigma_4}. \end{aligned} \quad (5.6.22)$$

To summarize, with Eqs. (5.6.15), (5.6.20) and (5.6.22) and the interaction matrix (D.2.19) we are now in the position to investigate any two-particle response function for our general class of multi-band models (2.4.3). As a first example, we study the magnetic susceptibility for a two-band model in the following chapter.

Chapter 6

Spin Susceptibility in the Time-Dependent Gutzwiller Approximation

As a first application, we calculate the frequency- and momentum-dependent transversal spin susceptibility for the translationally invariant two-band Hubbard model. Based on the spin susceptibility, we calculate the magnetic phase diagrams for different interaction parameters. We calculate the instability of the homogeneous paramagnet towards magnetically and orbitally ordered phases. While the *instability* of the paramagnet in comparison to a ferro- or anti-ferromagnetic state could in principle also be obtained from ground-state calculations, we are now also in the position to investigate the *stability* of the magnetically ordered phases by means of the TDGA. To this end, we prepare a ferromagnetic state and calculate the low-energy excitation spectrum, i.e., the magnon dispersion. We also calculate the high-energy excitation spectrum. The calculations are carried out both in three and infinite spatial dimensions. The results are compared to the corresponding results obtained in the HF approximation.

The results presented in Sections 6.3 and 6.4 shall illustrate the applicability of the TDGA in the context of strongly correlated multi-band systems. They are not meant to reproduce any experimental results in a quantitative manner.

6.1 Interaction Kernel

We consider two degenerate orbitals in a cubic environment. The cubic symmetry affects both the kinetic energy, since the hopping amplitudes are not independent from each other for equivalent directions, and the atomic

Hamiltonian, because the degrees of freedom for the interaction parameters are reduced. We skip the details of the cubic symmetry's influence to Section 6.3 and begin with the symmetry- and dimension-independent second-order expansion of the Lagrange functional.

6.1.1 Specification of Fluctuations

The formalism derived in Chapter 5 and Appendix D is still quite general. In this section, we re-derive the interaction kernels \tilde{K} and \tilde{V} for the two-band Hubbard model. We explicitly take the symmetries of two degenerated orbitals into account.

Since we are interested in magnetic excitations in this chapter, it is useful to classify the elements of the local density matrix by their spin components. To this end, we define the three categories

$$\{C_{i,ab}^{0,s}\} = \{C_{(i,as)(i,ab)}^0\}, \quad a, b = 1, 2 \quad \text{and} \quad s = \uparrow, \downarrow \quad (6.1.1)$$

$$\{C_{i,ab}^{0,+}\} = \{C_{(i,a\uparrow)(i,b\downarrow)}^0\}, \quad a, b = 1, 2 \quad (6.1.2)$$

$$\{C_{i,ab}^{0,-}\} = \{C_{(i,a\downarrow)(i,b\uparrow)}^0\}, \quad a, b = 1, 2 \quad (6.1.3)$$

of local density-matrix elements. We introduce the respective categories of fluctuations

$$\{\delta C_{i,ab}^{0,s}\} = \{\delta \langle \hat{c}_{i,as}^\dagger \hat{c}_{i,bs} \rangle\} \quad (6.1.4)$$

$$\{\delta C_{i,ab}^{0,+}\} = \{\delta \langle \hat{c}_{i,a\uparrow}^\dagger \hat{c}_{i,b\downarrow} \rangle\} \equiv \{\delta S_{i,ab}^+\} \quad (6.1.5)$$

$$\{\delta C_{i,ab}^{0,-}\} = \{\delta \langle \hat{c}_{i,a\downarrow}^\dagger \hat{c}_{i,b\uparrow} \rangle\} \equiv \{\delta S_{i,ab}^-\}, \quad (6.1.6)$$

with the abbreviation $\delta S_{i,ab}^+ = \delta \langle \hat{c}_{i,a\uparrow}^\dagger \hat{c}_{i,b\downarrow} \rangle$ and $\delta S_{i,ab}^- = \delta \langle \hat{c}_{i,a\downarrow}^\dagger \hat{c}_{i,b\uparrow} \rangle$ for the spin-flip components.

Each element of the local density matrix corresponds to a constraint of the form

$$g_{i,\sigma\sigma'} \equiv C_{i\sigma,i\sigma'}^0 - \langle \hat{c}_{i,\sigma}^\dagger \hat{P}_i^\dagger \hat{P}_i \hat{c}_{i,\sigma'} \rangle_{\Phi_0} = 0. \quad (6.1.7)$$

Classifying the constraints by the same criteria as in Eqs. (6.1.4)–(6.1.6), we divide the constraints (3.3.2) into the three sets

$$g_{i,ab}^s \equiv C_{i,(as)(bs)}^0 - \langle \hat{c}_{i,as}^\dagger \hat{P}_i^\dagger \hat{P}_i \hat{c}_{i,bs} \rangle_{\Phi_0} = 0 \quad (6.1.8)$$

$$g_{i,ab}^+ \equiv C_{i,(a\uparrow),(b\downarrow)}^0 - \langle \hat{c}_{i,a\uparrow}^\dagger \hat{P}_i^\dagger \hat{P}_i \hat{c}_{i,b\downarrow} \rangle_{\Phi_0} = 0 \quad (6.1.9)$$

$$g_{i,ab}^- \equiv C_{i,(a\downarrow),(b\uparrow)}^0 - \langle \hat{c}_{i,a\downarrow}^\dagger \hat{P}_i^\dagger \hat{P}_i \hat{c}_{i,b\uparrow} \rangle_{\Phi_0} = 0, \quad (6.1.10)$$

while the local completeness relation is written as

$$g_i^{(1)} \equiv 1 - \langle \hat{P}_i^\dagger \hat{P}_i \rangle_{\Phi_0} = 0. \quad (6.1.11)$$

As each constraint is multiplied by a Lagrange multiplier Λ , we introduce three respective sets of Lagrange parameters

$$\{\Lambda_{ab}^{i,s}\} \quad \text{for the} \quad \{g_{i,ab}^s\} \quad (6.1.12)$$

$$\{\Lambda_{ab}^{i,+}\} \quad \text{for the} \quad \{g_{i,ab}^+\} \quad (6.1.13)$$

$$\{\Lambda_{ab}^{i,-}\} \quad \text{for the} \quad \{g_{i,ab}^-\}. \quad (6.1.14)$$

For the expansion of the Lagrange functional, we denote the fluctuations of the Lagrange multipliers as $\{\delta\Lambda^{i,0}\}$, $\{\delta\Lambda^{i,+}\}$ and $\{\delta\Lambda^{i,-}\}$.

As can be seen from Table 2.5.1, the atomic eigenstates can be classified by the z -component of the total spin (see the last column of Table 2.5.1). We introduce the three classes of local variational parameters $\lambda_{i,\Gamma\Gamma'}$

$$\{\lambda_{i,\Gamma\Gamma'}^0\} \quad \text{for} \quad S_{\text{at},\Gamma}^z - S_{\text{at},\Gamma'}^z = 0 \quad (6.1.15)$$

$$\{\lambda_{i,\Gamma\Gamma'}^\pm\} \quad \text{for} \quad S_{\text{at},\Gamma}^z - S_{\text{at},\Gamma'}^z = \pm 1 \quad (6.1.16)$$

for the different contributions in the Gutzwiller correlator (3.5.1). The fluctuations $\{\delta\lambda_{i,\Gamma\Gamma'}^0\}$, $\{\delta\lambda_{i,\Gamma\Gamma'}^+\}$ and $\{\delta\lambda_{i,\Gamma\Gamma'}^-\}$ corresponding to the aforementioned sets of variational parameters are defined in the same way as for the Lagrange-multiplier fluctuations.

In the following, we introduce one single index γ for index pairs like ab and $\Gamma\Gamma'$, respectively. We then summarize the fluctuations of local density matrix elements and variational parameter fluctuations within the joint variable fluctuations

$$\{\delta A_\gamma^{i,0}\} = \{\delta C_{i,\gamma}^{0,s}, \delta\lambda_{i,\gamma}^0\} \quad (6.1.17)$$

$$\{\delta A_\gamma^{i,+}\} = \{\delta C_{i,\gamma}^{0,+}, \delta\lambda_{i,\gamma}^+\} \quad (6.1.18)$$

$$\{\delta A_\gamma^{i,-}\} = \{\delta C_{i,\gamma}^{0,-}, \delta\lambda_{i,\gamma}^-\}. \quad (6.1.19)$$

Together with the $\{\delta\Lambda^{i,0}\}$, $\{\delta\Lambda^{i,+}\}$ and $\{\delta\Lambda^{i,-}\}$, these are all local fluctuations that enter the expansion of the Lagrange functional.

The local density matrix is Hermitian, and so is the matrix of local variational parameters if we assume a Hermitian Gutzwiller correlator. With the inverse index $\bar{\gamma}$, we can express the Hermiticity of Eq. (3.5.1) as

$$\lambda_{i,\gamma}^* = \lambda_{i,\bar{\gamma}}, \quad (6.1.20)$$

while the Hermiticity of \tilde{C}^0 implies that the constraints $g_{i,\sigma\sigma'}$ can also be regarded as elements of a Hermitian matrix \tilde{g}_i and we therefore find

$$[\Lambda_\gamma^i]^* = \Lambda_{\bar{\gamma}}^i. \quad (6.1.21)$$

All in all, we obtain the useful relations

$$[\delta A_\gamma^{i,\pm}]^* = \delta A_\gamma^{i,\mp} \quad \text{and} \quad [\delta \Lambda_\gamma^{i,\pm}]^* = \delta \Lambda_\gamma^{i,\mp} \quad (6.1.22)$$

for fluctuations of local quantities which will be crucial for the derivation of the interaction kernel in a compact form, see below.

6.1.2 Second-Order Expansion in the Spin-Channel

We start with the Lagrange functional in its general form

$$\begin{aligned} L^{\text{GA}} &= \sum_{i \neq j} \sum_{\substack{ab \\ s}} \sum_{\substack{a's_1 \\ s_1 s_2}} t_{ij}^{ab} q_{i,as}^{a's_1} [q_{j,bs}^{b's_2}]^* \langle \hat{c}_{i,a's_1}^\dagger \hat{c}_{j,b's_2} \rangle + \sum_i E_{i,\text{loc}} \\ &+ \sum_i \left[\Lambda^{i,1} g_i^{(1)} + \sum_{s,\gamma} \Lambda_\gamma^{i,s} g_{i,\gamma}^s + \sum_{i,\gamma} \Lambda_\gamma^{i,+} g_{i,\gamma}^+ + \sum_\gamma \Lambda_\gamma^{i,-} g_{i,\gamma}^- \right] \quad (6.1.23) \\ &\equiv T + L_{\text{loc}} \end{aligned}$$

and allow for fluctuations of both the local quantities defined in the previous section and the expectation values of the non-local hopping processes $\langle \hat{c}_{i,a's_1}^\dagger \hat{c}_{j,b's_2} \rangle$.

The Lagrange functional contains the Lagrange multipliers $\{\Lambda\}$ which must be determined. In Appendix B we derive a scheme to deal with the system of equations

$$\frac{dL^{\text{GA}}}{d\lambda^{0,\pm}} \stackrel{!}{=} 0, \quad (6.1.24)$$

whose solution yields the saddle-point values of the Lagrange multipliers. We find that only the $\{\Lambda^{i,0}\}$ and $\Lambda^{i,1}$ are finite, while the $\{\Lambda^{i,\pm}\}$ vanish.

Since we assume a spin- and orbital-diagonal local density matrix, we have $C_{i\sigma,i\sigma'}^0 = \delta_{\sigma\sigma'} n_{i,\sigma}^0$. Bünemann *et al* stated that a spontaneous local hybridization may only occur for very small Hund's exchange coupling constants J [15], which justifies the assumption of a diagonal local density matrix for the studies of this chapter. Our numerical calculations then show that the diagonality of \tilde{C}^0 leads to a both spin- and orbital-diagonal renormalization matrix \tilde{q} at the saddle point. In order to keep the derivation of the interaction kernel well-structured, we expand the constraints (3.3.1) and (3.3.2), the local interaction energy (3.3.10) and (3.3.11), and the kinetic energy (3.3.22) and (3.3.23) separately. We explicitly show how the diagonality of \tilde{C}^0 and \tilde{q} simplifies the general expressions derived in Appendix D.

The expansion of the local interaction energy and the local constraints only involve the derivatives with respect to variables on the *same* lattice site. It is therefore a straight forward task to expand L_{loc} . The second derivatives

of the local interaction energy with respect to spin-flipping fluctuations are of the form

$$\frac{\partial^2 E_{i,\text{loc}}}{\partial A_{\tilde{\gamma}}^{i,\pm} \partial A_{\tilde{\gamma}'}^{i,\mp}} \neq 0. \quad (6.1.25)$$

For the completeness relation (3.3.1), we find that the diagonality of \tilde{C}^0 yields

$$\frac{\partial^2 g_i^{(1)}}{\partial A_{\tilde{\gamma}}^{i,\pm} \partial A_{\tilde{\gamma}'}^{i,\mp}} \neq 0 \quad (6.1.26)$$

for derivatives with respect to the $\{A^{i,\pm}\}$. The derivatives of the constraints concerning the local density matrix elements, Eq. (3.3.2), with respect to the $\{A^{i,\pm}\}$ turn out to be of the form

$$\frac{\partial g_{i,ab}^{\pm}}{\partial A_{\tilde{\gamma}}^{i,\pm}} \neq 0 \quad \text{and} \quad \frac{\partial^2 g_{i,ab}^s}{\partial A_{\tilde{\gamma}}^{i,\pm} \partial A_{\tilde{\gamma}'}^{i,\mp}} \neq 0. \quad (6.1.27)$$

Although there are also finite derivatives of the form

$$\frac{\partial^2 g_{i,ab}^{\pm}}{\partial A_{\tilde{\gamma}}^{i,0} \partial A_{\tilde{\gamma}'}^{i,\pm}} \neq 0 \quad (6.1.28)$$

mixing spin-conserving and spin-flipping fluctuations, we do not need to take them into account in our expansion, since the corresponding Lagrange multipliers are zero. Any derivatives of the form

$$\frac{\partial^2 E_{i,\text{loc}}}{\partial A_{\tilde{\gamma}}^{i,0} \partial A_{\tilde{\gamma}'}^{i,\pm}} \quad \text{or} \quad \frac{\partial^2 E_{i,\text{loc}}}{\partial A_{\tilde{\gamma}}^{i,\pm} \partial A_{\tilde{\gamma}'}^{i,\pm}} \quad \text{and} \quad \frac{\partial^2 g_i^{(1)}}{\partial A_{\tilde{\gamma}}^{i,0} \partial A_{\tilde{\gamma}'}^{i,\pm}} \quad \text{or} \quad \frac{\partial^2 g_i^{(1)}}{\partial A_{\tilde{\gamma}}^{i,\pm} \partial A_{\tilde{\gamma}'}^{i,\pm}} \quad (6.1.29)$$

also turn out to be zero.

One must also include the mixed terms $\sim \delta A_{\tilde{\gamma}}^i \delta \Lambda_{i,ab}$ in order to ensure that the expansion fulfills the constraints. As only the sets $\{g_{i,ab}^{\pm}\}$ yield finite first derivatives with respect to the $\{A^{i,\pm}\}$, it is sufficient to consider the fluctuations of the $\{\Lambda^{i,\pm}\}$ in the expansion of L .

The expansion of the kinetic energy is more complicated because it contains contributions which couple fluctuations of local variables on *different* lattice sites. Nevertheless, we still can split the expansion into a charge- and a spin-channel due to the diagonality of the renormalization matrix \tilde{q} , which is a direct consequence of the diagonality of \tilde{C}^0 .

We start with the derivatives of the renormalization factors $q_{i,as}^{a's'}$ with respect to the local quantities $\{A^{i,\pm}\}$. We find that—at the saddle point—derivatives of the form

$$\frac{\partial q_{i,a\uparrow}^{a'\downarrow}}{\partial A_\gamma^{i,+}} \neq 0 \quad \text{and} \quad \frac{\partial q_{i,a\downarrow}^{a'\uparrow}}{\partial A_\gamma^{i,-}} \neq 0 \quad \text{and} \quad \frac{\partial^2 q_{i,as}^{a's}}{\partial A_\gamma^{i,\pm} \partial A_{\gamma'}^{i,\mp}} \neq 0 \quad (6.1.30)$$

yield finite contributions, but there are also finite derivatives of the form

$$\frac{\partial^2 q_{i,as}^{a'\bar{s}}}{\partial A_\gamma^{i,0} \partial A_{\gamma'}^{i,\pm}} \neq 0 \quad (6.1.31)$$

mixing the charge- and spin-channel. Fortunately, the diagonality of \tilde{C}^0 and \tilde{q} leads to δ -relations that make all derivatives (6.1.31) dispensable and conserve the partition into the spin- and charge-channel. To address this point, we consider a typical term in the expansion of the kinetic energy

$$t_{ij}^{ab} \delta A_\gamma^i \frac{\partial^2 q_{i,as}^{a's_1}}{\partial A_\gamma^i \partial A_{\gamma'}^i} \delta A_{\gamma'}^i [q_{j,bs}^{b's_2}]^* \langle \hat{c}_{i,a's_1}^\dagger \hat{c}_{j,b's_2} \rangle \quad (6.1.32)$$

and figure out that the diagonality of \tilde{q} yields the factor δ_{ss_2} while the hopping expectation value yields $\delta_{s_1s_2}$, resulting in δ_{ss_1} .

We additionally allow for non-local fluctuations of the one-particle density matrix $\tilde{\rho}$. A typical term of this kind reads

$$t_{ij}^{ab} \delta A_\gamma^{i,+} \frac{\partial q_{i,as}^{a's_1}}{\partial A_\gamma^{i,+}} [q_{j,bs}^{b's_2}]^* \delta \langle \hat{c}_{i,a's_1}^\dagger \hat{c}_{j,b's_2} \rangle, \quad (6.1.33)$$

cf., the first line of Eq.(6.1.23). The diagonality of \tilde{q} yields the factor $\delta_{bb'}$ δ_{ss_2} , the derivative of the renormalization factor on lattice site \mathbf{R}_i yields the factor $\delta_{s\uparrow} \delta_{s_1\downarrow}$. Altogether, Eq.(6.1.33) can be written in the simplified form

$$t_{ij}^{ab} \delta A_\gamma^{i,+} \frac{\partial q_{i,a\uparrow}^{a'\downarrow}}{\partial A_\gamma^{i,+}} [q_{j,b\uparrow}^{b\uparrow}]^* \delta \langle \hat{c}_{i,a'\downarrow}^\dagger \hat{c}_{j,b\uparrow} \rangle \times \delta_{bb'} \delta_{ss_2} \delta_{s\uparrow} \delta_{s_1\downarrow}, \quad (6.1.34)$$

where we now see that the term $\delta \langle \hat{c}_{i,a'\downarrow}^\dagger \hat{c}_{j,b\uparrow} \rangle$ induces a ‘transitive’ spin-flip process with a ‘negative’ sign because the hopping process annihilates the electron with spin $s = \uparrow$ on lattice site \mathbf{R}_j and creates it on lattice site \mathbf{R}_i with spin $s = \downarrow$. An analog analysis for couplings to the $\{\delta A^{i,-}\}$ yields

$$\begin{aligned} & t_{ij}^{ab} \delta A_\gamma^{i,-} \frac{\partial q_{i,as}^{a's_1}}{\partial A_\gamma^{i,-}} [q_{j,bs}^{b's_2}]^* \delta \langle \hat{c}_{i,a's_1}^\dagger \hat{c}_{j,b's_2} \rangle \\ & = t_{ij}^{ab} \delta A_\gamma^{i,-} \frac{\partial q_{i,a\downarrow}^{a'\uparrow}}{\partial A_\gamma^{i,-}} [q_{j,b\downarrow}^{b\downarrow}]^* \delta \langle \hat{c}_{i,a'\uparrow}^\dagger \hat{c}_{j,b\downarrow} \rangle \times \delta_{bb'} \delta_{ss_2} \delta_{s\downarrow} \delta_{s_1\uparrow}, \end{aligned} \quad (6.1.35)$$

leading to a coupling to transitive spin-flip processes with a positive sign.

As we consider translationally invariant systems, all calculations are carried out in momentum space. Applying the Fourier transformation to the local fluctuations, we find for the local fluctuations $\{\delta A^{i,\pm}\}$ and $\{\delta \Lambda^{i,\pm}\}$

$$\delta A_\gamma^{i,\pm} = \frac{1}{\sqrt{N_s}} \sum_{\mathbf{q}} e^{-i\mathbf{R}_i \cdot \mathbf{q}} \delta A_\gamma^{\mathbf{q},\pm} \quad (6.1.36)$$

$$\delta \Lambda_\gamma^{i,\pm} = \frac{1}{\sqrt{N_s}} \sum_{\mathbf{q}} e^{-i\mathbf{R}_i \cdot \mathbf{q}} \delta \Lambda_\gamma^{\mathbf{q},\pm}. \quad (6.1.37)$$

With the ‘local’ part of the Lagrange functional

$$L_{\text{loc}} = \sum_i E_{i,\text{loc}} + \sum_i \left[\Lambda^{i,1} g_i^{(1)} + \sum_\gamma \Lambda_\gamma^{i,+} g_\gamma^{i,+} + \Lambda_\gamma^{i,-} g_\gamma^{i,-} \right], \quad (6.1.38)$$

Eq. (D.1.6) becomes

$$\delta L_{\text{loc}}^{(2)} = \sum_{\mathbf{q}} \sum_{\gamma\gamma'} \delta A_\gamma^{\mathbf{q},+} K_{\gamma\gamma'}^{\text{loc}} \delta A_{\gamma'}^{-\mathbf{q},-} \quad (6.1.39)$$

with the interaction matrix elements

$$K_{\gamma\gamma'}^{\text{loc}} = \frac{\partial^2 L_{\text{loc}}}{\partial A_\gamma^{i,+} \partial A_{\gamma'}^{i,-}} \quad (6.1.40)$$

and the Fourier transforms of the local fluctuations as they were defined in Eq. (6.1.36). The mixed terms connecting fluctuations $\{\delta A^{i,\pm}\}$ and $\{\delta \Lambda^{i,\pm}\}$ arising from the first-order expansion of the constraints (cf., Eq. (D.1.11)) are written as

$$\delta L_c^{(2)} = \sum_{\mathbf{q}} \sum_{\gamma\gamma'} \left[\delta \Lambda_\gamma^{\mathbf{q},-} K_{\gamma\gamma'}^c \delta A_{\gamma'}^{-\mathbf{q},-} + \delta A_\gamma^{\mathbf{q},+} [K_{\bar{\gamma}\bar{\gamma}'}^c]^* \delta \Lambda_{\gamma'}^{-\mathbf{q},+} \right], \quad (6.1.41)$$

with the interaction matrix elements

$$K_{\gamma\gamma'}^c = \frac{\partial g_\gamma^{i,-}}{\partial A_{\gamma'}^{i,-}} = \left[\frac{\partial g_{\bar{\gamma}}^{i,+}}{\partial A_{\bar{\gamma}}^{i,+}} \right]^*, \quad (6.1.42)$$

where the index γ now counts the constraints (6.1.9) and (6.1.10), respectively.

For the expansion of the kinetic energy, we have to address the question how derivatives of renormalization factors $q_{j,bs}^{b's_2}$ and their complex conjugated ones $[q_{j,bs}^{b's_2}]^*$ are related to each other. From the explicit expression for the renormalization factors (3.3.21) we conclude that

$$\frac{\partial [q_{j,bs}^{b's_2}]^*}{\partial A_\gamma^i} = \frac{\partial q_{j,bs}^{b's_2}}{\partial [A_\gamma^i]^*} = \frac{\partial q_{j,bs}^{b's_2}}{\partial A_{\bar{\gamma}}^i}, \quad (6.1.43)$$

and we can therefore write the local part $\delta T_1^{(2)}$ in Eq. (D.1.13) as

$$\delta T_1^{(2)} = \sum_{\mathbf{q}} \sum_{\gamma\gamma'} \delta A_{\gamma}^{\mathbf{q},+} K_{\mathbf{q},\gamma\gamma'}^1 \delta A_{\gamma'}^{-\mathbf{q},-}, \quad (6.1.44)$$

with the \mathbf{q} -dependent interaction-matrix element

$$\begin{aligned} K_{\mathbf{q},\gamma\gamma'}^1 &= \sum_{\substack{aa' \\ bb'}} \sum_s E_{ab,a'b'}^{\bar{s}}(\mathbf{q}) \left[\frac{\partial q_{as}^{a'\bar{s}}}{\partial A_{\gamma}^+} \frac{\partial q_{bs}^{b'\bar{s}}}{\partial A_{\gamma'}^+} + \frac{\partial q_{as}^{a'\bar{s}}}{\partial A_{\gamma}^-} \frac{\partial q_{bs}^{b'\bar{s}}}{\partial A_{\gamma'}^-} \right] \\ &+ \sum_{ab} \sum_s E_{ab,ab}^s \left[\frac{\partial^2 q_{as}^{as}}{\partial A_{\gamma}^+ \partial A_{\gamma'}^-} [q_{bs}^{bs}]^* + q_{as}^{as} \frac{\partial^2 q_{bs}^{bs}}{\partial A_{\gamma}^- \partial A_{\gamma'}^+} \right] \end{aligned} \quad (6.1.45)$$

and the tensor

$$E_{ab,a'b'}^s(\mathbf{q}) = \frac{1}{N_s} \sum_{\mathbf{k}} \varepsilon_{\mathbf{k}+\mathbf{q}}^{ab} \langle \hat{c}_{\mathbf{k},a's}^{\dagger} \hat{c}_{\mathbf{k},b's} \rangle_{\Phi_0}, \quad (6.1.46)$$

which is equivalent to the tensor defined in Eq. (D.1.21). Here, we decomposed the combined spin-orbit indices $\sigma = (as)$ again and kept only the relevant spin-index. The tensor (6.1.46) possesses the symmetry properties

$$E_{ab,a'b'}^s(\mathbf{q}) = E_{ab,a'b'}^s(-\mathbf{q}) \quad (6.1.47)$$

$$E_{ab,a'b'}^s(\mathbf{0}) \equiv E_{ab,ab}^s \times \delta_{aa'} \delta_{bb'}, \quad (6.1.48)$$

which were explicitly used to derive $K_{\mathbf{q},\gamma\gamma'}^1$ in the compact form Eq. (6.1.45). Note that Eq. (6.1.48) does not hold necessarily if systems of lower symmetry are investigated.

The expansion with respect to local and transitive fluctuations has already been sketched in Eq. (6.1.33) and has been carried out explicitly in Eq. (D.1.15). In Eq. (D.2.4), we define two auxiliary fluctuations

$$\delta B_w^{\mathbf{q},+} \equiv \delta B_{ab,a'b'}^{\mathbf{q},+} \equiv \frac{1}{\sqrt{N_s}} \sum_{\mathbf{k}} \varepsilon_{\mathbf{k}}^{ba} \delta \langle \hat{c}_{\mathbf{k},b'\uparrow}^{\dagger} \hat{c}_{\mathbf{k}+\mathbf{q},a'\downarrow} \rangle \quad (6.1.49)$$

$$\delta \bar{B}_w^{\mathbf{q},+} \equiv \delta \bar{B}_{ab,a'b'}^{\mathbf{q},+} \equiv \frac{1}{\sqrt{N_s}} \sum_{\mathbf{k}} \varepsilon_{\mathbf{k}+\mathbf{q}}^{ba} \langle \hat{c}_{\mathbf{k},b'\uparrow}^{\dagger} \hat{c}_{\mathbf{k}+\mathbf{q},a'\downarrow} \rangle \quad (6.1.50)$$

with their Hermitian conjugated counterparts

$$[\delta B_{ab,a'b'}^{\mathbf{q},+}]^{\dagger} = \frac{1}{\sqrt{N_s}} \sum_{\mathbf{k}} \varepsilon_{\mathbf{k}}^{ab} \delta \langle \hat{c}_{\mathbf{k}+\mathbf{q},a'\downarrow}^{\dagger} \hat{c}_{\mathbf{k},b'\uparrow} \rangle \equiv \delta \bar{B}_{ba,b'a'}^{-\mathbf{q},-} \quad (6.1.51)$$

$$[\delta \bar{B}_{ab,a'b'}^{\mathbf{q},+}]^{\dagger} = \frac{1}{\sqrt{N_s}} \sum_{\mathbf{k}} \varepsilon_{\mathbf{k}+\mathbf{q}}^{ab} \langle \hat{c}_{\mathbf{k}+\mathbf{q},a'\downarrow}^{\dagger} \hat{c}_{\mathbf{k},b'\uparrow} \rangle \equiv \delta B_{ba,b'a'}^{-\mathbf{q},-}. \quad (6.1.52)$$

The index $w = (ab, a'b')$ now contains only the orbital indices since we classified the fluctuations $\delta B^{\mathbf{q}}$ and $\delta \bar{B}^{\mathbf{q}}$ by their spin-flipping behavior. The expansion $\delta T_t^{(2)}$ of Eq. (D.1.13) then becomes

$$\begin{aligned} \delta T_1^{(2)} = \sum_{\mathbf{q}} \sum_{\gamma, w} & \left[\delta B_w^{\mathbf{q},+} K_{\gamma w}^{\mathbf{t},1} \delta A_{\gamma}^{-\mathbf{q},-} + \delta \bar{B}_w^{\mathbf{q},+} K_{\gamma w}^{\mathbf{t},2} \delta A_{\gamma}^{-\mathbf{q},-} \right. \\ & \left. + \delta A_{\gamma}^{\mathbf{q},+} [K_{\gamma w}^{\mathbf{t},2}]^* \delta B_w^{-\mathbf{q},-} + \delta A_{\gamma}^{\mathbf{q},+} [K_{\gamma w}^{\mathbf{t},1}]^* \delta \bar{B}_w^{-\mathbf{q},-} \right], \end{aligned} \quad (6.1.53)$$

with the interaction-matrix elements

$$K_{\gamma w}^{\mathbf{t},1} \equiv K_{\gamma, (ab, a'b')}^{\mathbf{t},1} = q_{a\uparrow}^{\alpha\uparrow} \frac{\partial [q_{b\uparrow}^{b'\downarrow}]^*}{\partial A_{\gamma}^+} \delta_{aa'} = q_{a\uparrow}^{\alpha\uparrow} \frac{\partial q_{b\uparrow}^{b'\downarrow}}{\partial A_{\bar{\gamma}}^-} \delta_{aa'} \quad (6.1.54)$$

$$K_{\gamma w}^{\mathbf{t},2} \equiv K_{\gamma, (ab, a'b')}^{\mathbf{t},2} = [q_{b\downarrow}^{b'\uparrow}]^* \frac{\partial q_{a\downarrow}^{a'\uparrow}}{\partial A_{\gamma}^-} \delta_{bb'}. \quad (6.1.55)$$

We finally obtain the second-order expansion in the spin-channel as

$$\delta L^{(2), \text{sc}} = \frac{1}{N_s} \sum_{\mathbf{q}} \begin{pmatrix} \delta \mathbf{A}^{\mathbf{q},+} & \delta \mathbf{B}^{\mathbf{q},+} & \delta \bar{\mathbf{B}}^{\mathbf{q},+} & \delta \mathbf{A}^{\mathbf{q},-} \end{pmatrix} \tilde{K}^{\mathbf{q}} \begin{pmatrix} \delta \mathbf{A}^{-\mathbf{q},-} \\ \delta \bar{\mathbf{B}}^{-\mathbf{q},-} \\ \delta \mathbf{B}^{-\mathbf{q},-} \\ \delta \mathbf{A}^{-\mathbf{q},+} \end{pmatrix}, \quad (6.1.56)$$

where the interaction kernel

$$\tilde{K}^{\mathbf{q}} = \begin{pmatrix} \tilde{K}^{AA} & \tilde{K}^{AB} & \tilde{K}^{A\bar{B}} & \tilde{K}^{A\Lambda} \\ [\tilde{K}^{A\bar{B}}]^{\dagger} & 0 & 0 & 0 \\ [\tilde{K}^{AB}]^{\dagger} & 0 & 0 & 0 \\ [\tilde{K}^{A\Lambda}]^{\dagger} & 0 & 0 & 0 \end{pmatrix} \quad (6.1.57)$$

is composed by the block matrices

$$\tilde{K}^{AA} = \tilde{K}^{\text{loc}} + \tilde{K}_{\mathbf{q}}^1 \quad (6.1.58)$$

$$\tilde{K}^{AB} = \tilde{K}^{\mathbf{t},1} \quad \tilde{K}^{A\bar{B}} = \tilde{K}^{\mathbf{t},2} \quad (6.1.59)$$

$$\tilde{K}^{A\Lambda} = \tilde{K}^{\text{c}}. \quad (6.1.60)$$

Note that, due to the relation $[\delta B_w^{\mathbf{q},+}]^* = \delta \bar{B}_{w'}^{-\mathbf{q},-}$, we had to interchange the order of $\delta B_{w'}^{-\mathbf{q},-}$ and $\delta \bar{B}_w^{\mathbf{q},+}$ in order to ensure that the interaction kernel can be written as a Hermitian matrix.

The representation of the Lagrange-functional expansion (6.1.56) requires that the fluctuations for the two spin-flip signs appear in a fixed order, since we had to interchange derivatives with respect to A_{γ}^+ by derivatives with respect to $A_{\bar{\gamma}}^-$. To this end, we define the index γ' counting the local fluctuations with negative sign by demanding that the relation

$$[\delta A_{\gamma}^{\mathbf{q},+}]^* \equiv \delta A_{\bar{\gamma}}^{-\mathbf{q},-} \stackrel{!}{=} \delta A_{\gamma'}^{-\mathbf{q},-} \quad (6.1.61)$$

holds. In the same manner, we require that the index w' counting the transitive fluctuations with negative signs fulfills the relations

$$[\delta B_w^{\mathbf{q},+}]^* = [\delta B_{ab,a'b'}^{\mathbf{q},+}]^* \equiv \delta \bar{B}_{ba,b'a'}^{-\mathbf{q},-} \stackrel{!}{=} \delta \bar{B}_{w'}^{-\mathbf{q},-} \quad (6.1.62)$$

$$[\delta \bar{B}_w^{\mathbf{q},+}]^* = [\delta \bar{B}_{ab,a'b'}^{\mathbf{q},+}]^* \equiv \delta B_{ba,b'a'}^{-\mathbf{q},-} \stackrel{!}{=} \delta B_{w'}^{-\mathbf{q},-}. \quad (6.1.63)$$

6.1.3 Anti-Adiabaticity and Effective Interaction Kernel

The anti-adiabaticity can now be applied for the $\delta\lambda^{\mathbf{q},+}$, $\delta\Lambda^{\mathbf{q},-}$ and the $\delta\lambda^{-\mathbf{q},-}$, $\delta\Lambda^{-\mathbf{q},+}$ separately. As in Eqs. (D.2.16) and (D.2.17), we decompose the matrices \tilde{K}^{AA} , \tilde{K}^{AB} , $\tilde{K}^{A\bar{B}}$ and $\tilde{K}^{A\Lambda}$ into their components coupling the local density-matrix fluctuations $\delta\mathbf{S}_\gamma^{\pm\mathbf{q},\pm}$ and the local variational-parameter fluctuations $\delta\lambda_\gamma^{\pm\mathbf{q},\pm}$. Requiring

$$\frac{\partial\delta L^{(2),\text{sc}}}{\partial\delta\lambda_\gamma^{\mathbf{q},+}} \stackrel{!}{=} 0 \quad \frac{\partial\delta L^{(2),\text{sc}}}{\partial\delta\Lambda_\gamma^{\mathbf{q},-}} \stackrel{!}{=} 0 \quad (6.1.64)$$

$$\frac{\partial\delta L^{(2),\text{sc}}}{\partial\delta\lambda_\gamma^{-\mathbf{q},-}} \stackrel{!}{=} 0 \quad \frac{\partial\delta L^{(2),\text{sc}}}{\partial\delta\Lambda_\gamma^{-\mathbf{q},+}} \stackrel{!}{=} 0 \quad (6.1.65)$$

yields the two independent systems of equations

$$\begin{pmatrix} \tilde{K}_{\lambda\lambda}^{AA} & \tilde{K}_\lambda^{A\Lambda} \\ [\tilde{K}_\lambda^{A\Lambda}]^\dagger & 0 \end{pmatrix} \begin{pmatrix} \delta\lambda^{-\mathbf{q},-} \\ \delta\Lambda^{-\mathbf{q},+} \end{pmatrix} = - \begin{pmatrix} \tilde{K}_{\lambda S}^{AA} & \tilde{K}_\lambda^{AB} & \tilde{K}_\lambda^{A\bar{B}} \\ [\tilde{K}_S^{A\Lambda}]^\dagger & 0 & 0 \end{pmatrix} \begin{pmatrix} \delta\mathbf{S}^{-\mathbf{q},-} \\ \delta\bar{\mathbf{B}}^{-\mathbf{q},-} \\ \delta\mathbf{B}^{-\mathbf{q},-} \end{pmatrix} \quad (6.1.66)$$

and

$$\begin{pmatrix} \tilde{K}_{\lambda\lambda}^{AA} & \tilde{K}_\lambda^{A\Lambda} \\ [\tilde{K}_\lambda^{A\Lambda}]^\dagger & 0 \end{pmatrix} \begin{pmatrix} \delta\lambda^{\mathbf{q},+} \\ \delta\Lambda^{\mathbf{q},-} \end{pmatrix} = - \begin{pmatrix} \tilde{K}_{\lambda S}^{AA} & \tilde{K}_\lambda^{AB} & \tilde{K}_\lambda^{A\bar{B}} \\ [\tilde{K}_S^{A\Lambda}]^\dagger & 0 & 0 \end{pmatrix} \begin{pmatrix} \delta\mathbf{S}^{\mathbf{q},+} \\ \delta\mathbf{B}^{\mathbf{q},+} \\ \delta\bar{\mathbf{B}}^{\mathbf{q},+} \end{pmatrix}, \quad (6.1.67)$$

where we used the index S instead of ρ in order to emphasize the spin-channel. The correction $\Delta\tilde{V}^{\mathbf{q}}$ in Eq. (D.2.20) then reads

$$\Delta\tilde{V}^{\mathbf{q}} = \begin{pmatrix} [\tilde{K}_{\lambda S}^{AA}]^\dagger & \tilde{K}_S^{A\Lambda} \\ [\tilde{K}_\lambda^{AB}]^\dagger & 0 \\ [\tilde{K}_\lambda^{A\bar{B}}]^\dagger & 0 \end{pmatrix} \times \begin{pmatrix} \tilde{K}_{\lambda\lambda}^{AA} & \tilde{K}_\lambda^{A\Lambda} \\ [\tilde{A}\Lambda_\lambda]^\dagger & 0 \end{pmatrix}^{-1} \times \begin{pmatrix} \tilde{K}_{\lambda S}^{AA} & \tilde{K}_\lambda^{AB} & \tilde{K}_\lambda^{A\bar{B}} \\ [\tilde{K}_S^{A\Lambda}]^\dagger & 0 & 0 \end{pmatrix}. \quad (6.1.68)$$

Finally, the effective interaction kernel is written as

$$\tilde{V}^{\mathbf{q}} = \begin{pmatrix} \tilde{K}_S^{AA} & \tilde{K}_S^{AB} & \tilde{K}_S^{A\bar{B}} \\ [\tilde{K}_S^{AB}]^\dagger & 0 & 0 \\ [\tilde{K}_S^{A\bar{B}}]^\dagger & 0 & 0 \end{pmatrix} - \Delta\tilde{V}^{\mathbf{q}}. \quad (6.1.69)$$

6.2 Transversal Spin Susceptibility

We define the transversal spin-susceptibility for the two-band model with degenerate orbitals. Explicit expressions for the different response functions are derived. The expressions derived in this section remain general, and we will point out which simplifications arise in the limit of infinite spatial dimensions.

6.2.1 Response Functions

In order to calculate response functions for fluctuations in the spin-channel, we define the reduced Green's function matrix as

$$\Pi_{\substack{\gamma, \gamma' \\ (w) (w')}}(\mathbf{q}, \omega) = \begin{pmatrix} \langle\langle \hat{S}_\gamma^{\mathbf{q},+}; \hat{S}_{\gamma'}^{-\mathbf{q},-} \rangle\rangle_\omega & \langle\langle \hat{S}_\gamma^{\mathbf{q},+}; \hat{B}_{w'}^{-\mathbf{q},-} \rangle\rangle_\omega & \langle\langle \hat{S}_\gamma^{\mathbf{q},+}; \hat{B}_{w'}^{-\mathbf{q},-} \rangle\rangle_\omega \\ \langle\langle \hat{B}_w^{\mathbf{q},+}; \hat{S}_{\gamma'}^{-\mathbf{q},-} \rangle\rangle_\omega & \langle\langle \hat{B}_w^{\mathbf{q},+}; \hat{B}_{w'}^{-\mathbf{q},-} \rangle\rangle_\omega & \langle\langle \hat{B}_w^{\mathbf{q},+}; \hat{B}_{w'}^{-\mathbf{q},-} \rangle\rangle_\omega \\ \langle\langle \hat{\hat{B}}_w^{\mathbf{q},+}; \hat{S}_{\gamma'}^{-\mathbf{q},-} \rangle\rangle_\omega & \langle\langle \hat{\hat{B}}_w^{\mathbf{q},+}; \hat{B}_{w'}^{-\mathbf{q},-} \rangle\rangle_\omega & \langle\langle \hat{\hat{B}}_w^{\mathbf{q},+}; \hat{B}_{w'}^{-\mathbf{q},-} \rangle\rangle_\omega \end{pmatrix}. \quad (6.2.1)$$

As in the derivation of the interaction kernel, we interchanged the order of $\hat{B}_{w'}^{-\mathbf{q},-}$ and $\hat{\hat{B}}_w^{\mathbf{q},+}$.

The sets of local operators consist of the intra-orbital and inter-orbital spin-flip operators $\hat{S}^{\mathbf{q},+}$

$$\hat{S}_{aa}^{\mathbf{q},+} = \frac{1}{\sqrt{N_s}} \sum_{\mathbf{k}} \hat{c}_{\mathbf{k},a\uparrow}^\dagger \hat{c}_{\mathbf{k}+\mathbf{q},a\downarrow} \quad (6.2.2)$$

$$\hat{S}_{a\bar{a}}^{\mathbf{q},+} = \frac{1}{\sqrt{N_s}} \sum_{\mathbf{k}} \hat{c}_{\mathbf{k},\bar{a}\uparrow}^\dagger \hat{c}_{\mathbf{k}+\mathbf{q},a\downarrow} \quad (6.2.3)$$

for $a = 1, 2$. The coupling to transitive fluctuations $\delta\mathbf{B}_{ab,a'b'}^{\mathbf{q},+}$ and $\delta\bar{\mathbf{B}}_{ab,a'b'}^{\mathbf{q},+}$ yields a δ -relation for two of their indices, cf., Eqs. (6.1.54) and (6.1.55). The remaining sixteen transitive spin-flip operators are

$$\hat{B}_{ab,a'b}^{\mathbf{q},+} = \frac{1}{\sqrt{N_s}} \sum_{\mathbf{k}} \varepsilon_{\mathbf{k}}^{ba} \hat{c}_{\mathbf{k},b\uparrow}^\dagger \hat{c}_{\mathbf{k}+\mathbf{q},a'\downarrow} \quad (6.2.4)$$

$$\hat{\hat{B}}_{ab,a'b'}^{\mathbf{q},+} = \frac{1}{\sqrt{N_s}} \sum_{\mathbf{k}} \varepsilon_{\mathbf{k}+\mathbf{q}}^{ba} \hat{c}_{\mathbf{k},b'\uparrow}^\dagger \hat{c}_{\mathbf{k}+\mathbf{q},a\downarrow}, \quad (6.2.5)$$

with $a^{(l)}, b^{(l)} = 1, 2$. The Hermitian conjugates of Eqs. (6.2.2)–(6.2.5) yield the corresponding operators with the opposite spin-flip sign.

The diagonalization of the effective one-particle Gutzwiller Hamiltonian

$$\hat{H}_0^{\text{eff}} = \sum_{\mathbf{k}} \sum_{\substack{ab \\ s}} [\bar{\varepsilon}_{\mathbf{k}}^{ab} + \delta_{ab}\eta_{ss}] \hat{c}_{\mathbf{k},as}^\dagger \hat{c}_{\mathbf{k},bs} \equiv \sum_{\mathbf{k}} \sum_{\alpha,s} [E_{\mathbf{k},\alpha s} + \eta_s] \hat{h}_{\mathbf{k},\alpha s}^\dagger \hat{h}_{\mathbf{k},\alpha s} \quad (6.2.6)$$

can be carried out analytically for the two-band model. Due to both the diagonality of the local density matrix \tilde{C}^0 and the orbital degeneracy, we introduce the orbital-independent variational parameter η_s to ensure the conservation of the particle number. Introducing the new parameters

$$\eta^\pm = \eta_\uparrow \pm \eta_\downarrow, \quad (6.2.7)$$

we re-write the spin-dependent part of Eq. (6.2.6)

$$\hat{H}_0^{\text{eff}} = \sum_{\mathbf{k}} \sum_{\alpha,s} [E_{\mathbf{k},\alpha s} + \frac{1}{2}s\eta^-] \hat{h}_{\mathbf{k},\alpha s}^\dagger \hat{h}_{\mathbf{k},\alpha s}. \quad (6.2.8)$$

According to Eqs. (5.6.18) and (5.6.19), the new creation operators are written as

$$h_{\mathbf{k},1s}^\dagger = \sum_a u_{a1}^{\mathbf{k},s} \hat{c}_{\mathbf{k},as}^\dagger = \cos \phi_{\mathbf{k}} \hat{c}_{\mathbf{k},1s}^\dagger + \sin \phi_{\mathbf{k}} \hat{c}_{\mathbf{k},2s}^\dagger \quad (6.2.9)$$

$$h_{\mathbf{k},2s}^\dagger = \sum_a u_{a2}^{\mathbf{k},s} \hat{c}_{\mathbf{k},as}^\dagger = -\sin \phi_{\mathbf{k}} \hat{c}_{\mathbf{k},1s}^\dagger + \cos \phi_{\mathbf{k}} \hat{c}_{\mathbf{k},2s}^\dagger \quad (6.2.10)$$

by means of the real 2×2 rotation matrix $\tilde{u}^{\mathbf{k}}$. The ‘mixing angle’ is obtained from

$$\tan 2\phi_{\mathbf{k}} = \frac{\tilde{\varepsilon}_{\mathbf{k}}^{12} + \tilde{\varepsilon}_{\mathbf{k}}^{21}}{\tilde{\varepsilon}_{\mathbf{k}}^1 - \tilde{\varepsilon}_{\mathbf{k}}^2} = \frac{\varepsilon_{\mathbf{k}}^{12} + \varepsilon_{\mathbf{k}}^{21}}{\varepsilon_{\mathbf{k}}^1 - \varepsilon_{\mathbf{k}}^2}. \quad (6.2.11)$$

Here, we made use of the orbital degeneracy (leading to $q_{1s}^1 \equiv q_{2s}^2$) and the diagonality of \tilde{C}^0 .

In our calculations, we take the viewpoint of the canonical ensemble. The zero of energy is kept fixed for all band fillings and the Fermi energy becomes a function of doping and (in case of ferromagnetism) of the spin-projection s . We calculate the Fermi energies independently for the two spin-projections s by means of the total electron density n_e and the magnetization m per lattice site. The fact that the diagonalization matrix is independent from the renormalization matrix (cf., Eq. (6.2.11)) and therefore independent from the actual interaction parameters, we define a ‘renormalized’ Fermi energy $\tilde{E}_F^s = E_F^s \cdot q_s^2$ and calculate it from

$$n_s = \frac{1}{N_s} \sum_{\mathbf{k}} \sum_{\alpha} \Theta[\tilde{E}_F^s - E_{\mathbf{k},\alpha s}] = \frac{1}{N_s} \sum_{\mathbf{k}} \sum_{\alpha} \Theta[E_F^s - E_{\mathbf{k},\alpha}], \quad (6.2.12)$$

where the relations

$$n_e = n_\uparrow + n_\downarrow \quad \text{and} \quad m = n_\uparrow - n_\downarrow \quad (6.2.13)$$

must be fulfilled. We then obtain η^- as

$$\eta^- = \tilde{E}_F^\uparrow - \tilde{E}_F^\downarrow. \quad (6.2.14)$$

The renormalized Fermi energy depends on the band filling only. The actual Fermi energy that depends on the interaction parameters is then easily calculated by a single minimization with respect to the variational parameters, but not within a self-consistency cycle which would increase the numerical effort.

With the ground state of Eq. (5.6.16), the elements of $\tilde{\Pi}^0$ explicitly read

$$\begin{aligned} & \langle\langle \hat{S}_{ab}^{\mathbf{q},+}; \hat{S}_{a'b'}^{-\mathbf{q},-} \rangle\rangle_{\omega}^0 \\ &= \frac{1}{N_s} \sum_{\mathbf{k}} \sum_{\alpha\beta} [u_{b\beta}^{\mathbf{k},\uparrow} u_{a'\beta}^{\mathbf{k},\uparrow}] [u_{a\alpha}^{\mathbf{k}+\mathbf{q},\downarrow} u_{b'\alpha}^{\mathbf{k}+\mathbf{q},\downarrow}] \frac{n_{\mathbf{k},\beta\uparrow}^0 - n_{\mathbf{k}+\mathbf{q},\alpha\downarrow}^0}{\omega - [E_{\mathbf{k}+\mathbf{q},\alpha\downarrow} - E_{\mathbf{k},\beta\uparrow}] + i\delta} \end{aligned} \quad (6.2.15)$$

$$\begin{aligned} & \langle\langle \hat{S}_{ab}^{\mathbf{q},+}; \hat{B}_{a'b',c'b'}^{-\mathbf{q},-} \rangle\rangle_{\omega}^0 \\ &= \frac{1}{N_s} \sum_{\mathbf{k}} \sum_{\alpha\beta} [u_{b\beta}^{\mathbf{k},\uparrow} u_{c'\beta}^{\mathbf{k},\uparrow}] [u_{a\alpha}^{\mathbf{k}+\mathbf{q},\downarrow} u_{b'\alpha}^{\mathbf{k}+\mathbf{q},\downarrow}] \frac{[n_{\mathbf{k},\beta\uparrow}^0 - n_{\mathbf{k}+\mathbf{q},\alpha\downarrow}^0] \times \varepsilon_{\mathbf{k}+\mathbf{q}}^{b'a'}}{\omega - [E_{\mathbf{k}+\mathbf{q},\alpha\downarrow} - E_{\mathbf{k},\beta\uparrow}] + i\delta} \end{aligned} \quad (6.2.16)$$

$$\begin{aligned} & \langle\langle \hat{S}_{ab}^{\mathbf{q},+}; \hat{B}_{a'b',a'c'}^{-\mathbf{q},-} \rangle\rangle_{\omega}^0 \\ &= \frac{1}{N_s} \sum_{\mathbf{k}} \sum_{\alpha\beta} [u_{b\beta}^{\mathbf{k},\uparrow} u_{c'\beta}^{\mathbf{k},\uparrow}] [u_{a\alpha}^{\mathbf{k}+\mathbf{q},\downarrow} u_{c'\alpha}^{\mathbf{k}+\mathbf{q},\downarrow}] \frac{[n_{\mathbf{k},\beta\uparrow}^0 - n_{\mathbf{k}+\mathbf{q},\alpha\downarrow}^0] \times \varepsilon_{\mathbf{k}}^{b'a'}}{\omega - [E_{\mathbf{k}+\mathbf{q},\alpha\downarrow} - E_{\mathbf{k},\beta\uparrow}] + i\delta} \end{aligned} \quad (6.2.17)$$

$$\begin{aligned} & \langle\langle \hat{B}_{ab,a'b}^{\mathbf{q},+}; \hat{B}_{\tilde{a}\tilde{b},\tilde{a}'\tilde{b}'}^{-\mathbf{q},-} \rangle\rangle_{\omega}^0 \\ &= \frac{1}{N_s} \sum_{\mathbf{k}} \sum_{\alpha\beta} [u_{b\beta}^{\mathbf{k},\uparrow} u_{\tilde{a}'\beta}^{\mathbf{k},\uparrow}] [u_{a'\alpha}^{\mathbf{k}+\mathbf{q},\downarrow} u_{\tilde{b}'\alpha}^{\mathbf{k}+\mathbf{q},\downarrow}] \frac{[n_{\mathbf{k},\beta\uparrow}^0 - n_{\mathbf{k}+\mathbf{q},\alpha\downarrow}^0] \times \varepsilon_{\mathbf{k}}^{ba} \varepsilon_{\mathbf{k}+\mathbf{q}}^{\tilde{b}\tilde{a}}}{\omega - [E_{\mathbf{k}+\mathbf{q},\alpha\downarrow} - E_{\mathbf{k},\beta\uparrow}] + i\delta} \end{aligned} \quad (6.2.18)$$

$$\begin{aligned} & \langle\langle \hat{B}_{ab,a'b}^{\mathbf{q},+}; \hat{B}_{\tilde{a}\tilde{b},\tilde{a}\tilde{b}'}^{-\mathbf{q},-} \rangle\rangle_{\omega}^0 \\ &= \frac{1}{N_s} \sum_{\mathbf{k}} \sum_{\alpha\beta} [u_{b\beta}^{\mathbf{k},\uparrow} u_{\tilde{a}\beta}^{\mathbf{k},\uparrow}] [u_{a'\alpha}^{\mathbf{k}+\mathbf{q},\downarrow} u_{\tilde{b}'\alpha}^{\mathbf{k}+\mathbf{q},\downarrow}] \frac{[n_{\mathbf{k},\beta\uparrow}^0 - n_{\mathbf{k}+\mathbf{q},\alpha\downarrow}^0] \times \varepsilon_{\mathbf{k}}^{ba} \varepsilon_{\mathbf{k}}^{\tilde{b}\tilde{a}}}{\omega - [E_{\mathbf{k}+\mathbf{q},\alpha\downarrow} - E_{\mathbf{k},\beta\uparrow}] + i\delta} \end{aligned} \quad (6.2.19)$$

$$\begin{aligned} & \langle\langle \hat{B}_{ab,a'b'}^{\mathbf{q},+}; \hat{B}_{\tilde{a}\tilde{b},\tilde{a}\tilde{b}'}^{-\mathbf{q},-} \rangle\rangle_{\omega}^0 \\ &= \frac{1}{N_s} \sum_{\mathbf{k}} \sum_{\alpha\beta} [u_{b'\beta}^{\mathbf{k},\uparrow} u_{\tilde{a}\beta}^{\mathbf{k},\uparrow}] [u_{a\alpha}^{\mathbf{k}+\mathbf{q},\downarrow} u_{\tilde{b}'\alpha}^{\mathbf{k}+\mathbf{q},\downarrow}] \frac{[n_{\mathbf{k},\beta\uparrow}^0 - n_{\mathbf{k}+\mathbf{q},\alpha\downarrow}^0] \times \varepsilon_{\mathbf{k}+\mathbf{q}}^{ba} \varepsilon_{\mathbf{k}}^{\tilde{b}\tilde{a}}}{\omega - [E_{\mathbf{k}+\mathbf{q},\alpha\downarrow} - E_{\mathbf{k},\beta\uparrow}] + i\delta}. \end{aligned} \quad (6.2.20)$$

The remaining non-diagonal blocks can be obtained from symmetry considerations.

6.2.2 Phase Diagram

In the first step, we look for instabilities of the homogeneous paramagnet. To reach this goal, one could evaluate the ground-state energy functional for different magnetizations m . As long as only second-order phase transitions are expected, one can alternatively find the instability line also by means of our TDGA.

In general, instabilities are indicated by a divergence of the real part of the response function or—equivalently—as a peak in the imaginary part. Instabilities of the homogeneous paramagnet towards magnetically ordered states are indicated by a divergence of the transversal spin susceptibility

$$\chi(\mathbf{q}, \omega) = \langle\langle \hat{S}_1^{\mathbf{q},+} + \hat{S}_2^{\mathbf{q},+}; \hat{S}_1^{-\mathbf{q},-} + \hat{S}_2^{-\mathbf{q},-} \rangle\rangle_{\omega}. \quad (6.2.21)$$

We can extract $\chi(\mathbf{q}, \omega)$ as the sum of elements of the first ‘block’ of the Green’s function matrix (6.2.1). From Eq. (5.6.15), we conclude that the divergence of $\tilde{\Pi}(\mathbf{q}, \omega)$ corresponds to the non-invertibility of the matrix $[1 + \tilde{\Pi}^0(\mathbf{q}, \omega)\tilde{V}^{\mathbf{q}}]$. Thus, we can alternatively obtain the instabilities if we solve

$$\text{DET}[1 + \tilde{\Pi}^0(\mathbf{q}, \omega)\tilde{V}^{\mathbf{q}}] \stackrel{!}{=} 0 \quad (6.2.22)$$

in dependence of the interaction parameters U , U' and J . The advantage of solving Eq. (6.2.22) instead of calculating the correlated Green’s function matrix is that the numerical effort of the matrix inversion is avoided. For the instability of the homogeneous paramagnet towards a homogeneous ferromagnet, we set $\mathbf{q} = \mathbf{0}$ and, since we are looking for spontaneous symmetry breaking, we additionally set $\omega = 0$. The imaginary part of $\tilde{\Pi}^0$ vanishes then. In order to examine the instability towards incommensurate ordered phases, we solve Eq. (6.2.22) for finite momenta $\mathbf{q} \neq \mathbf{0}$ and $\mathbf{q} \neq (\pi, \pi, \dots)$. For the investigation of the anti-ferromagnetically ordered system, we set $\mathbf{q} = (\pi, \pi, \dots)$. In this way, we look for the minimal interaction strength U that yields an instability towards any magnetically ordered phase.

The formation of an orbitally ordered phase is—besides breaking the spin symmetry—another possibility to lower the system’s energy. This phenomenon can also be observed in the two-site limit of the two-band model, cf., Appendix A.2. Mapping to a Kugel-Khomskii Hamiltonian [78] suggests the formation of an orbitally ordered ferromagnet at quarter filling. We therefore calculate the ground-state energy of the para- and ferromagnetic

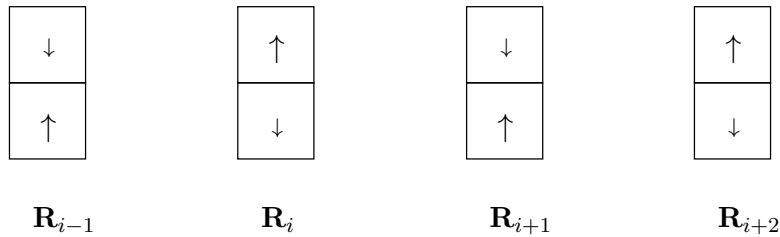


Figure 6.2.1: Schematic sketch of the ferromagnet with ‘anti-ferromagnetic’ orbital order. The gross magnetization is positive on each lattice site, the size of the arrows is proportional to the charge-density in each orbital. From site to site, each orbital takes turn as majority and minority orbital, respectively.

state with an additional ‘anti-ferromagnetic’ orbital order, cf., Fig. 6.2.1. Orbital ordering is a well-known phenomenon in multi-band systems and is already covered within a mean-field treatment [79, 80], with the known shortcoming that the stability of the orbitally ordered phases is over-estimated in comparison to results from the Gutzwiller approach [14]. DMFT calculations on this issue remain ambiguous [81, 82].

6.2.3 Magnon Dispersion and Excitation Spectrum

In the second step, we fix the interaction parameters to some values beyond the instability line of the paramagnet. We fix the elements of the local density matrix \tilde{C}^0 such that the ground-state energy functional is minimal with respect to the magnetization $m = n_{\uparrow}^0 - n_{\downarrow}^0$. To address the question of stability, we calculate the ferromagnetic magnon dispersion. To this end, we solve the equation

$$\text{DET}[1 + \tilde{\Pi}^0(\mathbf{q}, \varepsilon_{\mathbf{q}})\tilde{V}^{\mathbf{q}}] \stackrel{!}{=} 0 \quad (6.2.23)$$

and thus obtain the magnon dispersion $\varepsilon_{\mathbf{q}}$. This approach is valid for finite excitation energies as long as the imaginary part of the uncorrelated response functions is small compared to their real parts. This is the case as long as $\varepsilon_{\mathbf{q}}$ is small. The ferromagnetic state is considered to be stable if the curvature of the dispersion relation is positive. Magnon dispersions can be measured by neutron-scattering experiments. The quality of the choice of interaction parameters can thus be judged by comparison to experimental results.

Furthermore, we are interested in the calculation of high-energy excitation spectra. To this end, we calculate the correlated Green’s function matrix $\tilde{\Pi}(\mathbf{q}, \omega)$ and extract the imaginary part of the Green’s function (6.2.21) for a wide frequency and momentum range.

6.3 Spin Susceptibility in Infinite Dimensions

6.3.1 Model System

We begin our investigations with a two-band model on a hyper-cubic lattice. We keep all terms in the (cubic) interaction Hamiltonian and decouple the two orbitals by introducing the spin- and orbital-diagonal hopping amplitude

$$t_{ij}^{\sigma\sigma'} \equiv t_{ij}^{(bs)(b's')} = \delta_{bb'}\delta_{ss'} t \quad (6.3.1)$$

for nearest-neighbor sites \mathbf{R}_i and \mathbf{R}_j . The band energies then read

$$\varepsilon_{\mathbf{k}}^b = \frac{2t}{\sqrt{2D}} \sum_{n=1}^D \cos k_n \quad (6.3.2)$$

for the two orbitals $b = 1, 2$.

Due to the diagonality of the hopping amplitudes, the effective one-particle Gutzwiller Hamiltonian is already diagonal. The number of fluctuations that have to be taken into account in the calculation of the response functions are therefore reduced. We consider the four local and eight transitive intra-orbital spin-flips only. The effective interaction kernel and the response functions are therefore represented by 6×6 matrices.

The hopping amplitude is scaled $\sim \frac{1}{\sqrt{D}}$ in order to keep the energy expectation values finite in the limit $D \rightarrow \infty$. The limit $D \rightarrow \infty$ requires a special treatment of the \mathbf{k} -space summation. In Appendix F we show how any sum over the first Brillouin zone is replaced by a frequency integral by means of the density of states.

The momentum dependence in infinite spatial dimensions is included in a single scalar quantity $\eta_{\mathbf{q}}$, which is defined as

$$\eta_{\mathbf{q}} = \eta = \lim_{D \rightarrow \infty} \frac{1}{D} \sum_{n=1}^D \cos q_n \quad (6.3.3)$$

and lies within the interval $[-1, 1]$. $\eta_{\mathbf{q}} = +1$ corresponds to $\mathbf{q} = \mathbf{0}$ while $\eta_{\mathbf{q}} = -1$ corresponds to the vector $\mathbf{q} = (\pi, \pi, \dots)$. If $\eta_{\mathbf{q}}$ is used to characterize the ‘ordering vector’ of the system, $\eta_{\mathbf{q}} = +1$ corresponds to a homogeneous para- or ferromagnetic phase while $\eta_{\mathbf{q}} = -1$ indicates an anti-ferromagnetic ordering. Any states with an ordering vector $-1 < \eta_{\mathbf{q}} < +1$ will be denoted as incommensurate phases.

6.3.2 Results

We present numerical results for the models and susceptibilities introduced in the previous sections. Our findings have already been published and

discussed in [83]. First, we present the magnetic phase diagrams for four different ratios of interaction parameters in Fig. 6.3.1. We fix the ratio of J/U to 0.0, 0.1, 0.2 and 0.3, respectively, and carry out the calculations for the second-order phase transitions for different dopings δ . Due to particle-hole symmetry, we restrict ourselves to hole-doping only. We find that, for any J , the half-filled system ($\delta = 0$) undergoes a spontaneous phase transition towards a homogeneous anti-ferromagnet for $U = 0$. For small doping, the homogeneous paramagnet tends to incommensurate phases.

The phase diagram for $J = 0$ is shown in Fig. 6.3.1 a). It does not exhibit a ferromagnetic regime. This result is not surprising since previous variational calculations stated the existence of a critical J to favor itinerant ferromagnetism [7]. The existence of a critical J in a degenerate two-band model was also derived by means of quantum Monte-Carlo simulations within the DMFT [81]. The occurrence of incommensurate phases is restricted to a range of small doping $\delta \lesssim 0.07$ only. At half-filling ($\delta = 0$), previous calculations yield a metal-to-insulator transition (Brinkman–Rice transition) at a critical interaction U_{BR} which is now masked by the anti-ferromagnetic phase. Another localization transition appears for exactly quarter-filled systems, marked by the full square at $\delta = 0.25$. Both metal-to-insulator transitions are of second order for $J = 0$. The transition from the homogeneous paramagnet towards the orbitally ordered phase turns out to be of first order.

For $J/U = 0.1$, the range of incommensurate phases extends over the range from half- to quarter-filling, cf., Fig. 6.3.1 b). The ordering vector increases monotonically from $\eta_{\mathbf{q}} = -1$ to $\eta_{\mathbf{q}} = -0.3$. Within this range, we find also stable ferromagnetism (marked by the dashed line) if the interaction strengths U and J are further increased. The BR transition at half-filling is of first order for all finite J whereas the one at quarter-filling remains continuous also for finite J .

As expected, the boundary of stable ferromagnetism tends to smaller interaction strengths U if the ratio J/U is further increased. The regime of incommensurate ordered phases is restricted to a smaller doping range as illustrated in Fig. 6.3.1 c) for $J/U = 0.2$. At $\delta \approx 0.22$, the borders of the instability of the ferromagnetic phase and the stability of the ferromagnetic phase merge in a Quantum-Lifshitz-Point (QLP), similar to results obtained for the single-band model [84]. For larger doping, the two boundaries coincide until the BR transition sets in. We find an orbitally-ordered phase also for finite J/U masking the BR transition at quarter filling. Within the ferromagnetic state, the transition towards the orbitally ordered phase is

second order for $J/U = 0.2$.

For a ratio $J/U = 0.3$, the boundary of the stable ferromagnet is further shifted to smaller interaction strengths, cf., Fig. 6.3.1 d). The phase diagram exhibits also a QLP where the paramagnetic, the ferromagnetic and the incommensurate phases merge. The large value of J/U leads to the existence of a ferromagnetically ordered phase even for system below quarter-filling. A metal-to-insulator transition has not been found for interaction strengths $U/|t| < 45$. Although not shown in Fig. 6.3.1 d), a transition from the ferromagnetic state towards the orbitally ordered phase is found also for $J/U = 0.3$, and it is found to be of first order in contrast to the result for $J/U = 0.2$.

From Fig. 6.3.1 c) and d) we conclude that the ferromagnet is always stable if the critical interaction strength for $\mathbf{q} = \mathbf{0}$ is smaller than the critical interaction for a phase transition towards incommensurate phases. Furthermore, we find that the occurrence of a paramagnetic insulating phase both at $\delta = 0$ and $\delta = 0.25$ is prevented by either an anti-ferromagnetic or an orbitally ordered phase, similar to DMFT results for a three-band model [85].

For comparison, we present the same phase diagram obtained within HF approximation. In Fig. 6.3.2, we present the boundaries of the paramagnetic, the ferromagnetic and the incommensurate phases for the same interaction parameters as in Fig. 6.3.1. We find that the size of the Hund's exchange coupling influences the phase diagram only quantitatively. The HF approximation predicts phase transitions towards a stable ferromagnetic phase for all values J/U . This result confirms the overestimation of ferromagnetism in mean-field theories which is a known shortcoming of the HF approximation, since it cannot cover the multiplet structure of local electron configurations properly.

In Fig. 6.3.3, we present an example of a momentum- and frequency-dependent excitation spectrum for a ferromagnetic ground state with a magnetization of $n_{\uparrow} - n_{\downarrow} = 0.677$ per lattice site, and the doping is set to $\delta = 0.15$. The interaction parameters are $U/|t| = 10.5$ and $J/U = 0.2$, respectively. The spectrum consists of the low-energy magnon and the high-energy Stoner continuum. For $\eta \rightarrow 1$, the magnon excitation consists of a δ -peak at $\omega \rightarrow 0$ carrying the whole spectral weight, i.e., our calculations recover a Goldstone mode which serves as another consistency check of our formalism, cf., the inset of Fig. 6.3.3. For finite momenta \mathbf{q} (i.e., for $\eta_{\mathbf{q}} < +1$), the peaks appear at positive energies indicating the stability of the ferromagnetic state. The peaks are broadened with increasing momenta and their spectral weights

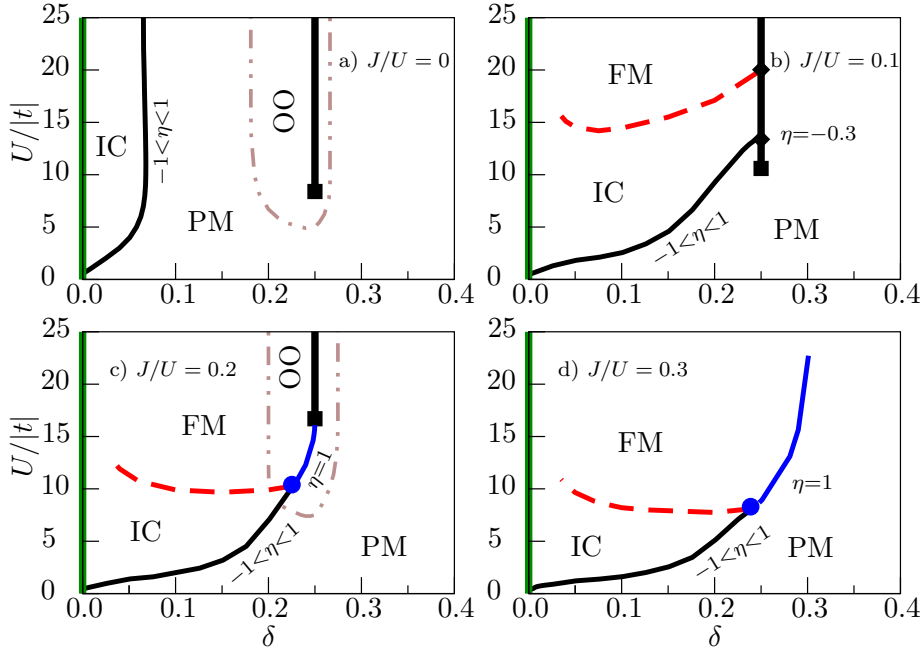


Figure 6.3.1: TDGA magnetic phase diagram for the two-band Hubbard model in infinite spatial dimensions as a function of doping. The solid lines mark second-order transitions from the homogeneous paramagnet (PM) to incommensurate (IC) and ferromagnetic (FM) phases, the thick lines mark the insulating phase due to the BR transition (black) and the anti-ferromagnetic phase (green). The dashed lines mark the boundary of stable ferromagnetism. The dash-dotted lines mark the orbitally ordered (OO) phases.

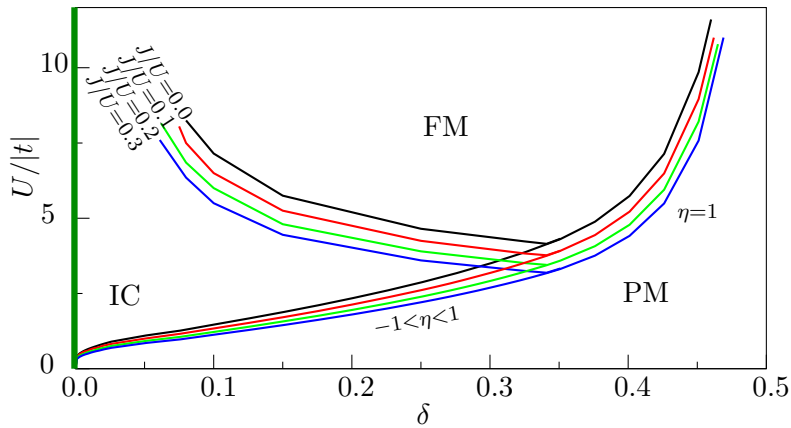


Figure 6.3.2: HF approximation magnetic phase diagram for the same interaction parameters as in Fig. 6.3.1.

decrease rapidly. The spectral weight is shifted to the higher energies where the Stoner continuum evolves with increasing momenta. Its mean position moves to smaller energies with increasing \mathbf{q} and merges with the broadened magnon peaks. The abrupt drop of the spin-wave intensity is also seen in inelastic neutron-scattering experiments and is usually interpreted as the intersection of the spin-wave excitation curve with the excitation continuum [86]. The magnon dispersion is a linear function of $1 - \eta$, i.e., it is quadratic in $|\mathbf{q}|$ for small momenta (cf., Eq. (F.1.11)) as expected for ferromagnetic magnons.

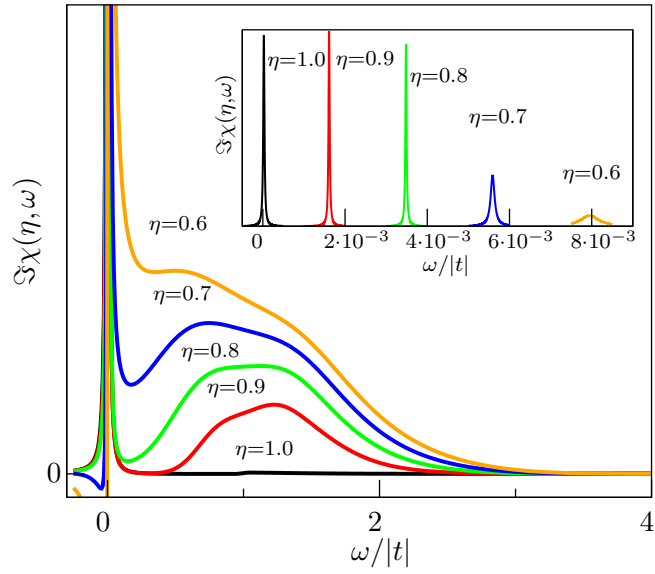


Figure 6.3.3: TDGA excitation spectrum for the stable ferromagnet. The plot displays the imaginary part of the transverse spin-susceptibility $\chi(\eta, \omega)$ obtained within the TDGA in a wide frequency range (main panel) and for small frequencies (input) for various ‘wave vectors’ η . The spectrum consist of the low-energy magnon and the high-energy Stoner continuum excitations. $U/|t| = 10.5$, $J/U = 0.2$, $\delta = 0.15$, $m = 0.677$.

6.4 Spin Susceptibility in Three Dimensions

6.4.1 Model System

We use a tight-binding Hamiltonian with nearest- and next-nearest neighbor hopping as it was already used in [7, 87, 88]. The diagonal hopping matrix elements between the $d_{3z^2-r^2}$ -orbital ($b = 1$) and the $d_{x^2-y^2}$ -orbital ($b = 2$)

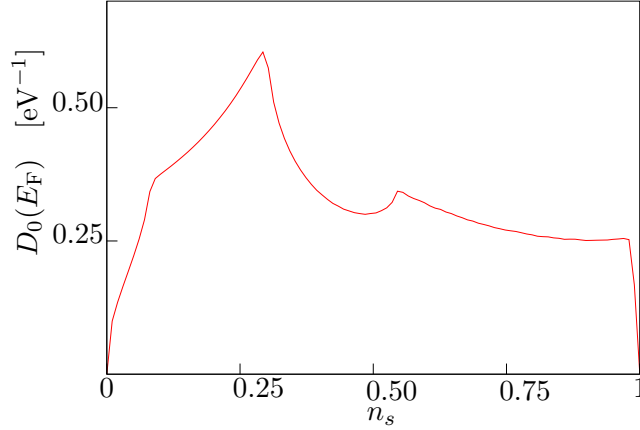


Figure 6.4.1: Density of states at the Fermi edge as a function of band filling n_s for uncorrelated electrons with the hopping parameters given in Table 6.4.1. The half-filled state (one electron per lattice site per orbital per spin direction) corresponds to $n_s = 0.5$.

in momentum space are given as [54]

$$\begin{aligned} \varepsilon_{\mathbf{k}}^{11} \equiv \varepsilon_{\mathbf{k}}^1 &= t_{dd\sigma}^{(1)} \left[\frac{1}{2} \cos k_x + \frac{1}{2} \cos k_y + 2 \cos k_z \right] + \frac{3}{2} t_{dd\delta}^{(1)} [\cos k_x + \cos k_y] \\ &+ t_{dd\sigma}^{(2)} \cos k_x \cos k_y + \left[\frac{1}{4} t_{dd\sigma}^{(2)} + 3t_{dd\pi}^{(2)} \right] [\cos k_x + \cos k_y] \cos k_z \\ &+ 3t_{dd\delta}^{(2)} \left[\cos k_x \cos k_y + \frac{1}{4} \cos k_x \cos k_z + \frac{1}{4} \cos k_y \cos k_z \right] \end{aligned} \quad (6.4.1)$$

$$\begin{aligned} \varepsilon_{\mathbf{k}}^{22} \equiv \varepsilon_{\mathbf{k}}^2 &= \frac{3}{2} t_{dd\sigma}^{(1)} [\cos k_x + \cos k_y] + t_{dd\delta}^{(1)} \left[\frac{1}{2} \cos k_x + \frac{1}{2} \cos k_y + 2 \cos k_z \right] \\ &+ 4t_{dd\pi}^{(2)} \cos k_x \cos k_y + \left[\frac{3}{4} t_{dd\sigma}^{(2)} + t_{dd\pi}^{(2)} + \frac{9}{4} t_{dd\delta}^{(2)} \right] [\cos k_x + \cos k_y] \cos k_z, \end{aligned} \quad (6.4.2)$$

while the band mixing (hybridization) reads

$$\begin{aligned} \varepsilon_{\mathbf{k}}^{12} = \varepsilon_{\mathbf{k}}^{21} &= \frac{\sqrt{3}}{2} [-t_{dd\sigma}^{(1)} + t_{dd\delta}^{(1)}] [\cos k_x - \cos k_y] \\ &+ \left[\frac{\sqrt{3}}{4} t_{dd\sigma}^{(2)} - \sqrt{3} t_{dd\pi}^{(2)} + \frac{3\sqrt{3}}{4} t_{dd\delta}^{(2)} \right] [\cos k_x - \cos k_y] \cos k_z. \end{aligned} \quad (6.4.3)$$

The values for the hopping amplitudes are listed in Table 6.4.1. This special choice of parameters avoids perfect nesting at half-filling and yields a density of states at the Fermi energy that exposes a peak at finite doping. The resulting density of states for electrons without correlation is shown in Fig. 6.4.1.

The local interaction Hamiltonian was introduced in Section 2.5.2, cf., Eq. (2.5.2). The eigenstates and eigenenergies of Eq. (2.5.2) have been listed in Table 2.5.1.

$t_{dd\sigma}^{(1)}$ [eV]	$t_{dd\pi}^{(1)}$ [eV]	$t_{dd\delta}^{(1)}$ [eV]	$t_{dd\sigma}^{(2)}$ [eV]	$t_{dd\pi}^{(2)}$ [eV]	$t_{dd\delta}^{(2)}$ [eV]
-1.0	0.3	-0.1	-0.25	0.075	-0.025

Table 6.4.1: Hopping amplitudes for nearest- ⁽¹⁾ and next-nearest ⁽²⁾ neighbors. The values are taken from [7] according to general experiences for energy bands in transition metals.

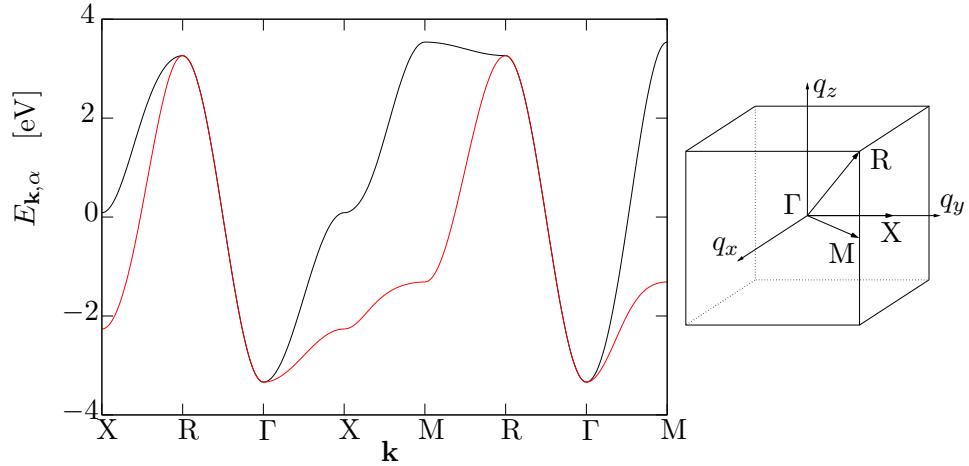


Figure 6.4.2: **Left:** generic dispersion relation for the two-band model in three dimensions along the usual symmetry axis. The zero of energy coincides with the one-particle on-site energies. The total bandwidth is $W = 6.875$ eV. Note the degeneracy along the (ξ, ξ, ξ) -direction. **Right:** sketch of the 1. Brillouin zone with symmetry points.

With the abbreviation $q_{1s}^1 = q_{2s}^2 \equiv q_s$, we can write the resulting eigenenergies as

$$E_{\mathbf{k},1s} = [q_s]^2 [\cos^2 \phi_{\mathbf{k}} \varepsilon_{\mathbf{k}}^1 + \sin^2 \phi_{\mathbf{k}} \varepsilon_{\mathbf{k}}^2 + 2 \sin \phi_{\mathbf{k}} \cos \phi_{\mathbf{k}} \varepsilon_{\mathbf{k}}^{12}] = [q_s]^2 E_{\mathbf{k},1} \quad (6.4.4)$$

$$E_{\mathbf{k},2s} = [q_s]^2 [\sin^2 \phi_{\mathbf{k}} \varepsilon_{\mathbf{k}}^1 + \cos^2 \phi_{\mathbf{k}} \varepsilon_{\mathbf{k}}^2 - 2 \sin \phi_{\mathbf{k}} \cos \phi_{\mathbf{k}} \varepsilon_{\mathbf{k}}^{12}] = [q_s]^2 E_{\mathbf{k},2}. \quad (6.4.5)$$

We plot the eigenenergies $E_{\mathbf{k},\alpha}$ of the Hamiltonian along the usual symmetry axis of a cubic Brillouin zone in Fig. 6.4.2.

Due to the finite hybridization, we must now take inter-orbital spin-flip processes into account in our calculation of the interaction kernel. The set of local spin-flip operators that enter the transversal spin-susceptibility thus are the four intra-orbital operators \hat{S}_{bb}^{\pm} and the four inter-orbital ones \hat{S}_{ab}^{\pm} ,

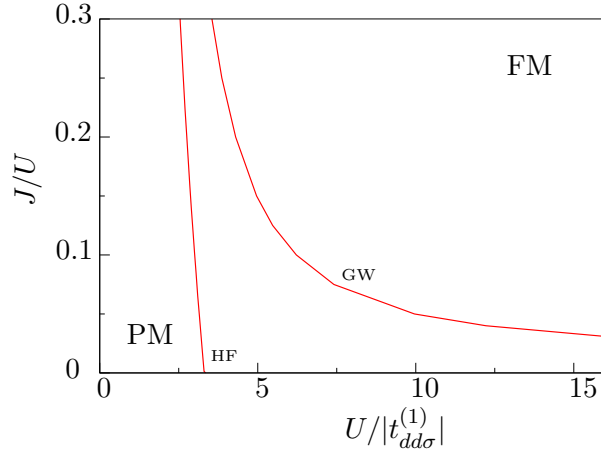


Figure 6.4.3: Borders of stability of the paramagnetic state for the two-band Hubbard model on a three-dimensional simple cubic lattice.

$a, b = 1, 2$. The hybridization also enlarges the number of transitive spin-flip operators $\hat{\mathbf{B}}^{\mathbf{q},\pm}$ and $\hat{\tilde{\mathbf{B}}}^{\mathbf{q},\pm}$ that must be taken into account in order to set up the full Green's function matrix $\tilde{\Pi}$. All in all, 32 transversal fluctuations yield finite contributions in the Lagrange-functional expansion. Hence, the effective interaction kernel and the Green's functions are included into 20×20 matrices.

6.4.2 Results

As can be seen from Fig. 6.4.1, the density of states at the Fermi level exhibits a peak at $n_s \approx 0.30$. The tendency to a spontaneous symmetry breaking towards a ferromagnetic phase is expected to be strongest at that peak. Due to the higher numerical effort, we did not scan the whole doping range. Note that our results have recently been published in [89].

We fix the doping to $n_s = 0.2975$ and calculate the borders of stability of the homogeneous paramagnet both within our TDGA and—for comparison—within HF theory. The curves are plotted in Fig. 6.4.3, where, for fixed n_s and J/U , we calculated the instability as a function of U . The same results have been obtained from ground-state calculations by Bünemann [7] and serve as consistency check here. It were these results that yielded the existence of a critical Hund's exchange coupling J for the occurrence of ferromagnetism within the Gutzwiller theory. In contrast, the HF approximation predicts an instability towards ferromagnetic ordering for *all* values of J . In addition, the J -dependence of the critical U in the HF treatment is almost negligible.

The instability towards the homogeneous ferromagnet is the first second-order phase transition that occurs in our TDGA calculations. In order to investigate the instability towards incommensurate phases, we scanned the \mathbf{q} -space around $\mathbf{q} = \mathbf{0}$ in certain directions, not only along the symmetry lines indicated in Fig. 6.4.2. There were no indicators of a second-order transition towards incommensurate phases before the homogeneous ferromagnet becomes energetically favored. Nevertheless, the ferromagnetic state just beyond the instability of the paramagnet is not stable yet, see below. One possible explanation is that our calculations do not cover possible first-order transitions with finite ordering vectors \mathbf{q} . Another reason for the absence of second-order transitions towards incommensurate phases might result from the finite discretization of the Brillouin zone in three dimensions. We cannot exclude that there are incommensurate phases with a finite ordering vector \mathbf{q} with $|\mathbf{q}| \ll 1$ that could not be resolved within our numerical implementation.

For a comparison of our TDGA to the commonly used HF approximation, we calculate the excitation spectrum of the ferromagnet. In general, both approaches lead to significantly different ground states for a common set of interaction parameters. For a meaningful comparison, we therefore adjust the interaction parameters to values that lead to an almost fully spin-polarized ground state within both techniques. We calculate the spectrum for the two directions $\mathbf{q} = (\xi, 0, 0)$ and $\mathbf{q} = (\xi, \xi, \xi)$, respectively. The spectra are plotted in Figs. 6.4.4 and 6.4.5.

All spectra are composed of the low-energy magnon peaks and the high-energy Stoner continuums. We find that our TDGA yields a Goldstone mode also in finite-dimensional systems. A first difference between the two methods concerns the excitation gap between the magnon and the Stoner excitations. This gap arises from the magnetic band splitting $\eta^- = E_{\text{F}}^{\uparrow} - E_{\text{F}}^{\downarrow}$ which in HF theory is given analytically as $\eta_{\text{HF}}^- = (U + J)m$. Within the TDGA, the band splitting η_{GA}^- is reduced by a factor of ~ 4 . The clear separation of the high-energy Stoner continuum from the low-energy magnon spectrum is therefore lifted, and both parts rapidly merge with increasing momentum transfer within the Gutzwiller approach. Consequently, the peak at $\omega \sim Jm$ corresponding to an inter-orbital spin-flip can only be seen in the time-dependent HF theory while it is covered by the broadening Stoner continuum in the Gutzwiller theory. Note that the overestimation of the excitation gap within time-dependent HF theory is a longstanding shortcoming in solid state theory. For a discussion about it, cf., [90].

In the insets of Figs. 6.4.4 and 6.4.5, we present the magnon dispersion

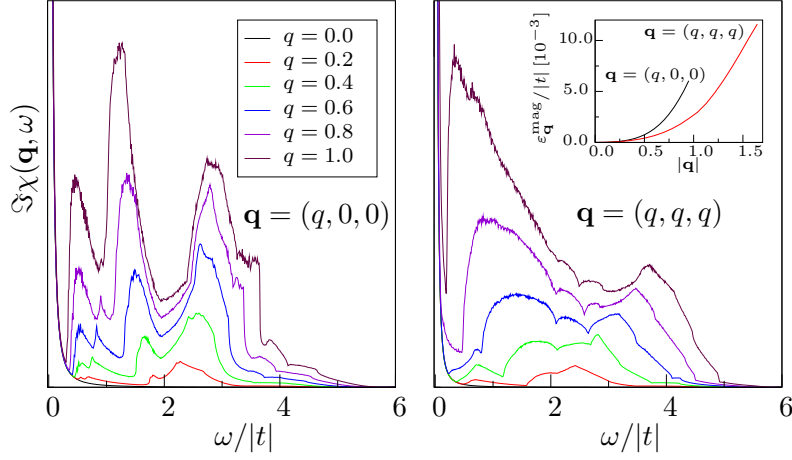


Figure 6.4.4: Gutzwiller excitation spectrum for a ferromagnet with $U/|t| = 10.0$ and $J/U = 0.30$. The ground-state magnetization is $m = 0.5728$ (close to maximum polarization), the excitation gap is $\eta_{\text{GA}}^- = E_{\text{F}}^\uparrow - E_{\text{F}}^\downarrow \approx 2.13 |t|$. The spin-wave stiffness is $D^{100} = 1.34 \times 10^{-3} |t|$ in $(\xi, 0, 0)$ -direction and $D^{111} = 1.30 \times 10^{-3} |t|$ in (ξ, ξ, ξ) -direction, respectively. The lattice constant is set to unity, thus $q_{x,y,z} \in [-\pi, \pi]$, the scaling is $t = t_{dd\sigma}^{(1)}$.

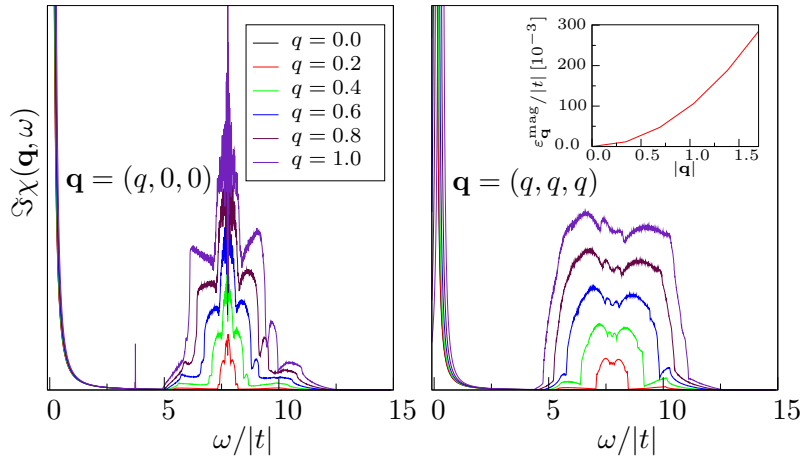


Figure 6.4.5: HF excitations with the same interaction parameters as in Fig. 6.4.4. The resulting ground-state magnetization is $m = 0.5975$ (fully polarized), the excitation gap is $\eta_{\text{HF}}^- \approx 7.77 |t|$. The isotropic spin-wave stiffness turns out to be $D^{100} \approx D^{111} = 100 \times 10^{-3} |t|$. The lattice constant is set to unity, thus $q_{x,y,z} \in [-\pi, \pi]$, the scaling is again $t = t_{dd\sigma}^{(1)}$.

as a function of the absolute value of \mathbf{q} for both the HF theory and the TDGA. The positive curvature indicates the stability of the ferromagnetic phase with respect to the fluctuations. The magnon dispersion in the TDGA exhibits a slight anisotropy. For a quantitative investigation, we calculate the ‘spin-wave stiffness’ D by fitting our numerical results according to

$$\varepsilon_{\mathbf{q}}^{\text{mag}} = D|\mathbf{q}|^2 [1 + \beta|\mathbf{q}|^2]. \quad (6.4.6)$$

Within HF theory, the magnon dispersion seems to be totally isotropic. The magnon excitation energies obtained within the HF theory are larger by nearly two orders of magnitude compared to those from the TDGA. To some extent, this large difference is probably due to the instability towards an incommensurate phase which we found for interaction parameters slightly smaller than those that we used in Fig. 6.4.4.

Chapter 7

Conclusions

7.1 Summary

In this work, we derived the TDGA for multi-band Hubbard models. The importance of the investigation of such models for a proper description of strongly correlated electron systems was motivated in the introduction in Chapter 1. The class of multi-band Hubbard models was derived in Chapter 2. Especially the local interaction Hamiltonian is affected by the multi-orbital character, since the amount of different local electron configurations yields a complex eigenvalue spectrum. We gave a short overview about Gutzwiller wave functions and the minimization scheme of the Gutzwiller energy functional in Chapter 3. In order to prepare the derivation of our new TDGA for multi-band Hubbard models, we derived the conventional RPA as a time-dependent generalization of the HF approximation in Chapter 4. There, we found an effective one-particle Hamiltonian whose ground-state one-particle density matrix obeys the RPA equations for small external perturbations.

In Chapter 5, we gave a detailed derivation of the TDGA for multi-band Hubbard models. To this end, we derived the ‘Gutzwiller Hamiltonian’ as the (first) derivative of the Gutzwiller energy functional with respect to density-matrix elements. In the following, the derivation of the time-dependent Gutzwiller approximation was based on three assumptions: Firstly, we assumed that the dynamics of the Slater determinant, used as starting ansatz for the Gutzwiller wave function, is determined by the effective one-particle ‘Gutzwiller’ Hamiltonian. Secondly, the dynamics of the variational parameters was determined from the assumption that the system is at any instant of time in its minimum with respect to all variational parameters. These assumptions lead to a linear dependence of the variational parameters on density-matrix fluctuations. In the effective interaction

kernel, i. e., the second derivatives of the Gutzwiller energy functional, the variational parameter fluctuations can be re-expressed by the density-matrix fluctuations. Thirdly it was assumed that the external perturbations and the thereby induced fluctuations of the single-particle density matrix are sufficiently small.

In general, the constraints arising from the evaluation of Gutzwiller wave functions in infinite dimensions cannot be fulfilled explicitly. We were thus faced with the question whether the expansion of the corresponding Lagrange functional instead of the Gutzwiller energy functional yields the same interaction kernel. We proved the validity of the Lagrange-functional expansion and presented a simple method how the Lagrange parameters at the saddle point can be calculated from the second-order expansion.

We showed that the resulting theory is consistent in several aspects. A second-order phase transition obtained from pure ground-state calculations is also signalled as instability in our Gutzwiller-RPA approach. Furthermore, we checked that the previous single-band results can be reproduced if we consider two totally decoupled electron bands. In Chapter 6, we applied our formalism to a two-band Hubbard model with two degenerate bands. We calculated magnetic phase diagrams and excitation spectra for various interaction parameters and dopings. In comparison with HF-RPA, our Gutzwiller-RPA approach leads to a more complex interaction kernel and thus to phase diagrams that exhibit a strong interaction dependence. We could further demonstrate that the application of the Gutzwiller-RPA scheme to ferromagnetic ground states leads to the appearance of a Goldstone mode, as expected for systems that break continuous spin symmetry.

We think that we could make plausible that the multi-band TDGA offers a valuable tool for the investigation of the dynamics of strongly correlated multi-band systems.

7.2 Outlook

The formalism derived in this work can straightforwardly be generalized to calculate pair and charge correlation functions for multi-band systems. The knowledge of pair correlation functions is important for the interpretation of Auger spectra, while charge correlations allow for the calculation of optical conductivity and polarizability, for example. Another issue of interest is the application of the TDGA to substances with non-collinear spin structures. In this case, the charge and spin channel are mixed in the second-order expansion, which enlarges the involved matrices and thus increases the numerical effort. Nevertheless, we expect that the resulting RPA equations

remain solvable.

The elimination of the variational parameter fluctuations via the ‘anti-adiabaticity’ condition has recently become obsolete. Schiró and Fabrizio recently developed a fully time-dependent generalization of the Gutzwiller approximation for the single-band model by deriving separate equations of motion for the variational parameters [91, 92]. Their approach allowed for the investigation of quantum quenches, for which the assumption of small amplitudes does not hold anymore. In this context, it will be interesting to study to what extent a fully time-dependent generalization to multi-band Hubbard models can be carried out and whether their approach recovers the previous results in the small-amplitude limit.

Appendix A

Two-Site Hubbard Models

We present exact results on the two-site Hubbard model with one and two orbitals per site, respectively. While the computational effort for the one-orbital model is manageable for all fillings, it exceeds the acceptable framework of this section in the two-orbital case. We thus limit ourselves to the quarter-filled two-orbital model.

A.1 The One-Orbital Model

The local one-band interaction Hamiltonian possesses four local eigenstates. Thus, the Hilbert space associated with the two-site model is 16-dimensional.

The Hubbard Hamiltonian for the two-site model with one orbital per lattice site reads

$$\hat{H}_{2s}^{1b} = t \sum_{s=\uparrow,\downarrow} [\hat{c}_{1,s}^\dagger \hat{c}_{2,s} + \hat{c}_{2,s}^\dagger \hat{c}_{1,s}] + U \sum_{i=1,2} \hat{n}_{i,\uparrow} \hat{n}_{i,\downarrow}. \quad (\text{A.1.1})$$

We denote the vacuum state with no electrons as $|0\rangle = |\circ\rangle_1 |\circ\rangle_2$.

The four local eigenstates of the interaction Hamiltonian $|\circ\rangle_i$, $|\uparrow\rangle_i$, $|\downarrow\rangle_i$ and $|\uparrow\downarrow\rangle_i$ for empty sites, singly and doubly occupied sites, respectively, are used to span the Hilbert space of two-site product states. Multi-particle states are generated by creation operators $\hat{c}_{i,s}^\dagger$ acting on $|0\rangle$. In the following, two-site states will be denoted as $|\cdots\rangle_1 |\cdots\rangle_2$, where the subscript at the ket-vectors labels the lattice site. Table A.1.1 shows the sixteen eigenstates of Eq. (A.1.1).

For $U > 0$ and half-filling, the ground state is a paramagnet described by

$$|\Psi_0^{1b}\rangle = \frac{\cos\phi}{\sqrt{2}} [|\uparrow\rangle_1 |\downarrow\rangle_2 - |\downarrow\rangle_1 |\uparrow\rangle_2] - \frac{\sin\phi}{\sqrt{2}} [|\uparrow\downarrow\rangle_1 |\circ\rangle_2 + |\circ\rangle_1 |\uparrow\downarrow\rangle_2], \quad (\text{A.1.2})$$

with the mixing angle ϕ explained in the caption of Table A.1.1. In the large-coupling limit, the ground-state energy $E_0 = \frac{U - \sqrt{U^2 + 16t^2}}{2}$ tends to $-\frac{4t^2}{U}$ as expected from perturbation theory.

No.	$ \Gamma\rangle$	$E_{ \Gamma\rangle}$
1	$ \circ\rangle_1 \circ\rangle_2$	0
2	$\frac{1}{\sqrt{2}}[\uparrow\rangle_1 + \uparrow\rangle_2]$	$+t$
3	$\frac{1}{\sqrt{2}}[\downarrow\rangle_1 + \downarrow\rangle_2]$	$+t$
4	$\frac{1}{\sqrt{2}}[\uparrow\rangle_1 - \uparrow\rangle_2]$	$-t$
5	$\frac{1}{\sqrt{2}}[\downarrow\rangle_1 - \downarrow\rangle_2]$	$-t$
6	$ \uparrow\rangle_1 \uparrow\rangle_2$	0
7	$\frac{1}{\sqrt{2}}[\uparrow\rangle_1 \downarrow\rangle_2 + \downarrow\rangle_1 \uparrow\rangle_2]$	0
8	$ \downarrow\rangle_1 \downarrow\rangle_2$	0
9	$\frac{1}{\sqrt{2}}[\uparrow\downarrow\rangle_1 - \uparrow\downarrow\rangle_2]$	U
10	$\frac{\cos\phi}{\sqrt{2}}[\uparrow\rangle_1 \downarrow\rangle_2 - \downarrow\rangle_1 \uparrow\rangle_2] + \frac{\sin\phi}{\sqrt{2}}[\uparrow\downarrow\rangle_1 + \uparrow\downarrow\rangle_2]$	$\frac{U + \sqrt{U^2 + 16t^2}}{2}$
11	$\frac{\cos\phi}{\sqrt{2}}[\uparrow\rangle_1 \downarrow\rangle_2 - \downarrow\rangle_1 \uparrow\rangle_2] - \frac{\sin\phi}{\sqrt{2}}[\uparrow\downarrow\rangle_1 + \uparrow\downarrow\rangle_2]$	$\frac{U - \sqrt{U^2 + 16t^2}}{2}$
12	$\frac{1}{\sqrt{2}}[\uparrow\downarrow\rangle_1 \uparrow\rangle_2 + \uparrow\rangle_1 \uparrow\downarrow\rangle_2]$	$U - t$
13	$\frac{1}{\sqrt{2}}[\uparrow\downarrow\rangle_1 \downarrow\rangle_2 + \downarrow\rangle_1 \uparrow\downarrow\rangle_2]$	$U - t$
14	$\frac{1}{\sqrt{2}}[\uparrow\downarrow\rangle_1 \uparrow\rangle_2 - \uparrow\rangle_1 \uparrow\downarrow\rangle_2]$	$U + t$
15	$\frac{1}{\sqrt{2}}[\uparrow\downarrow\rangle_1 \downarrow\rangle_2 - \downarrow\rangle_1 \uparrow\downarrow\rangle_2]$	$U + t$
16	$ \uparrow\downarrow\rangle_1 \uparrow\downarrow\rangle_2$	$2U$

Table A.1.1: The 16 eigenstates $|\Gamma\rangle$ and the corresponding eigenenergies $E_{|\Gamma\rangle}$ of the Hamiltonian (A.1.1) for the two-site model with one orbital per site. The mixing angle ϕ for the last pair of two-electron states is obtained from $\tan 2\phi = \frac{4t}{U}$.

A.2 The Two-Orbital Model

A.2.1 Exact Solution

We calculate the exact eigenstates and eigenenergies of the quarter-filled two-site Hubbard model with two orbitals per lattice site. The Hilbert space of local eigenstates of Eq. (2.5.2) containing zero, one or two electrons

is 11-dimensional. The two-site Hubbard model with two e_g -orbitals per site is described by the Hamiltonian

$$\hat{H}_{2s}^{2b} = t \sum_{\substack{a=1,2 \\ s=\uparrow\downarrow}} [\hat{c}_{1,as}^\dagger \hat{c}_{2,as} + \hat{c}_{2,as}^\dagger \hat{c}_{1,as}] + \sum_{i=1,2} \hat{H}_{i,\text{int}}, \quad (\text{A.2.1})$$

where we assumed an orbital-diagonal hopping amplitude $t_{12}^{\sigma_1\sigma_2} = t_{21}^{\sigma_1\sigma_2} \equiv t \delta_{\sigma_1\sigma_2}$. Following the notation of the previous section, we denote the two-site state with no electrons as $|0\rangle = |\circ, \circ\rangle_1 |\circ, \circ\rangle_2$, where the two states within each ket-vector represent the electronic configuration for the first and the second orbital, respectively, separated by a comma.

There are 28 two-electron eigenstates. They are listed in Table A.2.1 with their corresponding energies. Note that we dropped the ket-vector for empty sites in the product states to keep the notations as clear as possible.

The six mixing angles are obtained from

$$\tan 2\phi_1 = \tan 2\phi_2 = \tan 2\phi_5 = \frac{4t}{U' - J} \quad (\text{A.2.2})$$

$$\tan 2\phi_3 = \frac{4t}{U + J_C} \quad (\text{A.2.3})$$

$$\tan 2\phi_4 = \frac{4t}{U - J_C} \quad (\text{A.2.4})$$

$$\tan 2\phi_6 = \frac{4t}{U' + J}. \quad (\text{A.2.5})$$

Although a two-site model has no cubic symmetry, we restrict to the same interaction parameters that will be used in the calculations on higher-dimensional systems. In particular, we employ the relations $U - U' = 2J$ and $J_C = J$.

With these restrictions, we find for the ground-state energy

$$E_0 = \frac{U' - J - \sqrt{(U' - J)^2 + 16t^2}}{2}, \quad (\text{A.2.6})$$

which turns out to be three-fold degenerate (for finite on-site interactions). The three states associated with E_0 are highlighted with an asterisk. The most general expression for the ground-state wave function at finite interactions is

$$\begin{aligned} |\Psi_0\rangle = & \alpha_1 \left[\frac{\cos \phi_1}{\sqrt{2}} [|\uparrow, \circ\rangle_1 |\circ, \uparrow\rangle_2 - |\circ, \uparrow\rangle_1 |\uparrow, \circ\rangle_2] - \frac{\sin \phi_1}{\sqrt{2}} [|\uparrow, \uparrow\rangle_1 + |\uparrow, \uparrow\rangle_2] \right] \\ & + \alpha_2 \left[\frac{\cos \phi_2}{\sqrt{2}} [|\downarrow, \circ\rangle_1 |\circ, \downarrow\rangle_2 - |\circ, \downarrow\rangle_1 |\downarrow, \circ\rangle_2] - \frac{\sin \phi_2}{\sqrt{2}} [|\downarrow, \downarrow\rangle_1 + |\downarrow, \downarrow\rangle_2] \right] \\ & + \alpha_5 \left[\frac{\cos \phi_5}{2} [|\uparrow, \circ\rangle_1 |\circ, \downarrow\rangle_2 - |\circ, \downarrow\rangle_1 |\uparrow, \circ\rangle_2 + |\downarrow, \circ\rangle_1 |\circ, \uparrow\rangle_2 - |\circ, \uparrow\rangle_1 |\downarrow, \circ\rangle_2] + \right. \\ & \left. - \frac{\sin \phi_5}{2} [|\uparrow, \downarrow\rangle_1 + |\downarrow, \uparrow\rangle_1 + |\uparrow, \downarrow\rangle_2 + |\downarrow, \uparrow\rangle_2] \right], \end{aligned} \quad (\text{A.2.7})$$

with the constraint $|\alpha_1|^2 + |\alpha_2|^2 + |\alpha_5|^2 = 1$. Due to the degeneracy, the resulting ground state can be either para- or ferromagnetic.

No.	$ \Gamma\rangle$	$E_{ \Gamma\rangle}$
1	$ \uparrow, \circ\rangle_1 \uparrow, \circ\rangle_2$	0
2	$ \downarrow, \circ\rangle_1 \downarrow, \circ\rangle_2$	0
3	$ \circ, \uparrow\rangle_1 \circ, \uparrow\rangle_2$	0
4	$ \circ, \downarrow\rangle_1 \circ, \downarrow\rangle_2$	0
5	$\frac{1}{\sqrt{2}} [\uparrow, \circ\rangle_1 \circ, \uparrow\rangle_2 + \circ, \uparrow\rangle_1 \uparrow, \circ\rangle_2]$	0
6	$\frac{1}{\sqrt{2}} [\downarrow, \circ\rangle_1 \circ, \downarrow\rangle_2 + \circ, \downarrow\rangle_1 \downarrow, \circ\rangle_2]$	0
7	$\frac{1}{\sqrt{2}} [\uparrow, \circ\rangle_1 \circ, \downarrow\rangle_2 + \circ, \downarrow\rangle_1 \uparrow, \circ\rangle_2]$	0
8	$\frac{1}{\sqrt{2}} [\downarrow, \circ\rangle_1 \circ, \uparrow\rangle_2 + \circ, \uparrow\rangle_1 \downarrow, \circ\rangle_2]$	0
9	$\frac{1}{\sqrt{2}} [\uparrow, \circ\rangle_1 \downarrow, \circ\rangle_2 + \downarrow, \circ\rangle_1 \uparrow, \circ\rangle_2]$	0
10	$\frac{1}{\sqrt{2}} [\circ, \downarrow\rangle_1 \circ, \uparrow\rangle_2 + \circ, \uparrow\rangle_1 \circ, \downarrow\rangle_2]$	0
11	$\frac{1}{\sqrt{2}} [\uparrow, \uparrow\rangle_1 \circ, \circ\rangle_2 - \circ, \circ\rangle_1 \uparrow, \uparrow\rangle_2]$	$U' - J$
12	$\frac{1}{\sqrt{2}} [\downarrow, \downarrow\rangle_1 \circ, \circ\rangle_2 - \circ, \circ\rangle_1 \downarrow, \downarrow\rangle_2]$	$U' - J$
13	$\frac{1}{2} [\uparrow, \downarrow\rangle_1 + \downarrow, \uparrow\rangle_1 - \uparrow, \downarrow\rangle_2 - \downarrow, \uparrow\rangle_2]$	$U' - J$
14	$\frac{1}{2} [\uparrow, \downarrow\rangle_1 - \downarrow, \uparrow\rangle_1 - \uparrow, \downarrow\rangle_2 + \downarrow, \uparrow\rangle_2]$	$U' + J$
15	$\frac{1}{2} [\uparrow\downarrow, \circ\rangle_1 + \circ, \uparrow\downarrow\rangle_1 - \uparrow\downarrow, \circ\rangle_2 + \circ, \uparrow\downarrow\rangle_2]$	$U + J_C$
16	$\frac{1}{2} [\uparrow\downarrow, \circ\rangle_1 - \circ, \uparrow\downarrow\rangle_1 - \uparrow\downarrow, \circ\rangle_2 - \circ, \uparrow\downarrow\rangle_2]$	$U - J_C$
17	$\frac{\cos \phi_1}{\sqrt{2}} [\uparrow, \circ\rangle_1 \circ, \uparrow\rangle_2 - \circ, \uparrow\rangle_1 \uparrow, \circ\rangle_2] + \frac{\sin \phi_1}{\sqrt{2}} [\uparrow, \uparrow\rangle_1 + \uparrow, \uparrow\rangle_2]$	$\frac{U'-J}{2} + \frac{\sqrt{(U'-J)^2+16t^2}}{2}$
18*	$\frac{\cos \phi_1}{\sqrt{2}} [\uparrow, \circ\rangle_1 \circ, \uparrow\rangle_2 - \circ, \uparrow\rangle_1 \uparrow, \circ\rangle_2] + \frac{\sin \phi_1}{\sqrt{2}} [\uparrow, \uparrow\rangle_1 + \uparrow, \uparrow\rangle_2]$	$\frac{U'-J}{2} + \frac{\sqrt{(U'-J)^2+16t^2}}{2}$
19	$\frac{\cos \phi_2}{\sqrt{2}} [\downarrow, \circ\rangle_1 \circ, \downarrow\rangle_2 - \circ, \downarrow\rangle_1 \downarrow, \circ\rangle_2] + \frac{\sin \phi_2}{\sqrt{2}} [\downarrow, \downarrow\rangle_1 + \downarrow, \downarrow\rangle_2]$	$\frac{U'-J}{2} + \frac{\sqrt{(U'-J)^2+16t^2}}{2}$
20*	$\frac{\cos \phi_2}{\sqrt{2}} [\downarrow, \circ\rangle_1 \circ, \downarrow\rangle_2 - \circ, \downarrow\rangle_1 \downarrow, \circ\rangle_2] + \frac{\sin \phi_2}{\sqrt{2}} [\downarrow, \downarrow\rangle_1 + \downarrow, \downarrow\rangle_2]$	$\frac{U'-J}{2} + \frac{\sqrt{(U'-J)^2+16t^2}}{2}$
21	$\frac{\cos \phi_3}{2} [\uparrow, \circ\rangle_1 \downarrow, \circ\rangle_2 - \downarrow, \circ\rangle_1 \uparrow, \circ\rangle_2 + \circ, \uparrow\rangle_1 \circ, \downarrow\rangle_2 - \circ, \downarrow\rangle_1 \circ, \uparrow\rangle_2] + \frac{\sin \phi_3}{2} [\uparrow\downarrow, \circ\rangle_1 + \circ, \uparrow\downarrow\rangle_1 + \uparrow\downarrow, \circ\rangle_2 + \circ, \uparrow\downarrow\rangle_2]$	$\frac{U+J_C}{2} + \frac{\sqrt{(U+J_C)^2+16t^2}}{2}$
22	$\frac{\cos \phi_3}{2} [\uparrow, \circ\rangle_1 \downarrow, \circ\rangle_2 - \downarrow, \circ\rangle_1 \uparrow, \circ\rangle_2 + \circ, \uparrow\rangle_1 \circ, \downarrow\rangle_2 - \circ, \downarrow\rangle_1 \circ, \uparrow\rangle_2] + \frac{\sin \phi_3}{2} [\uparrow\downarrow, \circ\rangle_1 + \circ, \uparrow\downarrow\rangle_1 + \uparrow\downarrow, \circ\rangle_2 + \circ, \uparrow\downarrow\rangle_2]$	$\frac{U+J_C}{2} + \frac{\sqrt{(U+J_C)^2+16t^2}}{2}$
23	$\frac{\cos \phi_4}{2} [\uparrow, \circ\rangle_1 \downarrow, \circ\rangle_2 - \downarrow, \circ\rangle_1 \uparrow, \circ\rangle_2 + \circ, \uparrow\rangle_1 \circ, \downarrow\rangle_2 + \circ, \downarrow\rangle_1 \circ, \uparrow\rangle_2] + \frac{\sin \phi_4}{2} [\uparrow\downarrow, \circ\rangle_1 - \circ, \uparrow\downarrow\rangle_1 + \uparrow\downarrow, \circ\rangle_2 - \circ, \uparrow\downarrow\rangle_2]$	$\frac{U-J_C}{2} + \frac{\sqrt{(U-J_C)^2+16t^2}}{2}$

No.	$ \Gamma\rangle$	$E_{ \Gamma\rangle}$
24	$\frac{\cos \phi_4}{2} [\uparrow, \circ\rangle_1 \downarrow, \circ\rangle_2 - \downarrow, \circ\rangle_1 \uparrow, \circ\rangle_2 +$ $- \circ, \uparrow\rangle_1 \circ, \downarrow\rangle_2 + \circ, \downarrow\rangle_1 \circ, \uparrow\rangle_2] +$ $-\frac{\sin \phi_4}{2} [\uparrow, \circ\rangle_1 - \circ, \uparrow\rangle_1 + \uparrow, \circ\rangle_2 - \circ, \uparrow\rangle_2]$	$\frac{U-J_C}{2} +$ $-\frac{\sqrt{(U-J_C)^2+16t^2}}{2}$
25	$\frac{\cos \phi_5}{2} [\uparrow, \circ\rangle_1 \circ, \downarrow\rangle_2 - \circ, \downarrow\rangle_1 \uparrow, \circ\rangle_2 +$ $+ \downarrow, \circ\rangle_1 \circ, \uparrow\rangle_2 - \circ, \uparrow\rangle_1 \downarrow, \circ\rangle_2] +$ $+\frac{\sin \phi_5}{2} [\uparrow, \downarrow\rangle_1 + \downarrow, \uparrow\rangle_1 + \uparrow, \downarrow\rangle_2 + \downarrow, \uparrow\rangle_2]$	$\frac{U'-J}{2} +$ $+\frac{\sqrt{(U'-J)^2+16t^2}}{2}$
26*	$\frac{\cos \phi_5}{2} [\uparrow, \circ\rangle_1 \circ, \downarrow\rangle_2 - \circ, \downarrow\rangle_1 \uparrow, \circ\rangle_2 +$ $+ \downarrow, \circ\rangle_1 \circ, \uparrow\rangle_2 - \circ, \uparrow\rangle_1 \downarrow, \circ\rangle_2] +$ $-\frac{\sin \phi_5}{2} [\uparrow, \downarrow\rangle_1 + \downarrow, \uparrow\rangle_1 + \uparrow, \downarrow\rangle_2 + \downarrow, \uparrow\rangle_2]$	$\frac{U'-J}{2} +$ $-\frac{\sqrt{(U'-J)^2+16t^2}}{2}$
27	$\frac{\cos \phi_6}{2} [\uparrow, \circ\rangle_1 \circ, \downarrow\rangle_2 - \circ, \downarrow\rangle_1 \uparrow, \circ\rangle_2 +$ $- \downarrow, \circ\rangle_1 \circ, \uparrow\rangle_2 + \circ, \uparrow\rangle_1 \downarrow, \circ\rangle_2] +$ $+\frac{\sin \phi_6}{2} [\uparrow, \downarrow\rangle_1 - \downarrow, \uparrow\rangle_1 + \uparrow, \downarrow\rangle_2 - \downarrow, \uparrow\rangle_2]$	$\frac{U'+J}{2} +$ $+\frac{\sqrt{(U'+J)^2+16t^2}}{2}$
28	$\frac{\cos \phi_6}{2} [\uparrow, \circ\rangle_1 \circ, \downarrow\rangle_2 - \circ, \downarrow\rangle_1 \uparrow, \circ\rangle_2 +$ $- \downarrow, \circ\rangle_1 \circ, \uparrow\rangle_2 + \circ, \uparrow\rangle_1 \downarrow, \circ\rangle_2] +$ $-\frac{\sin \phi_6}{2} [\uparrow, \downarrow\rangle_1 - \downarrow, \uparrow\rangle_1 + \uparrow, \downarrow\rangle_2 - \downarrow, \uparrow\rangle_2]$	$\frac{U'+J}{2} +$ $-\frac{\sqrt{(U'+J)^2+16t^2}}{2}$

Table A.2.1: The 28 two-electron eigenstates $|\Gamma\rangle$ of the two-site model with two orbitals per site and the corresponding eigenenergies $E_{|\Gamma\rangle}$. The states highlighted with an asterisk mark the three-fold degenerate ground-state energy.

A.2.2 Exact Evaluation of the GW Wave Function

We demonstrate the Gutzwiller scheme for the two-site model of the two-band Hubbard model at quarter-filling. The local interaction Hamiltonian for the two-band model was introduced in Section 2.5.2. Its eigenstates are listed in Table A.2.2.

We will prove now that the Gutzwiller variational scheme yields the exact ground state if the one-particle product state $|\Phi_0\rangle$ is chosen properly. In Appendix A.2.1 we calculated the eigenenergies and eigenstates for the two-site model with a spin- and orbital-diagonal hopping matrix element t analytically. For $U = 0$, it follows $U' = J = J_C = 0$, and the ground state wave function is a linear combination of the states No. 17–28, see Table A.2.1. At finite U , the ground-state wave function is a linear combination of only three states, see Eq. (A.2.7). In the exact solution, the paramagnetic and the ferromagnetic states both have the same energy.

Only the states No. 18 and 20 can be written as one-particle product states, and both states are fully polarized ferromagnets. Without loss of generality, we choose the two-particle state

$$|\Phi_0^{\text{fm}}\rangle = \hat{h}_{1\uparrow}^\dagger \hat{h}_{2\uparrow}^\dagger |\circ\rangle \quad (\text{A.2.8})$$

with the one-particle states

$$\hat{h}_{1\uparrow}^\dagger = \frac{1}{\sqrt{2}}[\hat{c}_{1,1\uparrow}^\dagger - \hat{c}_{2,1\uparrow}^\dagger] \quad (\text{A.2.9})$$

$$\hat{h}_{2\uparrow}^\dagger = \frac{1}{\sqrt{2}}[\hat{c}_{1,2\uparrow}^\dagger - \hat{c}_{2,2\uparrow}^\dagger]. \quad (\text{A.2.10})$$

Here, the spin-symmetry is broken, but the orbital degeneracy is conserved.

For the Gutzwiller correlator $\hat{P}_G \equiv \hat{P}_{1,G}\hat{P}_{2,G}$, we make the simplified ansatz

$$\hat{P}_{i,G} = \lambda_o |o, o\rangle_{ii} \langle o, o| + \lambda_{1\uparrow} |\uparrow, o\rangle_{ii} \langle \uparrow, o| + \lambda_{2\uparrow} |o, \uparrow\rangle_{ii} \langle o, \uparrow| + \lambda_{\uparrow\uparrow} |\uparrow, \uparrow\rangle_{ii} \langle \uparrow, \uparrow| \quad (\text{A.2.11})$$

with lattice-site independent variational parameters.

A straightforward calculation yields that $|\Psi_G\rangle = \hat{P}_G|\Phi_0^{\text{fm}}\rangle$ leads to the exact ground state if we set

$$\lambda_{1\uparrow} = \lambda_{2\uparrow} = \sqrt{\sqrt{2} \cos \phi} \quad \text{and} \quad \lambda_{oo} = \lambda_d = \sqrt{\sqrt{2} |\sin \phi|}, \quad (\text{A.2.12})$$

with the mixing angle $\phi = \phi_1 = \phi_2 = \phi_5$ defined in Eq. (A.2.2). Hence, $|\Psi_G\rangle$ yields the same energy expectation value

$$E_0^{\text{GA}} = \frac{U' - J - \sqrt{(U' - J)^2 + 16t^2}}{2} \quad (\text{A.2.13})$$

for all interactions.

A.2.3 Comparison of the Exact Solution to the GA

As we have seen in the previous section, the exact evaluation of the Gutzwiller wave function for the two-site two-band model at quarter filling yields the exact ground state. In this section we compare the exact ground-state energy to the energy that we obtain within the GA. From Eq. (A.2.13) we see that the relevant interaction parameter is $U' - J = \tilde{U}$. We introduce the one-particle states

$$\hat{h}_{bs}^\dagger = \frac{1}{\sqrt{2}}[\hat{c}_{1,bs}^\dagger - \hat{c}_{2,bs}^\dagger] \quad (\text{A.2.14})$$

and define the two product states

$$|\Phi_0^{\text{pm}}\rangle = \hat{h}_{1\uparrow}^\dagger \hat{h}_{2\downarrow}^\dagger |o\rangle \quad (\text{A.2.15})$$

$$|\Phi_0^{\text{fm}}\rangle = \hat{h}_{1\uparrow}^\dagger \hat{h}_{2\uparrow}^\dagger |o\rangle \quad (\text{A.2.16})$$

$$(\text{A.2.17})$$

in order to set up the para- and ferromagnetic Gutzwiller wave functions $|\Psi_G^{\text{pm/fm}}\rangle$.

No.	$ \Gamma\rangle$	E_Γ	$\lambda_{\Gamma\Gamma}$
1	$ \circ, \circ\rangle$	0	λ_\circ
2	$ \uparrow, \circ\rangle$	0	$\lambda_{1\uparrow}$
3	$ \circ, \uparrow\rangle$	0	$\lambda_{2\uparrow}$
4	$ \downarrow, \circ\rangle$	0	$\lambda_{1\downarrow}$
5	$ \circ, \downarrow\rangle$	0	$\lambda_{2\downarrow}$
6	$ \uparrow, \uparrow\rangle$	$U' - J$	$\lambda_{\uparrow\uparrow}$
7	$\frac{1}{\sqrt{2}} [\uparrow, \downarrow\rangle + \downarrow, \uparrow\rangle]$	$U' - J$	$\lambda_{\uparrow\downarrow,+}$
8	$ \downarrow, \downarrow\rangle$	$U' - J$	$\lambda_{\downarrow\downarrow}$
9	$\frac{1}{\sqrt{2}} [\uparrow, \downarrow\rangle - \downarrow, \uparrow\rangle]$	$U' + J$	$\lambda_{\uparrow\downarrow,-}$
10	$\frac{1}{\sqrt{2}} [\uparrow\downarrow, \circ\rangle - \circ, \uparrow\downarrow\rangle]$	$U - J_C$	$\lambda_{d,-}$
11	$\frac{1}{\sqrt{2}} [\uparrow\downarrow, \circ\rangle + \circ, \uparrow\downarrow\rangle]$	$U + J_C$	$\lambda_{d,+}$

Table A.2.2: The zero-, one- and two-particle eigenstates $|\Gamma\rangle$ and their energies E_Γ . The last column contains the diagonal variational parameters associated with the corresponding states as they are used to set up the Gutzwiller correlator.

For $J = 0$, the paramagnetic and the ferromagnetic state are degenerate. In contrast to the exact solution, an infinitesimal Hund's exchange coupling J favors the formation of the ferromagnetic state in the GA. The energy of the system maybe lowered if we lift the orbital degeneracy, depending on the size of U' and J . To this end, we introduce the one-particle states

$$\hat{h}_{1\uparrow}^\dagger = [\cos \theta \hat{c}_{1,1\uparrow}^\dagger + \sin \theta \hat{c}_{2,1\uparrow}^\dagger] \quad (\text{A.2.18})$$

$$\hat{h}_{2\uparrow}^\dagger = [\sin \theta \hat{c}_{1,2\uparrow}^\dagger + \cos \theta \hat{c}_{2,2\uparrow}^\dagger] \quad (\text{A.2.19})$$

and define the orbitally-ordered ferromagnetic state

$$|\Phi_0^{\text{fm},\circ}\rangle = \hat{h}_{1\uparrow}^\dagger \hat{h}_{2\uparrow}^\dagger |\circ\rangle. \quad (\text{A.2.20})$$

The 'sublattice magnetization' Δ is defined as

$$\Delta = \langle \hat{n}_{1,1\uparrow} - \hat{n}_{2,1\uparrow} \rangle_{\Phi_0^{\text{fm},\circ}} = -\langle \hat{n}_{1,2\uparrow} - \hat{n}_{2,2\uparrow} \rangle_{\Phi_0^{\text{fm},\circ}} = \cos 2\theta. \quad (\text{A.2.21})$$

The minimization of the Gutzwiller ground-state energy functional with respect to Δ then allows for the determination of the occurrence of the orbitally-ordered state. In Fig. A.2.1 we plot the exact ground-state energy,

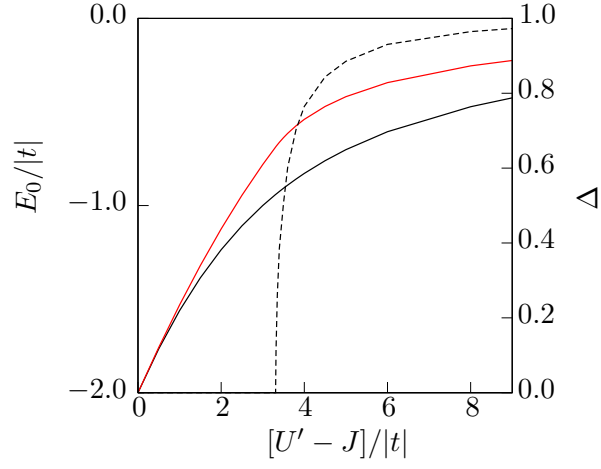


Figure A.2.1: Exact ground-state energy (black) and the GA energy (red) of the quarter-filled two-site model. The dashed line shows the sublattice magnetization Δ .

the GA energy and the sublattice magnetization in a common plot. The critical interaction strength \tilde{U}_c for the occurrence of the orbitally-ordered state is about a factor ~ 1.6 larger than the corresponding value in HF approximation, where the same orbital order is observed.

Appendix B

Determination of Lagrange parameters

B.1 Pseudo-Inverse Matrix

Since we expand the Lagrange functional L^{GA} instead of the energy functional in Section 5.5, we must determine the values of the Lagrange parameters Λ_n at the saddle point from the requirement

$$\frac{dL^{\text{GA}}}{d\lambda_\gamma} \stackrel{!}{=} 0 \quad \forall \gamma = 1 \dots n_\lambda \quad (\text{B.1.1})$$

or (in matrix notation)

$$\tilde{G}\mathbf{\Lambda} = -\mathbf{e}, \quad (\text{B.1.2})$$

where $\mathbf{\Lambda}$ contains the n_{con} Lagrange parameters. The $n_\lambda \times n_{\text{con}}$ matrix \tilde{G} is set up by the derivatives of the constraints and the r.h.s. vector \mathbf{e} contains the derivatives of the energy.

The existence of a stable ground state implies that Eq. (B.1.2) has at least one solution. There are two difficulties in solving Eq. (B.1.2):

- In general, there are more equations than constraints/Lagrange parameters: $n_\lambda > n_{\text{con}}$ or even $n_\lambda \gg n_{\text{con}}$.
- Round-off errors from the numerical minimization might lead to (analytically) unsolvable systems of equations.

To deal with these problems, we do not solve Eq. (B.1.2), but the—in case of unique resolvability—equivalent equation

$$\tilde{G}^T \tilde{G} \mathbf{\Lambda} = -\tilde{G}^T \mathbf{e} \quad (\text{B.1.3})$$

which is known to be solvable in any cases (not necessarily uniquely). If the matrix \tilde{G} has full rank (which can be checked easily by calculating its singular values), one can define the so-called ‘Moore–Penrose matrix inverse’ \tilde{G}^\dagger according to

$$\tilde{G}^\dagger = [\tilde{G}^T \tilde{G}]^{-1} \tilde{G}^T, \quad (\text{B.1.4})$$

which is known to yield the best approximation $\mathbf{\Lambda}^+$ to Eq. (B.1.2) via

$$\mathbf{\Lambda}^+ = -\tilde{G}^\dagger \mathbf{e}. \quad (\text{B.1.5})$$

The term ‘best approximation’ means that the error $\Delta_{\mathbf{x}}$ defined as

$$\Delta_{\mathbf{x}} = |\mathbf{x} + \tilde{G}\mathbf{e}| \quad (\text{B.1.6})$$

takes its minimal value for $\mathbf{x} = \mathbf{\Lambda}^+$. In the special case that Eq. (B.1.2) possesses a unique solution (which we expect physically), the solution $\mathbf{\Lambda}^+$ of Eq. (B.1.4) coincides with the one of Eq. (B.1.2). If Eq. (B.1.2) is not resolvable exactly due to numerical uncertainties of a certain order, the error of $\mathbf{\Lambda}$ is expected to be in the same order of magnitude. Hence, the strategy sketched here offers an appropriate and easy-to-use method to obtain the Lagrange parameters. For more profound statements on pseudo-inverse matrices, cf., [93].

Appendix C

Invariance of the Second-Order Expansions

C.1 Equivalence of the Lagrange-Functional Expansion

In this section, we show that the interaction kernel $\bar{K}_{YY'}^{\rho\rho}$, in Eq. (5.5.8) obtained from the second-order expansion of the Lagrange functional (LF) is identical to $K_{YY'}^{\rho\rho}$, in Eqs. (5.4.9) and (5.4.10). To this end, we choose again some arbitrary independent and dependent variational parameters λ_Z^i and λ_X^d , cf., Eq. (5.2.4). By construction, the constraints (5.2.3) are automatically fulfilled as a function of $\vec{\lambda}^i$ and $\vec{\rho}$, i.e., we have

$$g_n(\vec{\lambda}^d(\vec{\lambda}^i, \vec{\rho}), \vec{\lambda}^i, \vec{\rho}) = 0. \quad (\text{C.1.1})$$

Consequently, all first or higher-order derivatives of Eq. (C.1.1) with respect to λ_Z^i and ρ_Y vanish. For example, the first-order derivatives lead to

$$\frac{dg_n}{d\lambda_Z^i} = \frac{\partial g_n}{\partial \lambda_Z^i} + \sum_X \frac{\partial g_n}{\partial \lambda_X^d} \frac{\partial \lambda_X^d}{\partial \lambda_Z^i} = 0 \quad (\text{C.1.2})$$

$$\frac{dg_n}{d\rho_Y} = \frac{\partial g_n}{\partial \rho_Y} + \sum_X \frac{\partial g_n}{\partial \lambda_X^d} \frac{\partial \lambda_X^d}{\partial \rho_Y} = 0. \quad (\text{C.1.3})$$

Using the matrices

$$G_{nX} \equiv \frac{\partial g_n}{\partial \lambda_X^d}, \quad R_{XZ} \equiv \frac{\partial \lambda_X^d}{\partial \lambda_Z^i} \quad \text{and} \quad Q_{XY} \equiv \frac{\partial \lambda_X^d}{\partial \rho_Y}, \quad (\text{C.1.4})$$

we can write Eqs. (C.1.2) and (C.1.3) as

$$\frac{\partial g_n}{\partial \lambda_Z^i} = -[\tilde{G}\tilde{R}]_{nZ} \quad (\text{C.1.5})$$

$$\frac{\partial g_n}{\partial \rho_Y} = -[\tilde{G}\tilde{Q}]_{nY}. \quad (\text{C.1.6})$$

With the classification of dependent and independent variables we are in the position to evaluate the anti-adiabaticity conditions (5.5.6) and (5.5.7). First, Eq. (5.5.6) leads to

$$\sum_X \frac{\partial g_n}{\partial \lambda_X^d} \delta \lambda_X^d + \sum_Z \frac{\partial g_n}{\partial \lambda_Z^i} \delta \lambda_Z^i + \sum_Y \frac{\partial g_n}{\partial \rho_Y} \delta \rho_Y = 0 \quad (\text{C.1.7})$$

which, together with Eqs. (C.1.5) and (C.1.6), yields

$$\tilde{G} \left[\delta \vec{\lambda}^d - \tilde{R} \delta \vec{\lambda}^i - \tilde{Q} \delta \vec{\rho} \right] = \vec{0}. \quad (\text{C.1.8})$$

Since the square matrix \tilde{G} should be invertible, the bracket in Eq. (C.1.8) must vanish, and we find the relation

$$\delta \vec{\lambda}^d = \tilde{R} \delta \vec{\lambda}^i + \tilde{Q} \delta \vec{\rho}, \quad (\text{C.1.9})$$

which determines the dependent-parameters fluctuations $\delta \vec{\lambda}^d$ as a function of $\delta \vec{\lambda}^i$ and $\delta \vec{\rho}$.

Applying the separation of dependent and independent parameter fluctuations to the Eqs. (5.5.7) yields

$$\begin{pmatrix} \tilde{A}^T \\ \tilde{G}^T \end{pmatrix} \delta \vec{\Lambda} = - \begin{pmatrix} \tilde{L}^{ii} & \tilde{L}^{id} \\ \tilde{L}^{di} & \tilde{L}^{dd} \end{pmatrix} \begin{pmatrix} \delta \vec{\lambda}^i \\ \delta \vec{\lambda}^d \end{pmatrix} \begin{pmatrix} \tilde{L}^{i\rho} \\ \tilde{L}^{d\rho} \end{pmatrix} \delta \vec{\rho}, \quad (\text{C.1.10})$$

with $\tilde{A} = -\tilde{G}\tilde{R}$. Here we introduced the six matrices

$$L_{ZZ'}^{ii} \equiv \frac{\partial^2 L^{\text{GA}}}{\partial \lambda_Z^i \partial \lambda_{Z'}^i}, \quad L_{ZX}^{\text{id}} \equiv \frac{\partial^2 L^{\text{GA}}}{\partial \lambda_Z^i \partial \lambda_X^d}, \quad L_{XZ}^{\text{di}} \equiv \frac{\partial^2 L^{\text{GA}}}{\partial \lambda_X^d \partial \lambda_Z^i} \quad (\text{C.1.11})$$

$$L_{X'X'}^{\text{dd}} \equiv \frac{\partial^2 L^{\text{GA}}}{\partial \lambda_{X'}^d \partial \lambda_{X'}^d}, \quad L_{ZY}^{\text{i}\rho} \equiv \frac{\partial^2 L^{\text{GA}}}{\partial \lambda_Z^i \partial \rho_Y}, \quad L_{XY}^{\text{d}\rho} \equiv \frac{\partial^2 L^{\text{GA}}}{\partial \lambda_X^d \partial \rho_Y} \quad (\text{C.1.12})$$

of second derivatives. With Eq. (C.1.9) and the second ‘row’ of Eqs. (C.1.10) one can write the Lagrange-parameter fluctuations as a function of $\delta \vec{\lambda}^i$ and $\delta \vec{\rho}$,

$$\delta \vec{\Lambda} = - \left[\tilde{G}^T \right]^{-1} \left[\left[\tilde{L}^{\text{di}} + \tilde{L}^{\text{dd}} \tilde{R} \right] \delta \vec{\lambda}^i + \left[\tilde{L}^{\text{dd}} \tilde{Q} + \tilde{L}^{\text{d}\rho} \right] \delta \vec{\rho} \right]. \quad (\text{C.1.13})$$

Inserting this expression into the first row of Eqs. (C.1.10) we eventually find

$$\begin{aligned} \delta\vec{\lambda}^i = & - \left[\tilde{L}^{ii} + \tilde{L}^{id}\tilde{R} + \tilde{R}^T + \tilde{R}^T\tilde{L}^{dd}\tilde{R} \right]^{-1} \\ & \times \left[\tilde{L}^{i\rho} + \tilde{L}^{id}\tilde{Q} + \tilde{R}^T\tilde{L}^{d\rho} + \tilde{R}^T\tilde{L}^{dd}\tilde{Q} \right] \delta\vec{\rho}. \end{aligned} \quad (\text{C.1.14})$$

Equations (C.1.9), (C.1.13) and (C.1.14) now enable us to write all fluctuations $\delta\vec{\lambda}^i$, $\delta\vec{\lambda}^d$ and $\delta\vec{\Lambda}$ as functions of the density fluctuations $\delta\vec{\rho}$. These relations can be inserted into the second-order expansion of the Lagrange functional

$$\begin{aligned} 2\delta L^{(2)} = & (\delta\vec{\rho})^T \tilde{L}^{\rho\rho} \delta\vec{\rho} + (\delta\vec{\lambda}^i)^T \tilde{L}^{ii} \delta\vec{\lambda}^i + (\delta\vec{\lambda}^d)^T \tilde{L}^{dd} \delta\vec{\lambda}^d \\ & + (\delta\vec{\rho})^T \tilde{L}^{\rho d} \delta\vec{\lambda}^d + (\delta\vec{\rho})^T \tilde{L}^{\rho i} \delta\vec{\lambda}^i + (\delta\vec{\lambda}^i)^T \tilde{L}^{id} \delta\vec{\lambda}^d \\ & + (\delta\vec{\lambda}^d)^T \tilde{L}^{di} \delta\vec{\lambda}^i + (\delta\vec{\lambda}^d)^T \tilde{L}^{d\rho} \delta\vec{\rho} + (\delta\vec{\lambda}^i)^T \tilde{L}^{i\rho} \delta\vec{\rho} \\ & + 2(\delta\vec{\Lambda})^T \tilde{G} [\delta\vec{\lambda}^d - \tilde{R}\delta\vec{\lambda}^i - \tilde{Q}\delta\vec{\rho}] \end{aligned} \quad (\text{C.1.15})$$

in order to calculate $\bar{K}_{Y'Y'}^{\rho\rho}$, in Eq. (5.5.8). However, to prove just the identity of $\bar{K}_{Y'Y'}^{\rho\rho}$ and $K_{Y'Y'}^{\rho\rho}$, in Eq. (5.4.9) it is sufficient to apply only Eq. (C.1.9) to the expansion (C.1.15). This leads to

$$\begin{aligned} 2\delta L^{(2)} = & (\delta\vec{\rho})^T [\tilde{L}^{\rho\rho} + \tilde{Q}^T\tilde{L}^{d\rho} + \tilde{L}^{\rho d}\tilde{Q} + \tilde{Q}^T\tilde{L}^{dd}\tilde{Q}] \delta\vec{\rho} \\ & + (\delta\vec{\lambda}^i)^T [\tilde{L}^{ii} + \tilde{L}^{id}\tilde{R} + \tilde{R}^T\tilde{L}^{di} + \tilde{R}^T\tilde{L}^{dd}\tilde{R}] \delta\vec{\lambda}^i \\ & + (\delta\vec{\rho})^T [\tilde{L}^{\rho i} + \tilde{L}^{\rho i}\tilde{R} + \tilde{Q}^T\tilde{L}^{di} + \tilde{Q}^T\tilde{L}^{dd}\tilde{R}] \delta\vec{\lambda}^i \\ & + (\delta\vec{\lambda}^i)^T [\tilde{L}^{i\rho} + \tilde{R}^T\tilde{L}^{i\rho} + \tilde{L}^{id}\tilde{Q} + \tilde{R}^T\tilde{L}^{dd}\tilde{Q}] \delta\vec{\rho}. \end{aligned} \quad (\text{C.1.16})$$

As we will show below, the matrices (5.4.2)–(5.4.4) which determine the second-order expansion (5.4.5) are the same as the corresponding matrices in Eq. (C.1.16). Hence, we have

$$\delta E^{(2)} = \delta L^{(2)}. \quad (\text{C.1.17})$$

Since the anti-adiabaticity condition

$$\frac{\partial \delta E^{(2)}}{\partial \delta \lambda_Z^i} = \frac{\partial \delta L^{(2)}}{\partial \delta \lambda_Z^i} = 0 \quad (\text{C.1.18})$$

for $\delta E^{(2)}$ reproduces Eq. (C.1.14), the identity of $\bar{K}_{Y'Y'}^{\rho\rho}$ and $K_{Y'Y'}^{\rho\rho}$ is then finally demonstrated.

It remains to be shown that the matrices (5.4.2)–(5.4.4) agree with those in Eq. (C.1.16). To this end, we use the explicit form Eq. (5.2.5) of the energy functional (5.2.1) that appears in the definition of the matrices (5.4.2)–(5.4.4). As an example, we consider the matrix $\tilde{M}^{\rho\rho}$ and show that it is

identical to the matrix in the first line of Eq. (C.1.16). With similar derivations one can prove the same for the other matrices (5.4.3), (5.4.4) and their counterparts in Eq. (C.1.16).

Using Eqs. (5.2.5) and (5.4.2) we find

$$M_{YY'}^{\rho\rho} = [\tilde{E}^{\rho\rho} + \tilde{Q}^T \tilde{E}^{\text{d}\rho} + \tilde{E}^{\rho\text{d}} \tilde{Q} + \tilde{Q}^T \tilde{E}^{\text{dd}} \tilde{Q}]_{YY'} + 2 \sum_X \frac{\partial E}{\partial \lambda_X^{\text{d}}} \frac{\partial^2 \lambda_X^{\text{d}}}{\partial \rho_Y \partial \rho_{Y'}}. \quad (\text{C.1.19})$$

Here, the matrices

$$\tilde{E}^{\alpha\beta} = \tilde{L}^{\alpha\beta} - \sum_n \Lambda_n \tilde{g}_n^{\alpha\beta} \quad \text{and} \quad \tilde{g}_n^{\alpha\beta} \quad (\text{C.1.20})$$

with $\alpha\beta \in \{\rho\rho, \text{d}\rho, \rho\text{d}, \text{dd}\}$ are defined as in Eq. (C.1.11) only with L^{GA} replaced by E or g_n , respectively. Obviously, the matrix in the first line of Eq. (C.1.16) is identical to $\tilde{M}^{\rho\rho}$ if

$$2 \sum_X \frac{\partial E}{\partial \lambda_X^{\text{d}}} \frac{\partial^2 \lambda_X^{\text{d}}}{\partial \rho_Y \partial \rho_{Y'}} = - \sum_n \Lambda_n [\tilde{g}_n^{\rho\rho} + \tilde{Q}^T \tilde{g}_n^{\text{d}\rho} + \tilde{g}_n^{\rho\text{d}} \tilde{Q} + \tilde{Q}^T \tilde{g}_n^{\text{dd}} \tilde{Q}]_{YY'}. \quad (\text{C.1.21})$$

To prove Eq. (C.1.21), we use the fact that the second (total) derivatives of Eq. (C.1.1) with respect to the densities ρ_Y vanish:

$$\frac{\text{d}^2 g_n}{\text{d}\rho_Y \text{d}\rho_{Y'}} = [\tilde{g}_n^{\rho\rho} + \tilde{Q}^T \tilde{g}_n^{\text{d}\rho} + \tilde{g}_n^{\rho\text{d}} \tilde{Q} + \tilde{Q}^T \tilde{g}_n^{\text{dd}} \tilde{Q}]_{YY'} + 2 \sum_X \frac{\partial g_n}{\partial \lambda_X^{\text{d}}} \frac{\partial^2 \lambda_X^{\text{d}}}{\partial \rho_Y \partial \rho_{Y'}} = 0. \quad (\text{C.1.22})$$

Equation (C.1.21) is therefore fulfilled if

$$\sum_X \left[\frac{\partial E}{\partial \lambda_X^{\text{d}}} + \sum_n \Lambda_n \frac{\partial g_n}{\partial \lambda_X^{\text{d}}} \right] \frac{\partial^2 \lambda_X^{\text{d}}}{\partial \rho_Y \partial \rho_{Y'}} = 0. \quad (\text{C.1.23})$$

This equation, however, holds trivially, since Eq. (5.5.2) leads to

$$\frac{\partial L^{\text{GA}}}{\partial \lambda_Z} = \frac{\partial E}{\partial \lambda_Z} + \sum_n \Lambda_n \frac{\partial g_n}{\partial \lambda_Z} = 0 \quad (\text{C.1.24})$$

for all parameters λ_Z and in particular for $\lambda_Z = \lambda_X^{\text{d}}$ as it appears in Eq. (C.1.24).

C.2 Linear Transformations of the Density Matrix

In investigations of our translationally invariant lattice systems Eq. (2.4.3), it turns out to be more convenient to work with fluctuations $\delta\vec{\mu}$ which are linearly related to the density-matrix fluctuations,

$$\delta\vec{\rho} = \tilde{\Xi} \cdot \delta\vec{\mu}, \quad (\text{C.2.1})$$

cf., Eqs. (D.2.4) and (D.2.5) and the resulting Green's function matrix in Eq. (5.6.14). The effective second-order functional (5.4.9) and (5.4.10) in terms of the fluctuations $\delta\vec{\mu}$ is then given as

$$\delta E^{(2)}(\delta\vec{\mu}) = \frac{1}{2}(\delta\vec{\mu})^T \tilde{\Xi}^T \tilde{K}^{\rho\rho} \tilde{\Xi} \delta\vec{\mu}, \quad (\text{C.2.2})$$

with $\tilde{K}^{\rho\rho}$ as defined in Eq. (5.4.10). For numerical calculations it is important to show that one obtains the same kernel

$$\tilde{K}^{\mu\mu} \equiv \tilde{\Xi}^T \tilde{K}^{\rho\rho} \tilde{\Xi} \quad (\text{C.2.3})$$

as in Eq. (C.2.2) if the transformation Eq. (C.2.1) and the anti-adiabaticity condition are applied in the reverse order: If we apply Eq. (C.2.1) first to Eq. (5.4.5), we obtain

$$\delta E^{(2)} = \frac{1}{2} \left[(\delta\vec{\mu})^T \tilde{\Xi}^T \tilde{M}^{\rho\rho} \tilde{\Xi} \delta\vec{\mu} + 2(\delta\vec{\lambda}^i)^T \tilde{M}^{\lambda\rho} \tilde{\Xi} \delta\vec{\mu} + (\delta\vec{\lambda}^i)^T \tilde{M}^{\lambda\lambda} \delta\vec{\lambda}^i \right]. \quad (\text{C.2.4})$$

The anti-adiabaticity condition for $\delta\vec{\mu}$ then reads

$$\delta\vec{\lambda}^i = -[\tilde{M}^{\lambda\lambda}]^{-1} \tilde{M}^{\lambda\rho} \tilde{\Xi} \delta\vec{\mu}. \quad (\text{C.2.5})$$

Inserted into Eq. (C.2.4) this equation yields

$$\begin{aligned} \delta E^{(2)}(\delta\vec{\mu}) &= E_0 + \frac{1}{2}(\delta\vec{\mu})^T \tilde{K}^{\mu\mu} \delta\vec{\mu} \\ \tilde{K}^{\mu\mu} &= \tilde{\Xi}^T \tilde{M}^{\rho\rho} \tilde{\Xi} - \tilde{\Xi}^T \tilde{M}^{\rho\lambda} \left[\tilde{M}^{\lambda\lambda} \right]^{-1} \tilde{M}^{\lambda\rho} \tilde{\Xi} = \tilde{\Xi}^T \tilde{K}^{\rho\rho} \tilde{\Xi}, \end{aligned} \quad (\text{C.2.6})$$

as claimed above.

Appendix D

Explicit Form of the Second-Order Expansion

We calculate the second-order expansion of the Lagrange functional with respect to the variational parameters $\lambda_{i,\Gamma'}$ and the density matrix (4.1.2). For the general consideration in Chapter 5 and Appendix C it was convenient to subsume the parameters $\lambda_{\Gamma'}$ and their conjugates $\lambda_{\Gamma'}^*$ in a set of n_p parameters λ_Z , cf., Eq. (5.2.2). In this appendix, where we aim to resolve the explicit structure of the second-order expansion, it is better to take the difference between $\lambda_{\Gamma'}$ and $\lambda_{\Gamma'}^*$ into account.

D.1 Local Fluctuations

The constraints (3.3.1) and (3.3.2), the local energy (3.3.10) and (3.3.11), and the renormalization matrix (3.3.20) are all functions only of $\lambda_{i,\Gamma'}^*$, $\lambda_{i,\Gamma'}$ and of the local density matrix elements $C_{i\sigma,i\sigma'}^0$. For simplicity, we use the joint variables A_v^i and $(A_v^i)^*$ for all these local variables, i.e., it is either

$$A_v^i = A_{\sigma_1,\sigma_2}^i = \langle \hat{c}_{i,\sigma_2}^\dagger \hat{c}_{i,\sigma_1} \rangle \quad \text{or} \quad A_v^i = A_{\Gamma'}^i = \lambda_{i,\Gamma'}. \quad (\text{D.1.1})$$

With respect to the parameters $\lambda_{i,\Gamma'}^*$ and $\lambda_{i,\Gamma'}$, the second derivatives of Eqs. (3.3.1), (3.3.2), (3.3.10), (3.3.11) and (3.3.20) are quadratic functions of the form $\sim (A_v^i)^* A_v^i$. Due to the Hermiticity of the density matrix the same can be achieved for derivatives with respect to the local density matrix. Then the only finite second derivatives of the Lagrange functional

$$\begin{aligned} L^{\text{GA}} &= T + \sum_i E_{i,\text{loc}}(\{(A_v^i)^*\}, \{A_v^i\}) + \sum_{i,n} \Lambda_{i,n} g_{i,n}(\{(A_v^i)^*\}, \{A_v^i\}) \\ &\equiv T + L_{\text{loc}}, \end{aligned} \quad (\text{D.1.2})$$

with the kinetic energy

$$T = \sum_{i \neq j} \sum_{\substack{\sigma_1 \sigma_2 \\ \sigma'_1 \sigma'_2}} t_{ij}^{\sigma_1 \sigma_2} q_{i, \sigma_1}^{\sigma'_1} [q_{j, \sigma_2}^{\sigma'_2}]^* \langle \hat{c}_{i \sigma'_1}^\dagger \hat{c}_{j \sigma'_2} \rangle_{\Phi_0}, \quad (\text{D.1.3})$$

are

$$\frac{\partial^2 L^{\text{GA}}}{\partial (A_v^i)^* \partial A_{v'}^i} \neq 0, \quad (\text{D.1.4})$$

whereas

$$\frac{\partial^2 L^{\text{GA}}}{\partial (A_v^i)^* \partial (A_{v'}^i)^*} = \frac{\partial^2 L^{\text{GA}}}{\partial A_v^i \partial A_{v'}^i} = 0. \quad (\text{D.1.5})$$

Since only local fluctuations δA_v^i couple in the expressions for the local energy and the constraints, their second-order expansion is a straightforward task leading to

$$\delta L_{\text{loc}}^{(2)} = \sum_{\mathbf{q}} \sum_{vv'} (\delta A_v^{\mathbf{q}})^* K_{vv'}^{\text{loc}} \delta A_{v'}^{\mathbf{q}}, \quad (\text{D.1.6})$$

where we introduced

$$K_{vv'}^{\text{loc}} = \frac{\partial^2 L_{\text{loc}}}{\partial (A_v^i)^* \partial A_{v'}^i} \quad (\text{D.1.7})$$

and the Fourier transforms of the local fluctuations

$$\delta A_v^i = \frac{1}{\sqrt{N_s}} \sum_{\mathbf{q}} e^{-i\mathbf{R}_v \cdot \mathbf{q}} \delta A_v^{\mathbf{q}}. \quad (\text{D.1.8})$$

All derivatives in this section (e.g., Eq. (D.1.7)) have to be evaluated for the ground-state values of the variational parameters $\lambda_{i, \Gamma \Gamma'}$, the density matrix $\tilde{\rho}$ and the Lagrange parameters $\Lambda_{i, n}$. Note that the density-matrix fluctuations $\delta A_{\sigma_2, \sigma_1}^{\mathbf{q}}$ can be written as

$$\begin{aligned} \delta A_{\sigma_2, \sigma_1}^{\mathbf{q}} &= \frac{1}{\sqrt{N_s}} \sum_i e^{i\mathbf{R}_i \cdot \mathbf{q}} \delta \langle \hat{c}_{i, \sigma_1}^\dagger \hat{c}_{i, \sigma_2} \rangle = \frac{1}{\sqrt{N_s}} \sum_{\mathbf{k}} \delta \langle \hat{c}_{\mathbf{k}, \sigma_1}^\dagger \hat{c}_{\mathbf{k} + \mathbf{q}, \sigma_2} \rangle \\ &= \delta \langle \hat{A}_{\sigma_2, \sigma_1}^{\mathbf{q}} \rangle, \end{aligned} \quad (\text{D.1.9})$$

where the operator $\hat{A}_v^{\mathbf{q}}$ has been defined in Eq. (5.6.5).

In addition to Eq. (D.1.6), we need to take into account the mixed terms $\sim \delta A_v^i \delta \Lambda_{i, n}$. In real space, their contribution is given as

$$\delta L_c^{(2)} = \sum_{i, n, v} \left(\frac{\partial g_{i, n}}{\partial (A_v^i)^*} \delta (A_v^i)^* + \frac{\partial g_{i, n}}{\partial A_v^i} \delta A_v^i \right) \delta \Lambda_{i, n}. \quad (\text{D.1.10})$$

If we introduce the Fourier transforms $\delta \Lambda_n^{\mathbf{q}}$ of the fluctuations $\delta \Lambda_{i, n}$, we can write Eq. (D.1.10) as

$$\delta L_c^{(2)} = \sum_{\mathbf{q}} \sum_{n, v} (\delta A_v^{\mathbf{q}})^* K_{vn}^c \delta \Lambda_n^{\mathbf{q}} + (\delta \Lambda_n^{\mathbf{q}})^* (K_{vn}^c)^* \delta A_v^{\mathbf{q}}. \quad (\text{D.1.11})$$

Here, we used that the constraints $g_{i,n}$ are assumed to be real and lattice-site independent such that

$$K_{vn}^c \equiv \frac{\partial g_{i,n}}{\partial (A_v^i)^*} = \left[\frac{\partial g_{i,n}}{\partial A_v^i} \right]^*. \quad (\text{D.1.12})$$

More involved than the calculation of Eq. (D.1.6) is the expansion of the kinetic energy. Here we find

$$\delta T^{(2)} = \delta T_1^{(2)} + \delta T_t^{(2)}, \quad (\text{D.1.13})$$

with

$$\begin{aligned} \delta T_1^{(2)} = & \sum_{i \neq j} \sum_{\substack{\sigma_1 \sigma_2 \\ \sigma_1' \sigma_2'}} t_{ij}^{\sigma_1 \sigma_2} \langle \hat{c}_{i\sigma_1}^\dagger \hat{c}_{j\sigma_2} \rangle \sum_{vv'} \left[\frac{\partial^2 q_{i,\sigma_1}^{\sigma_1'}}{\partial (A_v^i)^* \partial A_{v'}^i} [q_{j,\sigma_2}^{\sigma_2'}]^* (\delta A_v^i)^* \delta A_{v'}^i \right. \\ & \left. + \frac{1}{2} \left(\frac{\partial q_{i,\sigma_1}^{\sigma_1'}}{\partial (A_v^i)^*} \frac{\partial [q_{j,\sigma_2}^{\sigma_2'}]^*}{\partial A_{v'}^j} (\delta A_v^i)^* \delta A_{v'}^j + \frac{\partial q_{i,\sigma_1}^{\sigma_1'}}{\partial A_v^i} \frac{\partial [q_{j,\sigma_2}^{\sigma_2'}]^*}{\partial (A_{v'}^j)^*} \delta A_v^i (\delta A_{v'}^j)^* \right) \right] \\ & + \text{c.c.} \end{aligned} \quad (\text{D.1.14})$$

and

$$\begin{aligned} \delta T_t^{(2)} = & \sum_{i \neq j} \sum_{\substack{\sigma_1 \sigma_2 \\ \sigma_1' \sigma_2'}} t_{ij}^{\sigma_1 \sigma_2} \delta \langle \hat{c}_{i\sigma_1}^\dagger \hat{c}_{j\sigma_2} \rangle \\ & \times \sum_v \left[\frac{\partial q_{i,\sigma_1}^{\sigma_1'}}{\partial (A_v^i)^*} [q_{j,\sigma_2}^{\sigma_2'}]^* (\delta A_v^i)^* + q_{i,\sigma_1}^{\sigma_1'} \frac{\partial [q_{j,\sigma_2}^{\sigma_2'}]^*}{\partial (A_v^j)^*} (\delta A_v^j)^* \right] + \text{c.c.} \end{aligned} \quad (\text{D.1.15})$$

The fact that the complex conjugates yield the terms not explicitly shown in Eqs. (D.1.14) and (D.1.15) follows from the relations

$$\left[\frac{\partial q_\sigma^{\sigma'}}{\partial A_v} \right]^* = \frac{\partial [q_\sigma^{\sigma'}]^*}{\partial (A_v)^*} \quad (\text{D.1.16})$$

$$\left[\frac{\partial^2 q_\sigma^{\sigma'}}{\partial (A_v)^* \partial A_{v'}} \right]^* = \frac{\partial^2 [q_\sigma^{\sigma'}]^*}{\partial (A_{v'})^* \partial A_v} \quad (\text{D.1.17})$$

$$\left[t_{ij}^{\sigma \sigma'} \right]^* = t_{ji}^{\sigma' \sigma}. \quad (\text{D.1.18})$$

For our translationally invariant ground state it is more convenient to write Eqs. (D.1.14) and (D.1.15) in momentum space. With the Fourier transforms of the local fluctuations the term (D.1.14) reads

$$\delta T_1^{(2)} = \sum_{\mathbf{q}} \sum_{vv'} (\delta A_v^{\mathbf{q}})^* [K_{\mathbf{q},vv'}^1 + (K_{\mathbf{q},v'v}^1)^*] \delta A_v^{\mathbf{q}}, \quad (\text{D.1.19})$$

where

$$K_{\mathbf{q},vv'}^1 \equiv \sum_{\substack{\sigma_1\sigma_2 \\ \sigma'_1\sigma'_2}} \left[\frac{1}{2} E_{\sigma_1\sigma_2,\sigma'_1\sigma'_2}(\mathbf{q}) \left(\frac{\partial q_{\sigma_1}^{\sigma'_1}}{\partial(A_v)^*} \frac{\partial [q_{\sigma_2}^{\sigma'_2}]^*}{\partial A_{v'}} + \frac{\partial q_{\sigma_1}^{\sigma'_1}}{\partial A_{v'}} \frac{\partial [q_{\sigma_2}^{\sigma'_2}]^*}{\partial(A_v)^*} \right) \right. \\ \left. + E_{\sigma_1\sigma_2,\sigma'_1\sigma'_2} \frac{\partial^2 q_{\sigma_1}^{\sigma'_1}}{\partial(A_v)^* \partial A_{v'}} [q_{\sigma_2}^{\sigma'_2}]^* \right]. \quad (\text{D.1.20})$$

Here we assumed that the renormalization matrix is lattice-site independent and introduced the tensor

$$E_{\sigma_1\sigma_2,\sigma'_1\sigma'_2}(\mathbf{q}) = \frac{1}{N_s} \sum_{\mathbf{k}} \epsilon_{\mathbf{k}+\mathbf{q}}^{\sigma_1\sigma_2} \langle \hat{c}_{\mathbf{k},\sigma'_1}^\dagger \hat{c}_{\mathbf{k},\sigma'_2} \rangle \quad (\text{D.1.21})$$

with

$$\epsilon_{\mathbf{k}}^{\sigma_1\sigma_2} = \frac{1}{N_s} \sum_{i \neq j} t_{ij}^{\sigma_1\sigma_2} e^{i\mathbf{k}(\mathbf{R}_i - \mathbf{R}_j)}. \quad (\text{D.1.22})$$

Note that for $\mathbf{q} = \mathbf{0}$ the tensor (D.1.21),

$$E_{\sigma_1\sigma_2,\sigma'_1\sigma'_2} = E_{\sigma_1\sigma_2,\sigma'_1\sigma'_2}(\mathbf{0}), \quad (\text{D.1.23})$$

has already been defined in Eq. (3.3.23).

D.2 Transitive Fluctuations

For the evaluation of the ‘transitive’ term (D.1.15) we write the non-local density-matrix fluctuations as

$$\delta \langle \hat{c}_{i\sigma'_1}^\dagger \hat{c}_{j\sigma'_2} \rangle = \frac{1}{N_s} \sum_{\mathbf{k}\mathbf{k}'} e^{i(\mathbf{R}_i \cdot \mathbf{k} - \mathbf{R}_j \cdot \mathbf{k}')} \delta \langle \hat{c}_{\mathbf{k},\sigma'_1}^\dagger \hat{c}_{\mathbf{k}',\sigma'_2} \rangle. \quad (\text{D.2.1})$$

Together with Eq. (D.1.8) this yields

$$\delta T_t^{(2)} = \frac{1}{N_s} \sum_{\mathbf{q}\mathbf{k}} \sum_{v,\sigma'_1\sigma'_2} (\delta A_v^{\mathbf{q}})^* \bar{K}_{\mathbf{k}\mathbf{q},v,\sigma'_1\sigma'_2}^t \delta \langle \hat{c}_{\mathbf{k},\sigma'_1}^\dagger \hat{c}_{\mathbf{k}+\mathbf{q},\sigma'_2} \rangle + \text{c.c.}, \quad (\text{D.2.2})$$

with

$$\bar{K}_{\mathbf{k}\mathbf{q},v,\sigma'_1\sigma'_2}^t = \sum_{\sigma_1\sigma_2} \left[\frac{\partial q_{\sigma_1}^{\sigma'_1}}{\partial(A_v)^*} [q_{\sigma_2}^{\sigma'_2}]^* \epsilon_{\mathbf{k}+\mathbf{q}}^{\sigma_1\sigma_2} + q_{\sigma_1}^{\sigma'_1} \frac{\partial [q_{\sigma_2}^{\sigma'_2}]^*}{\partial(A_v)^*} \epsilon_{\mathbf{k}}^{\sigma_1\sigma_2} \right]. \quad (\text{D.2.3})$$

In principle, Eqs. (D.2.2) and (D.2.3) allow us to calculate all second-order couplings of density-matrix and parameter fluctuations that arise from $\delta T_t^{(2)}$. For numerical calculations, however, these equations are not very

useful due to the explicit \mathbf{k} -dependence of Eq. (D.2.3). It is much easier to introduce the two auxiliary fluctuations

$$\delta B_w^{\mathbf{q}} \equiv \delta B_{\sigma_2 \sigma_1, \sigma'_2 \sigma'_1}^{\mathbf{q}} \equiv \frac{1}{\sqrt{N_s}} \sum_{\mathbf{k}} \epsilon_{\mathbf{k}}^{\sigma_1 \sigma_2} \delta \langle \hat{c}_{\mathbf{k}, \sigma'_1}^\dagger \hat{c}_{\mathbf{k}+\mathbf{q}, \sigma'_2} \rangle \quad (\text{D.2.4})$$

$$\delta \bar{B}_w^{\mathbf{q}} \equiv \delta \bar{B}_{\sigma_2 \sigma_1, \sigma'_2 \sigma'_1}^{\mathbf{q}} \equiv \frac{1}{\sqrt{N_s}} \sum_{\mathbf{k}} \epsilon_{\mathbf{k}+\mathbf{q}}^{\sigma_1 \sigma_2} \delta \langle \hat{c}_{\mathbf{k}, \sigma'_1}^\dagger \hat{c}_{\mathbf{k}+\mathbf{q}, \sigma'_2} \rangle, \quad (\text{D.2.5})$$

where $w \equiv (\sigma_2 \sigma_1, \sigma'_2 \sigma'_1)$ is an abbreviation for quadruples of indices σ . With these definitions we can write Eq. (D.2.2) as

$$\begin{aligned} \delta T_t^{(2)} = \sum_{\mathbf{q}} \sum_{v,w} \left[(\delta A_v^{\mathbf{q}})^* K_{vw}^{t(1)} \delta B_w^{\mathbf{q}} + (\delta A_v^{\mathbf{q}})^* K_{vw}^{t(2)} \delta \bar{B}_w^{\mathbf{q}} \right. \\ \left. + (\delta B_w^{\mathbf{q}})^* (K_{vw}^{t(1)})^* \delta A_v^{\mathbf{q}} + (\delta \bar{B}_w^{\mathbf{q}})^* (K_{vw}^{t(2)})^* \delta A_v^{\mathbf{q}} \right], \end{aligned} \quad (\text{D.2.6})$$

where

$$K_{v, (\sigma_2 \sigma_1, \sigma'_2 \sigma'_1)}^{t(1)} \equiv q_{\sigma_1}^{\sigma'_1} \frac{\partial [q_{\sigma_2}^{\sigma'_2}]^*}{\partial (A_v)^*} \quad (\text{D.2.7})$$

$$K_{v, (\sigma_2 \sigma_1, \sigma'_2 \sigma'_1)}^{t(2)} \equiv \frac{\partial q_{\sigma_1}^{\sigma'_1}}{\partial (A_v)^*} [q_{\sigma_2}^{\sigma'_2}]^*. \quad (\text{D.2.8})$$

Note that we introduced the *two* different fluctuations (D.2.4) and (D.2.5) only because they allow us to write the second-order expansion in a relatively simple form. In fact, these fluctuations are not independent but related through

$$\delta \bar{B}_{\sigma_1 \sigma_2, \sigma'_1 \sigma'_2}^{\mathbf{q}} = [\delta B_{\sigma_2 \sigma_1, \sigma'_2 \sigma'_1}^{-\mathbf{q}}]^*. \quad (\text{D.2.9})$$

Altogether we end up with the following second-order expansion of the Lagrange functional

$$\delta L^{(2)} = \frac{1}{N_s} \sum_{\mathbf{q}} (\delta \mathbf{A}^{\mathbf{q}} \quad \delta \mathbf{B}^{\mathbf{q}} \quad \delta \bar{\mathbf{B}}^{\mathbf{q}} \quad \delta \mathbf{\Lambda}^{\mathbf{q}})^* \tilde{K}^{\mathbf{q}} \begin{pmatrix} \delta \mathbf{A}^{\mathbf{q}} \\ \delta \mathbf{B}^{\mathbf{q}} \\ \delta \bar{\mathbf{B}}^{\mathbf{q}} \\ \delta \mathbf{\Lambda}^{\mathbf{q}} \end{pmatrix}, \quad (\text{D.2.10})$$

where

$$\tilde{K}^{\mathbf{q}} \equiv \begin{pmatrix} \tilde{K}^{AA} & \tilde{K}^{AB} & \tilde{K}^{A\bar{B}} & \tilde{K}^{A\Lambda} \\ [\tilde{K}^{AB}]^\dagger & 0 & 0 & 0 \\ [\tilde{K}^{A\bar{B}}]^\dagger & 0 & 0 & 0 \\ [\tilde{K}^{A\Lambda}]^\dagger & 0 & 0 & 0 \end{pmatrix} \quad (\text{D.2.11})$$

and

$$\tilde{K}^{AA} \equiv \tilde{K}^{\text{loc}} + \tilde{K}_{\mathbf{q}}^1 + [\tilde{K}_{\mathbf{q}}^1]^\dagger \quad (\text{D.2.12})$$

$$\tilde{K}^{AB} \equiv \tilde{K}^{\text{t}(1)} \quad (\text{D.2.13})$$

$$\tilde{K}^{A\bar{B}} \equiv \tilde{K}^{\text{t}(2)} \quad (\text{D.2.14})$$

$$\tilde{K}^{A\Lambda} \equiv \tilde{K}^{\text{c}}. \quad (\text{D.2.15})$$

As described in Section 5.5, the anti-adiabaticity condition leads an effective second-order functional only of the density matrix. This condition can be evaluated directly for the second-order expansion (D.2.10) since the fluctuations $\delta\mathbf{A}^{\mathbf{q}}$, $\delta\mathbf{B}^{\mathbf{q}}$, $\delta\bar{\mathbf{B}}^{\mathbf{q}}$ are some linear functions of the density-matrix fluctuations $\delta\langle\hat{c}_{\mathbf{k},\sigma_1}^\dagger\hat{c}_{\mathbf{k}+\mathbf{q},\sigma_2}\rangle$, cf., Appendix C.2. To this end, we distinguish the fluctuations of the local density matrix $\delta\mathbf{A}_\rho^{\mathbf{q}}$ and of the variational parameters $\delta\mathbf{A}_\lambda^{\mathbf{q}}$ as well as the corresponding blocks in the matrix (D.2.11),

$$\tilde{K}^{AA} = \begin{pmatrix} \tilde{K}_{\lambda\lambda}^{AA} & \tilde{K}_{\lambda\rho}^{AA} \\ [\tilde{K}_{\lambda\rho}^{AA}]^\dagger & \tilde{K}_{\rho\rho}^{AA} \end{pmatrix} \quad \tilde{K}^{AB} = \begin{pmatrix} \tilde{K}_\lambda^{AB} \\ \tilde{K}_\rho^{AB} \end{pmatrix} \quad (\text{D.2.16})$$

$$\tilde{K}^{A\bar{B}} = \begin{pmatrix} \tilde{K}_\lambda^{A\bar{B}} \\ \tilde{K}_\rho^{A\bar{B}} \end{pmatrix} \quad \tilde{K}^{A\Lambda} = \begin{pmatrix} \tilde{K}_\lambda^{A\Lambda} \\ \tilde{K}_\rho^{A\Lambda} \end{pmatrix}. \quad (\text{D.2.17})$$

The resulting expansion of the Lagrange functional is then given as

$$\delta\bar{L}^{(2)} = \frac{1}{N_s} \sum_{\mathbf{q}} (\delta\mathbf{A}_\rho^{\mathbf{q}} \quad \delta\mathbf{B}^{\mathbf{q}} \quad \delta\bar{\mathbf{B}}^{\mathbf{q}})^* \tilde{V}^{\mathbf{q}} \begin{pmatrix} \delta\mathbf{A}_\rho^{\mathbf{q}} \\ \delta\mathbf{B}^{\mathbf{q}} \\ \delta\bar{\mathbf{B}}^{\mathbf{q}} \end{pmatrix} \quad (\text{D.2.18})$$

with the new kernel

$$\tilde{V}^{\mathbf{q}} \equiv \begin{pmatrix} \tilde{V}^{AA} & \tilde{V}^{AB} & \tilde{V}^{A\bar{B}} \\ \tilde{V}^{BA} & \tilde{V}^{BB} & \tilde{V}^{B\bar{B}} \\ \tilde{V}^{\bar{B}A} & \tilde{V}^{\bar{B}B} & \tilde{V}^{\bar{B}\bar{B}} \end{pmatrix} = \begin{pmatrix} \tilde{K}_{\rho\rho}^{AA} & \tilde{K}_\rho^{AB} & \tilde{K}_\rho^{A\bar{B}} \\ [\tilde{K}_\rho^{AB}]^\dagger & 0 & 0 \\ [\tilde{K}_\rho^{A\bar{B}}]^\dagger & 0 & 0 \end{pmatrix} - \Delta\tilde{V}^{\mathbf{q}}, \quad (\text{D.2.19})$$

where

$$\Delta\tilde{V}^{\mathbf{q}} \equiv \begin{pmatrix} [\tilde{K}_{\lambda\rho}^{AA}]^\dagger & \tilde{K}_\rho^{A\Lambda} \\ [\tilde{K}_\lambda^{AB}]^\dagger & 0 \\ [\tilde{K}_\lambda^{A\bar{B}}]^\dagger & 0 \end{pmatrix} \times \begin{pmatrix} \tilde{K}_{\lambda\lambda}^{AA} & \tilde{K}_\lambda^{A\Lambda} \\ [\tilde{K}_\lambda^{A\Lambda}]^\dagger & 0 \end{pmatrix}^{-1} \times \begin{pmatrix} \tilde{K}_{\lambda\rho}^{AA} & \tilde{K}_\lambda^{AB} & \tilde{K}_\lambda^{A\bar{B}} \\ [\tilde{K}_\rho^{A\Lambda}]^\dagger & 0 & 0 \end{pmatrix}. \quad (\text{D.2.20})$$

Note that $\tilde{V}^{\mathbf{q}}$ (unlike $\tilde{K}^{\mathbf{q}}$) includes finite couplings also between the fluctuations $\delta\mathbf{B}^{\mathbf{q}}$ and $\delta\bar{\mathbf{B}}^{\mathbf{q}}$. The calculation of $\tilde{V}^{\mathbf{q}}$ (for fixed \mathbf{q}) only involves the handling of finite-dimensional matrices. In contrast, the evaluation of the functional (D.2.2) (instead of (D.2.6)) would have led to significantly more complicated equations.

Appendix E

Explicit Form of the Gutzwiller RPA Equations

In this appendix, we prove that the general Gutzwiller-RPA equations given in Eqs. (5.3.12) lead to the Green's function matrix (5.6.15) if applied to our multi-band Hamiltonian (2.4.3).

E.1 Gutzwiller-RPA Equations

With the abbreviations $\delta D_\mu^{\mathbf{q}}$, $\hat{D}_\mu^{\mathbf{q}}$ for the three fluctuations $\delta A_v^{\mathbf{q}}$, $\delta B_w^{\mathbf{q}}$ and $\delta \bar{B}_w^{\mathbf{q}}$ and the corresponding operators $\hat{A}_v^{\mathbf{q}}$, $\hat{B}_w^{\mathbf{q}}$ and $\hat{\bar{B}}_w^{\mathbf{q}}$, we have to show that the Green's function matrix

$$\Pi_{\mu\mu'}(\mathbf{q}, \omega) = \langle\langle \hat{D}_\mu^{\mathbf{q}}; (\hat{D}_{\mu'}^{\mathbf{q}})^\dagger \rangle\rangle_\omega, \quad (\text{E.1.1})$$

as given in Eq. (5.6.15), obeys the equation

$$\delta D_\mu^{\mathbf{q}} = \sum_{\mu'} \langle\langle \hat{D}_\mu^{\mathbf{q}}; (\hat{D}_{\mu'}^{\mathbf{q}})^\dagger \rangle\rangle_\omega \delta f_{\mu'}^{\mathbf{q}}. \quad (\text{E.1.2})$$

Using the explicit form Eq. (5.6.15) of $\tilde{\Pi}(\mathbf{q}, \omega)$, this equation can also be written as

$$\sum_{\mu'} [1 + \tilde{\Pi}^0(\mathbf{q}, \omega) \tilde{V}^{\mathbf{q}}]_{\mu\mu'} \delta D_{\mu'}^{\mathbf{q}} = \sum_{\mu'} \Pi_{\mu\mu'}^0(\mathbf{q}, \omega) \delta f_{\mu'}^{\mathbf{q}}. \quad (\text{E.1.3})$$

Note that the excitation amplitudes $\delta f_\mu^{\mathbf{q}}$ enter the problem through the perturbation operator

$$\begin{aligned} \delta \hat{V}_f \equiv \sum_{\mu} \delta f_{\mu}^{\mathbf{q}} (\hat{D}_{\mu}^{\mathbf{q}})^\dagger \equiv & \frac{1}{\sqrt{N_s}} \sum_{\mathbf{k}} \sum_{\substack{\sigma_1 \sigma_2 \\ \sigma'_1 \sigma'_2}} \hat{c}_{\mathbf{k}+\mathbf{q}, \sigma'_1}^\dagger \hat{c}_{\mathbf{k}, \sigma'_2} \left[\delta f_{\sigma_1 \sigma_2}^{A; \mathbf{q}} \delta_{\sigma_1 \sigma'_1} \delta_{\sigma_2 \sigma'_2} \right. \\ & \left. + \delta f_{\sigma_1 \sigma_2, \sigma'_1 \sigma'_2}^{B; \mathbf{q}} \epsilon_{\mathbf{k}}^{\sigma_1 \sigma_2} + \delta f_{\sigma_1 \sigma_2, \sigma'_1 \sigma'_2}^{\bar{B}; \mathbf{q}} \epsilon_{\mathbf{k}+\mathbf{q}}^{\sigma_1 \sigma_2} \right], \end{aligned} \quad (\text{E.1.4})$$

which is needed to define the general Green's functions (5.6.14).

E.2 Decoupled Fluctuations

Before we prove Eq. (E.1.3), it is instructive to consider the case $\tilde{V}^{\mathbf{q}} = 0$ in which the three fluctuations $\delta A_w^{\mathbf{q}}$, $\delta B_w^{\mathbf{q}}$ and $\delta \bar{B}_w^{\mathbf{q}}$ are decoupled and we can set $f_w^{B;\mathbf{q}} = f_w^{\bar{B};\mathbf{q}} = 0$. We start this derivation in the eigenbasis of the Gutzwiller Hamiltonian (5.6.16). It leads to the simplest form of the matrix \tilde{E} in Eq. (5.3.12) which then reads

$$\begin{aligned} & [\omega - (E_{\mathbf{k}+\mathbf{q},\alpha_1} - E_{\mathbf{k},\alpha_2})] \delta \langle \hat{h}_{\mathbf{k},\alpha_2}^\dagger \hat{h}_{\mathbf{k}+\mathbf{q},\alpha_1} \rangle^{\text{hp/ph}} \\ &= \frac{1}{\sqrt{N_s}} (n_{\mathbf{k},\alpha_2}^0 - n_{\mathbf{k}+\mathbf{q},\alpha_1}^0) \delta f_{(\mathbf{k}+\mathbf{q},\alpha_1)(\mathbf{k},\alpha_2)}. \end{aligned} \quad (\text{E.2.1})$$

Here, the excitation amplitude is given as

$$\delta f_{(\mathbf{k}+\mathbf{q},\alpha_1)(\mathbf{k},\alpha_2)} = \sum_{\sigma_1\sigma_2} \delta f_{\sigma_1\sigma_2}^{A;\mathbf{q}} [u_{\sigma_1,\alpha_1}^{\mathbf{k}+\mathbf{q}}]^* u_{\sigma_2,\alpha_2}^{\mathbf{k}}. \quad (\text{E.2.2})$$

Note that the factor $n_{\mathbf{k},\alpha_2}^0 - n_{\mathbf{k}+\mathbf{q},\alpha_1}^0 = \pm 1$ in Eq. (E.2.1) represents the particle-hole and the hole-particle channels in Eq. (5.3.12). For simplicity, we will drop the corresponding labels hp/ph in the following.

With the transformations (5.6.18) and (5.6.19), Eq. (E.2.1) leads to

$$\begin{aligned} \delta A_{\sigma_1,\sigma_2}^{\mathbf{q}} &= \frac{1}{\sqrt{N_s}} \sum_{\mathbf{k}} \delta \langle \hat{c}_{\mathbf{k},\sigma_2}^\dagger \hat{c}_{\mathbf{k}+\mathbf{q},\sigma_1} \rangle \\ &= \frac{1}{\sqrt{N_s}} \sum_{\mathbf{k}} \sum_{\alpha_1\alpha_2} [u_{\sigma_2,\alpha_2}^{\mathbf{k}}]^* u_{\sigma_1,\alpha_1}^{\mathbf{k}+\mathbf{q}} \delta \langle \hat{h}_{\mathbf{k},\alpha_2}^\dagger \hat{h}_{\mathbf{k}+\mathbf{q},\alpha_1} \rangle \\ &= \frac{1}{N_s} \sum_{\mathbf{k}} \sum_{\substack{\alpha_1\alpha_2 \\ \sigma_1'\sigma_2'}} \frac{[u_{\sigma_2,\alpha_2}^{\mathbf{k}}]^* u_{\sigma_1,\alpha_1}^{\mathbf{k}+\mathbf{q}} [u_{\sigma_1',\alpha_1}^{\mathbf{k}+\mathbf{q}}]^* u_{\sigma_2',\alpha_2}^{\mathbf{k}}}{\omega - (E_{\mathbf{k}+\mathbf{q},\alpha_1} - E_{\mathbf{k},\alpha_2})} [n_{\mathbf{k},\alpha_2}^0 - n_{\mathbf{k}+\mathbf{q},\alpha_1}^0] \delta f_{\sigma_1'\sigma_2'}^{\mathbf{q}}. \end{aligned} \quad (\text{E.2.3})$$

As expected, we therefore find

$$\delta A_{\sigma_1,\sigma_2}^{\mathbf{q}} = \sum_{\sigma_1'\sigma_2'} \langle \langle \hat{A}_{\sigma_1,\sigma_2}^{\mathbf{q}}; (\hat{A}_{\sigma_1',\sigma_2'}^{\mathbf{q}})^\dagger \rangle \rangle_\omega^0 \delta f_{\sigma_1'\sigma_2'}^{\mathbf{q}}, \quad (\text{E.2.4})$$

with the ('retarded') Green's function

$$\begin{aligned} & \langle \langle \hat{A}_{\sigma_1,\sigma_2}^{\mathbf{q}}; (\hat{A}_{\sigma_1',\sigma_2'}^{\mathbf{q}})^\dagger \rangle \rangle_\omega^0 \\ &= \frac{1}{N_s} \sum_{\mathbf{k}} \sum_{\alpha_1\alpha_2} \frac{[u_{\sigma_2,\alpha_2}^{\mathbf{k}}]^* u_{\sigma_1,\alpha_1}^{\mathbf{k}+\mathbf{q}} [u_{\sigma_1',\alpha_1}^{\mathbf{k}+\mathbf{q}}]^* u_{\sigma_2',\alpha_2}^{\mathbf{k}}}{\omega - (E_{\mathbf{k}+\mathbf{q},\alpha_1} - E_{\mathbf{k},\alpha_2}) + i\delta} [n_{\mathbf{k},\alpha_2}^0 - n_{\mathbf{k}+\mathbf{q},\alpha_1}^0] \end{aligned} \quad (\text{E.2.5})$$

as introduced in Eq. (5.6.20).

E.3 Coupled Fluctuations

Now we consider the case of a finite interaction matrix $\tilde{V}^{\mathbf{q}}$. Using our abbreviation δD_μ for the amplitudes δA_v , δB_w and $\delta \bar{B}_w$ the Lagrange functional $\delta \bar{L}^{(2)}$ has the form

$$\delta \bar{L}^{(2)} = \sum_{\mathbf{q}} \sum_{\mu\mu'} (\delta D_\mu^{\mathbf{q}})^* V_{\mu\mu'}^{\mathbf{q}} (\delta D_{\mu'}^{\mathbf{q}}). \quad (\text{E.3.1})$$

With this additional interaction term, Eq. (E.2.1) reads

$$\begin{aligned} & [\omega - (E_{\mathbf{k}+\mathbf{q},\alpha_1} - E_{\mathbf{k},\alpha_2})] \delta \langle \hat{h}_{\mathbf{k},\alpha_2}^\dagger \hat{h}_{\mathbf{k}+\mathbf{q},\alpha_1} \rangle \\ & + [n_{\mathbf{k},\alpha_2}^0 - n_{\mathbf{k}+\mathbf{q},\alpha_1}^0] \times \sum_{\mathbf{k}'} \sum_{\alpha_3\alpha_4} U_{\mathbf{k},\alpha_1\alpha_2}^{\mathbf{k}',\alpha_3\alpha_4}(\mathbf{q}) \delta \langle \hat{h}_{\mathbf{k}',\alpha_4}^\dagger \hat{h}_{\mathbf{k}'+\mathbf{q},\alpha_3} \rangle \\ & = \frac{1}{\sqrt{N_s}} [n_{\mathbf{k},\alpha_2}^0 - n_{\mathbf{k}+\mathbf{q},\alpha_1}^0] \delta f_{(\mathbf{k}+\mathbf{q},\alpha_1)(\mathbf{k},\alpha_2)}, \end{aligned} \quad (\text{E.3.2})$$

where

$$U_{\mathbf{k},\alpha_1\alpha_2}^{\mathbf{k}',\alpha_3\alpha_4}(\mathbf{q}) = \frac{\partial}{\partial \delta \langle \hat{h}_{\mathbf{k}+\mathbf{q},\alpha_1}^\dagger \hat{c}_{\mathbf{k},\alpha_2} \rangle} \frac{\partial}{\partial \delta \langle \hat{h}_{\mathbf{k}',\alpha_4}^\dagger \hat{h}_{\mathbf{k}'+\mathbf{q},\alpha_3} \rangle} \delta \bar{L}^{(2)} \quad (\text{E.3.3})$$

$$= \sum_{\mu\mu'} V_{\mu\mu'}^{\mathbf{q}} \frac{\partial (\delta D_\mu^{\mathbf{q}})^*}{\partial \delta \langle \hat{h}_{\mathbf{k}+\mathbf{q},\alpha_1}^\dagger \hat{h}_{\mathbf{k},\alpha_2} \rangle} \frac{\partial \delta D_{\mu'}^{\mathbf{q}}}{\partial \delta \langle \hat{h}_{\mathbf{k}',\alpha_4}^\dagger \hat{h}_{\mathbf{k}'+\mathbf{q},\alpha_3} \rangle} \quad (\text{E.3.4})$$

and

$$\begin{aligned} \delta f_{(\mathbf{k}+\mathbf{q},\alpha_1)(\mathbf{k},\alpha_2)} &= \sum_{\substack{\sigma_1\sigma_2 \\ \sigma'_1\sigma'_2}} [u_{\sigma'_1,\alpha_1}^{\mathbf{k}+\mathbf{q}}]^* u_{\sigma_2,\alpha_2}^{\mathbf{k}} \left(\delta f_{\sigma_1,\sigma_2}^{A;\mathbf{q}} \delta_{\sigma_1\sigma'_1} \delta_{\sigma_2\sigma'_2} \right. \\ & \quad \left. + \delta f_{\sigma_1\sigma_2,\sigma'_1\sigma'_2}^{B;\mathbf{q}} \epsilon_{\mathbf{k}}^{\sigma_1\sigma_2} + \delta f_{\sigma_1\sigma_2,\sigma'_1\sigma'_2}^{\bar{B};\mathbf{q}} \epsilon_{\mathbf{k}+\mathbf{q}}^{\sigma_1\sigma_2} \right). \end{aligned} \quad (\text{E.3.5})$$

The derivatives in Eq. (E.3.4) can be further evaluated using the transformations (5.6.18) and (5.6.19),

$$\frac{\partial (\delta D_\mu^{\mathbf{q}})^*}{\partial \delta \langle \hat{h}_{\mathbf{k}+\mathbf{q},\alpha_1}^\dagger \hat{h}_{\mathbf{k},\alpha_2} \rangle} = \sum_{\sigma_1\sigma_2} \frac{\partial (\delta D_\mu^{\mathbf{q}})^*}{\partial \delta \langle \hat{c}_{\mathbf{k}+\mathbf{q},\sigma_1}^\dagger \hat{c}_{\mathbf{k},\sigma_2} \rangle} [u_{\sigma_1,\alpha_1}^{\mathbf{k}+\mathbf{q}}]^* u_{\sigma_2,\alpha_2}^{\mathbf{k}} \quad (\text{E.3.6})$$

$$\frac{\partial \delta D_{\mu'}^{\mathbf{q}}}{\partial \delta \langle \hat{h}_{\mathbf{k}',\alpha_4}^\dagger \hat{h}_{\mathbf{k}'+\mathbf{q},\alpha_3} \rangle} = \sum_{\sigma_3\sigma_4} \frac{\partial \delta D_{\mu'}^{\mathbf{q}}}{\partial \delta \langle \hat{c}_{\mathbf{k}',\sigma_4}^\dagger \hat{c}_{\mathbf{k}'+\mathbf{q},\sigma_3} \rangle} [u_{\sigma_4,\alpha_4}^{\mathbf{k}'}]^* u_{\sigma_3,\alpha_3}^{\mathbf{k}'+\mathbf{q}}. \quad (\text{E.3.7})$$

Depending on the particular fluctuations $\delta D_\mu^{\mathbf{q}}$, the remaining derivatives on the r.h.s. of Eqs. (E.3.6) and (E.3.7) are given as

$$\delta D_\mu^{\mathbf{q}} = \delta A_v^{\mathbf{q}} : \frac{\partial \delta A_{\sigma_2, \sigma_1}^{\mathbf{q}}}{\partial \delta \langle \hat{c}_{\mathbf{k}, \sigma}^\dagger \hat{c}_{\mathbf{k}+\mathbf{q}, \sigma'} \rangle} = \frac{\partial (\delta A_{\sigma_1, \sigma_2}^{\mathbf{q}})^*}{\partial \delta \langle \hat{c}_{\mathbf{k}+\mathbf{q}, \sigma}^\dagger \hat{c}_{\mathbf{k}, \sigma'} \rangle} = \frac{\delta_{\sigma \sigma_1} \delta_{\sigma' \sigma_2}}{\sqrt{N_s}} \quad (\text{E.3.8})$$

$$\delta D_\mu^{\mathbf{q}} = \delta B_w^{\mathbf{q}} : \frac{\partial \delta B_{\sigma_2 \sigma_1, \sigma'_2 \sigma'_1}^{\mathbf{q}}}{\partial \delta \langle \hat{c}_{\mathbf{k}, \sigma}^\dagger \hat{c}_{\mathbf{k}+\mathbf{q}, \sigma'} \rangle} = \frac{\partial (B_{\sigma_1 \sigma_2, \sigma'_1 \sigma'_2}^{\mathbf{q}})^*}{\partial \delta \langle \hat{c}_{\mathbf{k}+\mathbf{q}, \sigma}^\dagger \hat{c}_{\mathbf{k}, \sigma'} \rangle} = \frac{\delta_{\sigma \sigma_1} \delta_{\sigma' \sigma'_2}}{\sqrt{N_s}} \epsilon_{\mathbf{k}}^{\sigma_1 \sigma_2} \quad (\text{E.3.9})$$

$$\delta D_\mu^{\mathbf{q}} = \delta \bar{B}_w^{\mathbf{q}} : \frac{\partial \delta \bar{B}_{\sigma_2 \sigma_1, \sigma'_2 \sigma'_1}^{\mathbf{q}}}{\partial \delta \langle \hat{c}_{\mathbf{k}, \sigma}^\dagger \hat{c}_{\mathbf{k}+\mathbf{q}, \sigma'} \rangle} = \frac{\partial (\bar{B}_{\sigma_1 \sigma_2, \sigma'_1 \sigma'_2}^{\mathbf{q}})^*}{\partial \delta \langle \hat{c}_{\mathbf{k}+\mathbf{q}, \sigma}^\dagger \hat{c}_{\mathbf{k}, \sigma'} \rangle} = \frac{\delta_{\sigma \sigma_1} \delta_{\sigma' \sigma'_2}}{\sqrt{N_s}} \epsilon_{\mathbf{k}+\mathbf{q}}^{\sigma_1 \sigma_2}. \quad (\text{E.3.10})$$

With Eqs. (E.3.3)–(E.3.10), we are now in the position to evaluate the Gutzwiller-RPA equation (E.3.2). To this end, we proceed as in Eq. (E.2.3),

$$\begin{aligned} \delta A_{\sigma_1, \sigma_2}^{\mathbf{q}} &= \frac{1}{\sqrt{N_s}} \sum_{\mathbf{k}} \sum_{\alpha_1 \alpha_2} [u_{\sigma_2, \alpha_2}^{\mathbf{k}}]^* u_{\sigma_1, \alpha_1}^{\mathbf{k}+\mathbf{q}} \delta \langle \hat{h}_{\mathbf{k}, \alpha_2}^\dagger \hat{h}_{\mathbf{k}+\mathbf{q}, \alpha_1} \rangle \\ &= - \sum_{\mu \mu'} V_{\mu \mu'}^{\mathbf{q}} \left\{ \left[\frac{1}{\sqrt{N_s}} \sum_{\mathbf{k}} \sum_{\substack{\alpha_1 \alpha_2 \\ \sigma'_1 \sigma'_2}} \frac{[u_{\sigma_2, \alpha_2}^{\mathbf{k}}]^* u_{\sigma_1, \alpha_1}^{\mathbf{k}+\mathbf{q}} [u_{\sigma'_1, \alpha_1}^{\mathbf{k}+\mathbf{q}}]^* u_{\sigma'_2, \alpha_2}^{\mathbf{k}}}{\omega - (E_{\mathbf{k}+\mathbf{q}, \alpha_1} - E_{\mathbf{k}, \alpha_2})} \right. \right. \\ &\quad \times [n_{\mathbf{k}, \alpha_2}^0 - n_{\mathbf{k}+\mathbf{q}, \alpha_1}^0] \frac{\partial (\delta D_\mu^{\mathbf{q}})^*}{\partial \delta \langle \hat{c}_{\mathbf{k}+\mathbf{q}, \sigma'_1}^\dagger \hat{c}_{\mathbf{k}, \sigma'_2} \rangle} \left. \right. \\ &\quad \times \sum_{\mathbf{k}'} \sum_{\sigma_3 \sigma_4} \frac{\partial \delta D_{\mu'}^{\mathbf{q}}}{\partial \delta \langle \hat{c}_{\mathbf{k}', \sigma_4}^\dagger \hat{c}_{\mathbf{k}'+\mathbf{q}, \sigma_3} \rangle} \delta \langle \hat{c}_{\mathbf{k}', \sigma_4}^\dagger \hat{c}_{\mathbf{k}'+\mathbf{q}, \sigma_3} \rangle \left. \right\} \\ &\quad + \sum_{\mu} \langle \langle \hat{A}_{\sigma_1, \sigma_2}^{\mathbf{q}}; (\hat{D}_\mu^{\mathbf{q}})^\dagger \rangle \rangle_\omega^0 \delta f_\mu^{\mathbf{q}}. \end{aligned} \quad (\text{E.3.11})$$

The sums over μ and μ' lead to nine contributions which can all be evaluated using Eqs. (E.3.8)–(E.3.10). As a result we find

$$\delta A_v^{\mathbf{q}} + \sum_{\mu \mu'} \langle \langle \hat{A}_v^{\mathbf{q}}; (\hat{D}_\mu^{\mathbf{q}})^\dagger \rangle \rangle_\omega^0 V_{\mu \mu'}^{\mathbf{q}} \delta D_{\mu'}^{\mathbf{q}} = \sum_{\mu} \langle \langle \hat{A}_v^{\mathbf{q}}; (\hat{D}_\mu^{\mathbf{q}})^\dagger \rangle \rangle_\omega^0 \delta f_\mu^{\mathbf{q}}, \quad (\text{E.3.12})$$

where the ‘non-interacting’ Green’s functions $\langle \langle \hat{A}_v^{\mathbf{q}}; (\hat{D}_\mu^{\mathbf{q}})^\dagger \rangle \rangle_\omega^0$ in Eq. (E.3.12) are given as in Eq. (E.2.5), apart from additional factors $\epsilon_{\mathbf{k}}^{\sigma_3 \sigma_4}$ or $\epsilon_{\mathbf{k}+\mathbf{q}}^{\sigma_3 \sigma_4}$:

$$\begin{aligned} &\left(\begin{aligned} &\langle \langle \hat{A}_{\sigma_1, \sigma_2}^{\mathbf{q}}; (\hat{B}_{\sigma_3 \sigma_4, \sigma'_3 \sigma'_4}^{\mathbf{q}})^\dagger \rangle \rangle_\omega^0 \\ &\langle \langle \hat{A}_{\sigma_1, \sigma_2}^{\mathbf{q}}; (\hat{B}_{\sigma_3 \sigma_4, \sigma'_3 \sigma'_4}^{\mathbf{q}})^\dagger \rangle \rangle_\omega^0 \end{aligned} \right) \\ &= \frac{1}{N_s} \sum_{\mathbf{k}} \sum_{\alpha_1 \alpha_2} \frac{[u_{\sigma_2, \alpha_2}^{\mathbf{k}}]^* u_{\sigma_1, \alpha_1}^{\mathbf{k}+\mathbf{q}} [u_{\sigma'_3, \alpha_1}^{\mathbf{k}+\mathbf{q}}]^* u_{\sigma'_4, \alpha_2}^{\mathbf{k}}}{\omega - (E_{\mathbf{k}+\mathbf{q}, \alpha_1} - E_{\mathbf{k}, \alpha_2}) + i\delta} \begin{pmatrix} \epsilon_{\mathbf{k}}^{\sigma_3 \sigma_4} \\ \epsilon_{\mathbf{k}+\mathbf{q}}^{\sigma_3 \sigma_4} \end{pmatrix}. \end{aligned} \quad (\text{E.3.13})$$

With Eq. (E.3.12), we have proven the ‘first’ set of Eqs. (E.1.3), i.e., those with $\mu = \nu = (\sigma, \sigma')$. If we replace $\delta A_{\sigma_1, \sigma_2}$ in the first line of Eq. (E.3.11) by

$$\delta B_{\sigma_1 \sigma_2, \sigma'_1 \sigma'_2} = \frac{1}{\sqrt{N_s}} \sum_{\mathbf{k}} \sum_{\alpha_1 \alpha_2} [u_{\sigma'_2, \alpha_2}^{\mathbf{k}}]^* u_{\sigma'_1, \alpha_1}^{\mathbf{k}+\mathbf{q}} \delta \langle \hat{h}_{\mathbf{k}, \alpha_2}^\dagger \hat{h}_{\mathbf{k}+\mathbf{q}, \alpha_1} \rangle \epsilon_{\mathbf{k}}^{\sigma_2 \sigma_1} \quad (\text{E.3.14})$$

or by

$$\delta \bar{B}_{\sigma_1 \sigma_2, \sigma'_1 \sigma'_2} = \frac{1}{\sqrt{N_s}} \sum_{\mathbf{k}} \sum_{\alpha_1 \alpha_2} [u_{\sigma'_2, \alpha_2}^{\mathbf{k}}]^* u_{\sigma'_1, \alpha_1}^{\mathbf{k}+\mathbf{q}} \delta \langle \hat{h}_{\mathbf{k}, \alpha_2}^\dagger \hat{h}_{\mathbf{k}+\mathbf{q}, \alpha_1} \rangle \epsilon_{\mathbf{k}+\mathbf{q}}^{\sigma_2 \sigma_1}, \quad (\text{E.3.15})$$

the remaining Eqs. (E.1.3) are derived in the very same way as Eq. (E.3.12). This closes our proof of Eq. (5.6.15).

Appendix F

Kinetic Energy in Infinite Dimensions

The limit of infinite spatial dimensions, $D \rightarrow \infty$, was first introduced by Metzner and Vollhardt [63] and was adopted by Müller-Hartmann [94]. Since the GA turned out to yield the exact result for expectation values of the single-band Hubbard model in $D = \infty$, their works provided a starting point for a systematic calculations of corrections to the GA for finite-dimensional systems.

F.1 Simplification of momentum-space sums

For a single-band Hubbard model with nearest-neighbor-hopping (hopping amplitude t) on a simple cubic lattice, the authors point out that the density of states in the limit of large D reads

$$\rho(\varepsilon) = \frac{1}{\sqrt{2\pi t^2}} e^{-\frac{\varepsilon^2}{2t^2}}. \quad (\text{F.1.1})$$

In the limit $D = \infty$, the number of particles per band and per spin-direction is given by

$$n_{bs} = \int_{-\infty}^{E_F^s} d\varepsilon \rho(\varepsilon) = \frac{1}{2} \left[1 + \text{ERF}\left(\frac{E_F^s}{\sqrt{2}}\right) \right], \quad (\text{F.1.2})$$

from which the Fermi energy E_F^s for s -electrons must be determined. $\text{ERF}(\varepsilon)$ denotes the error function. The \mathbf{k} -sum of one-particle energies is then written as

$$\frac{1}{N_s} \sum_{\mathbf{k}} \varepsilon_{\mathbf{k}} \langle \hat{n}_{\mathbf{k}} \rangle \stackrel{D \rightarrow \infty}{=} \int_{-\infty}^{E_F} d\varepsilon \varepsilon \rho(\varepsilon). \quad (\text{F.1.3})$$

For the calculation of response functions, momentum-space summations of the form

$$\frac{1}{N_s} \sum_{\mathbf{k}} \frac{n_{\mathbf{k},\alpha}^0 - n_{\mathbf{k}+\mathbf{q},\alpha}^0}{\omega - [E_{\mathbf{k}+\mathbf{q},\alpha} - E_{\mathbf{k},\alpha}]} \quad (\text{F.1.4})$$

must be evaluated. To this end, we write Eq. (F.1.4) as

$$\frac{1}{N_s} \sum_{\mathbf{k}} \frac{n_{\mathbf{k},\alpha}^0 - n_{\mathbf{k}+\mathbf{q},\alpha}^0}{\omega - [E_{\mathbf{k}+\mathbf{q},\alpha} - E_{\mathbf{k},\alpha}]} = \frac{1}{N_s} \sum_{\mathbf{k}\mathbf{k}'} \frac{n_{\mathbf{k},\alpha}^0 - n_{\mathbf{k}',\alpha}^0}{\omega - [E_{\mathbf{k}',\alpha} - E_{\mathbf{k},\alpha}]} \delta_{\mathbf{k}',\mathbf{k}+\mathbf{q}} \quad (\text{F.1.5})$$

and express the one-particle energies as

$$E_{\mathbf{k},\alpha} = \int_{-\infty}^{+\infty} d\Omega \Omega \cdot \delta[\Omega - E_{\mathbf{k},\alpha}], \quad (\text{F.1.6})$$

leading to the final expression

$$\frac{1}{N_s} \sum_{\mathbf{k}} \frac{n_{\mathbf{k},\alpha}^0 - n_{\mathbf{k}+\mathbf{q},\alpha}^0}{\omega - [E_{\mathbf{k}+\mathbf{q},\alpha} - E_{\mathbf{k},\alpha}]} = \iint_{-\infty}^{+\infty} d\Omega d\tilde{\Omega} \frac{\Theta[E_F - \Omega] - \Theta[E_F - \tilde{\Omega}]}{\omega - [\tilde{\Omega} - \Omega]} \Lambda_{\mathbf{q}}(\Omega, \tilde{\Omega}), \quad (\text{F.1.7})$$

where the information about the transferred momentum is contained in the function

$$\Lambda_{\mathbf{q}}(\Omega, \tilde{\Omega}) = \frac{1}{2\pi t^2} \frac{1}{\sqrt{1 - \eta_{\mathbf{q}}^2}} e^{-\frac{1}{4t^2} \left[\frac{[\Omega - \tilde{\Omega}]^2}{1 - \eta_{\mathbf{q}}} + \frac{[\Omega + \tilde{\Omega}]^2}{1 + \eta_{\mathbf{q}}} \right]}, \quad (\text{F.1.8})$$

with the scalar quantity $\eta_{\mathbf{q}}$ defined in Eq. (6.3.3). In the limit $\eta \rightarrow \pm 1$, $\Lambda_{\mathbf{q}}$ takes the form

$$\Lambda_{\mathbf{q}}(\Omega, \tilde{\Omega}) \rightarrow \begin{cases} \rho(\Omega) \cdot \delta[\Omega - \tilde{\Omega}] & \text{for } \eta_{\mathbf{q}} \rightarrow +1 \\ \rho(\Omega) \cdot \delta[\Omega + \tilde{\Omega}] & \text{for } \eta_{\mathbf{q}} \rightarrow -1 \end{cases}, \quad (\text{F.1.9})$$

and one of the frequency integrations can be carried out analytically.

The momentum dependence described by $\eta_{\mathbf{q}}$ can be evaluated for small momenta leading to

$$\eta_{\mathbf{q}} = \lim_{D \rightarrow \infty} \frac{1}{D} \sum_{n=1}^D \cos q_n \stackrel{|\mathbf{q}| \ll 1}{\approx} \lim_{D \rightarrow \infty} \frac{1}{D} \sum_{n=1}^D [1 - \frac{1}{2} q_n^2] = 1 - \frac{1}{2} q^2, \quad (\text{F.1.10})$$

where the last relation holds for ‘diagonal’ wave vectors $\mathbf{q} \sim (q, q, \dots)$. We can then write

$$|q| \stackrel{|\mathbf{q}| \ll 1}{\approx} \sqrt{2[1 - \eta_{\mathbf{q}}]}. \quad (\text{F.1.11})$$

Bibliography

- [1] Walter Metzner and Dieter Vollhardt. *Phys. Rev. Lett.*, 59:121–124, 1987.
- [2] D. Vollhardt. *New. J. Mod. Phys. B*, 3:2189–2209, 1989.
- [3] V. J. Emery, editor. *Correlated Electron Systems*, volume 9. World Scientific, Singapore, 1993.
- [4] A. Georges, G. Kotliar, W. Krauth, and M. J. Rozenberg. *Rev. Mod. Phys.*, 68:13–125, 1996.
- [5] F. Gebhard. *The Mott Metal-Insulator Transition—Models and Methods*. Springer, Heidelberg, 1997.
- [6] J. Büneemann, F. Gebhard, and W. Weber. *J. Phys. Cond. Mat*, 9:7343, 1997.
- [7] J. Büneemann, W. Weber, and F. Gebhard. *Phys. Rev. B*, 57(12):6896–6916, 1998.
- [8] J. Büneemann, F. Gebhard, and R. Thul. *Phys. Rev. B*, 67:75103, 2003.
- [9] M. C. Gutzwiller. *Phys. Rev. Lett.*, 10:159–162, 1963.
- [10] M. C. Gutzwiller. *Phys. Rev.*, 134:A923–A941, 1964.
- [11] M. C. Gutzwiller. *Phys. Rev.*, 137:A1726–A1735, 1965.
- [12] Claudio Attaccalite and Michele Fabrizio. *Phys. Rev. B*, 68:155117, 2003.
- [13] Michel Ferrero, Federico Becca, Michele Fabrizio, and Massimo Capone. *Phys. Rev. B*, 72:205126, Nov 2005.
- [14] J. Büneemann, K. Jávorne-Radnóczy, P. Fazekas, and F. Gebhard. *J. Phys. Cond. Matt.*, 19:326217, 2007.

- [15] J. Bünemann, D. Rasch, and F. Gebhard. *J. Phys. Cond. Matt.*, 19:436206, 2007.
- [16] Nicola Lanatà, Paolo Barone, and Michele Fabrizio. *Phys. Rev. B*, 78:155127, Oct 2008.
- [17] Bünemann *et al.* *Europhys. Lett.*, 61:667–673, 2003.
- [18] Giovanni Borghi, Michele Fabrizio, and Erio Tosatti. *Phys. Rev. Lett.*, 102:066806, Feb 2009.
- [19] J. Bünemann, F. Gebhard, T. Ohm, S. Weiser, and W. Weber. *Phys. Rev. Lett.*, 101:236404, Dec 2008.
- [20] A. Hofmann, X. Y. Cui, J. Schäfer, S. Meyer, P. Höpfner, C. Blumenstein, M. Paul, L. Patthey, E. Rotenberg, J. Bünemann, F. Gebhard, T. Ohm, W. Weber, and R. Claessen. *Phys. Rev. Lett.*, 102:187204, May 2009.
- [21] Sen Zhou and Ziqiang Wang. *Phys. Rev. Lett.*, 105:096401, Aug 2010.
- [22] T. Schickling, F. Gebhard, and J. Bünemann. *Phys. Rev. Lett.*, 106:146402, Apr 2011.
- [23] J.-P. Julien and J. Bouchet. *Physica B: Condensed Matter*, 359-361:783–785, 2005. Proceedings of the International Conference on Strongly Correlated Electron Systems.
- [24] K. M. Ho, J. Schmalian, and C. Z. Wang. *Phys. Rev. B*, 77:073101, Feb 2008.
- [25] XiaoYu Deng, Lei Wang, Xi Dai, and Zhong Fang. *Phys. Rev. B*, 79:075114, Feb 2009.
- [26] Jia Ning Zhuang, Lei Wang, Zhong Fang, and Xi Dai. *Phys. Rev. B*, 79:165114, Apr 2009.
- [27] GuangTao Wang, Yumin Qian, Gang Xu, Xi Dai, and Zhong Fang. *Phys. Rev. Lett.*, 104:047002, Jan 2010.
- [28] Gabriel Kotliar and Andrei E. Ruckenstein. *Phys. Rev. Lett.*, 57:1362–1365, 1986.
- [29] G. Seibold. *Phys. Rev. B*, 58:15520–15527, Dec 1998.
- [30] G. Seibold and J. Lorenzana. *Phys. Rev. B*, 69:134513, 2004.

- [31] F. Lechermann, A. Georges, G Kotliar, and O. Parcollet. *Phys. Rev. B*, 76:155102, 2007.
- [32] J. Büнемann. *physica status solidi (b)*, 248(1):203–211, 2011.
- [33] Michel Ferrero, Pablo S. Cornaglia, Lorenzo De Leo, Olivier Parcollet, Gabriel Kotliar, and Antoine Georges. *Phys. Rev. B*, 80:064501, 2009.
- [34] A. Isidori and M. Capone. *Phys. Rev. B*, 80:115120, 2009.
- [35] Frank Lechermann. *Phys. Rev. Lett.*, 102:046403, 2009.
- [36] J. Büнемann and F. Gebhard. *Phys. Rev. B*, 76:193104, 2007.
- [37] G. Seibold, E. Sigmund, and V. Hizhnyakov. *Phys. Rev. B*, 57:6937–6942, 1998.
- [38] G. Seibold and J. Lorenzana. *Phys. Rev. Lett.*, 86:2605–2608, 2001.
- [39] J. Lorenzana and G. Seibold. *Phys. Rev. Lett.*, 90:066404, Feb 2003.
- [40] G. Seibold, F. Becca, P. Rubin, and J. Lorenzana. *Phys. Rev. B*, 69:155113, 2004.
- [41] J. Lorenzana, G. Seibold, and R. Coldea. *Phys. Rev. B*, 72:224511, 2005.
- [42] G. Seibold and J. Lorenzana. *Phys. Rev. Lett.*, 94:107006, 2005.
- [43] G. Seibold and J. Lorenzana. *Phys. Rev. B*, 73:144515, 2006.
- [44] G. Seibold and J. Lorenzana. *Journal of Superconductivity and Novel Magnetism*, 20:619–622, 2007. 10.1007/s10948-007-0249-0.
- [45] G. Seibold, F. Becca, and J. Lorenzana. *Phys. Rev. Lett.*, 100:016405, 2008.
- [46] G. Seibold, F. Becca, and J. Lorenzana. *Phys. Rev. B*, 78:045114, 2008.
- [47] Götz S. Uhrig. *Phys. Rev. Lett.*, 77:3629–3632, 1996.
- [48] Thomas Obermeier, Thomas Pruschke, and Joachim Keller. *Phys. Rev. B*, 56:R8479–R8482, 1997.
- [49] F. Günther, G. Seibold, and J. Lorenzana. *physica status solidi (b)*, 248:339–351, 2011.

- [50] E. von Oelsen, A. Di Ciolo, J. Lorenzana, G. Seibold, and M. Grilli. *Phys. Rev. B*, 81:155116, 2010.
- [51] G. Czycholl. *Theoretische Festkörperphysik*, volume 2. Springer-Verlag Berlin Heidelberg, 2004.
- [52] M. Born and Oppenheimer. *R. Annalen der Physik*, 389:457–484, 1927.
- [53] F. Bloch. *Zeitschrift für Physik A*, 52:555–600, 1928.
- [54] J. C. Slater and G. F. Koster. *Phys. Rev.*, 94(6):1498–1524, 1954.
- [55] J. Hubbard. *Proc. Roy. Soc.*, A276:238, 1963.
- [56] Junjiro Kanamori. *Prog. Theor. Phys.*, 30:275–289, 1963.
- [57] V. J. Emery. *Phys. Rev. Lett.*, 58(26):2794–2797, 1987.
- [58] Patrik Fazekas. *Lecture Notes on Electron Correlation and Magnetism*. World Scientific Publishing Co. Pte. Ltd., 1999.
- [59] J. Spalek. *Acta Physica Polonica A*, 111:409, 2007.
- [60] J. Büneemann, F. Gebhard, K. Radnóczy, and P. Fazekas. *J. Phys.: Condens. Matter*, 17:3807–3814, 2005.
- [61] J. Büneemann. *Eur. Phys. J. B*, 4:29–38, 1998.
- [62] Dieter Vollhardt. *Rev. Mod. Phys.*, 56:99–120, Jan 1984.
- [63] Walter Metzner and Dieter Vollhardt. *Phys. Rev. Lett.*, 62:324–327, 1989.
- [64] F. Gebhard. *Phys. Rev. B*, 41:9452–9473, 1990.
- [65] W. Metzner and D. Vollhardt. *Phys. Rev. B*, 37:7382–7399, 1988.
- [66] J. Büneemann, F. Gebhard, and W. Weber. In A. Narlikar, editor, *Frontiers in Magnetic Materials*. Springer, Berlin, 2005.
- [67] J. Büneemann, F. Gebhard, and W. Weber. *arXiv:cond-mat/0503332v1*, 2005.
- [68] D. J. Thouless. *The Quantum Mechanics of Many-Body Systems*. Academic Press, New York, 1972.
- [69] J. Büneemann, F. Gebhard, T. Schickling, and W. Weber. Numerical minimisation of gutzwiller energy functionals. in preparation, 2011.

- [70] J. Bünemann, 2011. private communication.
- [71] Elliott H. Lieb and F. Y. Wu. *Phys. Rev. Lett.*, 20:1445–1448, 1968.
- [72] W. F. Brinkman and T. M. Rice. *Phys. Rev. B*, 2:4302–4304, Nov 1970.
- [73] P. v. Dongen, F. Gebhard, and D. Vollhardt. *Zeitschrift für Physik B Condensed Matter*, 76:199–210, 1989. 10.1007/BF01312685.
- [74] D. Pines, editor. *Elementary excitations in Solids*. W. A. Benjamin, Inc., New York, 1963.
- [75] R. Kubo. *J. Phys. Soc. Japan*, 12:570–586, 1957.
- [76] R. Kubo. *Lectures in Theoretical Physics*. Wiley-Interscience, New York, 1959.
- [77] G. D. Mahan. *Many Particle Physics*. Springer, Berlin, 2005.
- [78] K. I. Kugel and D. I. Khomskii. *Sov. Phys. JETP*, 37:725, 1973.
- [79] Laura M. Roth. *Phys. Rev.*, 149:306–308, 1966.
- [80] A. Takahashi and H. Shiba. *J. Phys. Soc. Jpn.*, 69:3328–3333, 2000.
- [81] K. Held and D. Vollhardt. *Eur. Phys. J. B*, 5:473, 1998.
- [82] Tsutomu Momoi and Kenn Kubo. *Phys. Rev. B*, 58:R567–R570, 1998.
- [83] E. von Oelsen, G. Seibold, and J. Bünemann. *Phys. Rev. Lett.*, 107:076402, 2011.
- [84] F. Günther, G. Seibold, and J. Lorenzana. *Phys. Rev. Lett.*, 98:176404, 2007.
- [85] Ching-Kit Chan, Philipp Werner, and Andrew J. Millis. *Phys. Rev. B*, 80:235114, 2009.
- [86] H. A. Mook, R. M. Nicklow, E. D. Thompson, and M. K. Wilkinson. *J. Appl. Phys.*, 40:1450, 1969.
- [87] J. Bünemann and W. Weber. *Phys. Rev. B*, 55:4011–4014, 1997.
- [88] J. Bünemann and W. Weber. *Physica B*, 230-232:412, 1997.
- [89] E. von Oelsen, G. Seibold, and J. Bünemann. *New Journal of Physics*, 13:113031, 2011.

- [90] Gernot Stollhoff, Andrzej M. Oleś, and Volker Heine. *Phys. Rev. B*, 41:7028–7041, 1990.
- [91] Marco Schiró and Michele Fabrizio. *Phys. Rev. Lett.*, 105:076401, 2010.
- [92] Marco Schiró and Michele Fabrizio. *Phys. Rev. B*, 83:165105, 2011.
- [93] Dennis S. Bernstein. *Matrix Mathematics. Theory, Facts, and Formulas*. Princeton University Press, Princeton and Oxford, 2 edition, 2009.
- [94] E. Müller-Hartmann. *Z. Phys. B–Condensed Matter*, 74:507–512, 1989.

Acknowledgment

A list of acknowledgments shall close this thesis.

First of all, I want to thank my supervisor Prof. Götz Seibold for his patience and the support that I received during the research period resulting in this thesis. Special thanks go to my co-worker Dr. Jörg Bünemann, whose previous research on Gutzwiller wave functions yielded the basis for the numerical implementation of our theory. I express my gratitude to both of them for various fruitful discussions about strongly correlated systems and their computational treatment and the careful proofreading of the manuscript.

I want to express my gratefulness to Prof. Vladimir Hizhnyakov and Prof. Florian Gebhard for their readiness to act as referees.

Furthermore, I want to thank Dr. Dominic Merkt for fruitful discussions on computational topics. I want to thank all my colleagues for the familiar atmosphere in the institute.

Finally, I want to thank all the people that accompanied me during the last years, and that supported, encouraged or diverted me during some frustrating periods.

Plaudite, amici, comedia finita est.

LUDWIG VAN BEETHOVEN, 1827

Plaudite, amici, tragedia finita est.

ERNST VON OELSEN, 2011